THESIS

BETWEEN A BOULDER AND A HARD PLACE:
AN ACTUALISTIC EXPERIMENT TO INFER THE IMPACT OF CAVE ROOF FALL ON LIMB BONES AND ITS IMPLICATIONS FOR THE ARCHAEOLOGICAL RECORD

Submitted by

Alexandru Hajdu

Department of Anthropology and Geography

In partial fulfillment of the requirements

For the Degree of Master of Arts

Colorado State University

Fort Collins, Colorado

Summer 2022

Master's Committee

Advisor: Michelle Glantz

Michael Pante
Anne Hess

Copyright by Alexandru Hajdu 2022

All Rights Reserved

ABSTRACT

BETWEEN A BOULDER AND A HARD PLACE:
AN ACTUALISTIC EXPERIMENT TO INFER THE IMPACT OF CAVE ROOF FALL ON LIMB BONES AND ITS IMPLICATIONS FOR THE ARCHAEOLOGICAL RECORD

Over 50 years of research has highlighted the important role hominins and carnivores play as agents of bone fragmentation. The work has largely been focused on differentiating the assemblages created by hominins from those modified by carnivores. Consequently, cave roof fall and other agents have received relatively little attention in this rich literature. Previous studies of cave roof fall have suggested it can modify assemblages in a manner that mimics hammerstone-on-anvil percussion of bones indicating the need for reliable criteria to distinguish between these two processes. Here, we conduct an actualistic experiment designed to simulate the effects of cave roof fall on bone assemblages.

Sixteen (n=16) bison tibiae were fractured in four experiments with drop heights of 4.6 and 7.6 meters and rock weights of 6.8 and 13.6 kilograms. To represent a hominin assemblage sixteen (n=16) tibiae were randomly selected from a hammerstone-on-anvil collection created by Robert Kaplan and stored at Colorado State University. Bone surface modifications (BSM) counts that include pits, notches, grooves, and striations were created for both groups. Additionally, notch measurement ratios, Incipient notch counts, fragment counts, general fragment size frequency distributions, epiphyseal fragment measurements, percentages of fragments with BSMs, and presence/absence of stress relief traces (hackle marks and ribs) were collected from both groups.

Results suggest that flake count, pit count and the percentage of fragments with pits and/or grooves are the variables which are different between cave roof fall and hammerstone-on-anvil percussion. These variables are significantly different between the two assemblages; however, they are not applicable to the archaeological record. This is because the traces that these variables were built upon are not distinguishable between the two actors. This qualitative approach to address the equifinality between cave roof fall and hammerstone-on-anvil percussion has failed to provide any valuable insights.

ACKNOWLEDGEMENTS

Firstly, I am indebted to my committee members for their support and feedback for this thesis. I would like to thank Dr. Mica Glantz for providing me with a sound board, feedback, and encouragement. The same goes for Dr. Michael Pante, who provided encouragement, feedback and his taphonomic expertise. Finally, I would like to thank Dr. Ann Hess for her feedback and statistical guidance. Additionally, I would like to acknowledge Dr. Andrew Du for providing additional statistical guidance and insight. Finally, I would like to thank the College of Liberal Arts and the Department of Anthropology and Geography for providing me a portion of funding for the experiment and classes needed to complete my Master's Degree.

Secondly, I would like to thank my family for supporting me and encouraging me to pursue a Master's Degree. This thesis would not have been possible without their support.

Next, I would like to thank my partner, Denise Frazier, and her family. The actualistic experiment at the heart of this thesis would not have been possible without Denise helping me set up the pulley system, break the bones, endure the bone boiling process, and endless editing. As well as her family for encouraging both of us.

Lastly, I would like to thank my cohort for their comradery and support. Many of us depended on the Friday pitchers at Avo's to keep some sanity. Special mention goes to Robert "Bobby" Kaplan for creating the hammerstone-on-anvil sample used in this thesis.

I am grateful for everyone that has helped and supported me on this journey. This is dedicated to you!

TABLE OF CONTENTS

ABSTRACT ii
ACKNOWLEDGEMENTS iv
LIST OF TABLES vii
LIST OF FIGURES viii
Chapter I - Introduction 1
1.1 Research Question and Theoretical Framework 3
1.2 Summary of Chapters 7
Chapter II - Background 8
2.1 Taphonomy and Paleoanthropology 8
2.2 Traces and Taphonomic Site Interpretation 18
2.3 Traces and Cave Site Taphonomy 24
Chapter III – Materials and Methods 32
3.1 Materials 32
3.2 Methodology 32
3.3 Data Collection from Fractured Bones 46
3.3.1 Visual – No Magnification 49
3.3.2 Visual – With Magnification 61
3.3.3 Presence/Absence 67
3.3.4 Measurement 70
3.3.5 Composite Variables 81
3.4 Hypothesis Testing and Statistics 82
Chapter IV - Results 89
4.1 Experimental Results 90
4.2 Data Distribution and Summary Statistics 91
4.3 Statistical Test Results and P-values 96
4.4 Significant Variables 99
4.5 Non-Significant Variables 101
4.6 Research Question Assessment 103
4.7 Summary 103

Chapter V - Discussion 104
5.1 Significantly Different Variables 104
5.2 Non-Significant Variables 107
5.3 Archaeological Implications 112
5.4 Limitations of This Study 115
5.5 Summary 116
Chapter VI - Conclusion 118
6.1 The Experiment 118
6.2 Future Directions 119
APPENDICES 121
Appendix 1: Materials 121
Appendix 2: Cave Roof Fall Raw Data Tables 123
Appendix 3: Results Histograms 129
Appendix 4: Results Violin Plots 144
Appendix 5: Scatter Plots 159
REFERENCES 164

LIST OF TABLES

Table 1 Archaeological and Paleontological Cave Sites with Evidence of Cave Roof Fall 26
Table 2 Traces of Dynamic Loading on Bones Modified By Hominins at Open Air Sites and Roof Fall at Cave Sites 30
Table 3: Measurements of boulders used in the cave roof fall simulation 33
Table 4: Pleistocene Archaeological Rock Shelter Sites with Cave Heights 36
Table 5 Cave Roof Fall Simulation Summary with Defined Drop Height and Boulder Weight For Each Experiemnt 42
Table 6: Variables Collected from Fractured Bison Bones 47
Table 7: Notch Variations and Pseudo Notches Definitions 52
Table 8 Statistical Tests with Assigned Variables from Both Assemblages 85
Table 9 Predictions for the Outcome of each Tested Variable for Each Actor 86
Table 10 Reaserch Question with Hypotheses and Statistical Tests with Hypotheses 89
Table 11 Summary Statistics for Number of Blows Attributed to Cave Roof Fall to Fracture the Bison Tibiae 90
Table 12 Summary Statistics for Number of Blows Attributed to HAP to Fracture the Bison Tibiae 90
Table 13 Summary Statistics for Each Collected Variable 95
Table 14 P-values from Fisher's Exact Test for Notch and Incipient Notch Presence 96
Table 15 P-values and Correlation Coefficients From Spearman's Rank Order on Fragemnt Size Categories Between both Actors 96
Table 16 P-values for All Variables Testes Using the Mann-Whitney U Test 97
Table 17 Variables That Could not be Tested or Were Not Designed to be Tested with Supporting Reasoning 98
Table 18 Materials used in Cave Roof Fall and Percussion Actualistic Studies 121
Table 19 7.6 m Boulder Drops 123
Table 20 4.6 m Boulder Drops 124
Table 21 Raw Data from the Roof Fall Simulation Experiment Trials 125
Table 22 Raw Cave Roof Fall and Hammerstone-on-Anvil Percussion Collected from All Fractured Bison Bones 126
Table 23 Notch and Incipient Notch Dimensions, Ratios and Release Angle 127
Table 24 Total Fragment Size Categories per Assemblage and Percentage of Fragment Size Categories to Total Fragment Count 128

LIST OF FIGURES

Figure 1 An illustration of the processes that encompass middle-range theory and middle-range research. 6
Figure 2 Nestled hierarchy of steps necessary to build a proper network of inferences between steps..... 13
Figure 3 Boulder number 1 (6.8 kg) 34
Figure 4 Boulder number 2 (13.6 kg) 34
Figure 5 Boulder number 3 (6.8 kg) 34
Figure 6 Tibia positioned on tarp underneath the boulder..... 38
Figure 7 Rock fastened with string 39
Figure 8 Cave roof fall simulation..... 40
Figure 9 Bone in canning pot..... 43
Figure 10 Hammerstone-on-anvil fragments..... 49
Figure 11 Cave roof fall created fragments 50
Figure 12 Bone flakes created by cave roof fall 51
Figure 13 Bone flakes created by hammerstone-on anvil percussion..... 51
Figure 14 Incipient notch created by cave roof fall 53
Figure 15 Incipient notch created by hammerstone-on-anvil percussion 53
Figure 16 Percussion notch on the cortical side of the fragment..... 54
Figure 17 Percussion notch on the medullary side of the fragment..... 55
Figure 18 Impact notch on the cortical side of the fragment 55
Figure 19 Impact notch on the medullary side of the fragment..... 56
Figure 20 Pseudo-notch on the cortical side of a cave roof fall fragment 57
Figure 21 Pseudo-notch on the internal part of a cave roof fall fragment 57
Figure 22 Pseudo-notch on the cortical side of a hammerstone-on-anvil fragment 58
Figure 23 Pseudo-notch on the medullary side of hammerstone-on-anvil fragment..... 58
Figure 24 Fragments with a cortical surface on the left, fragments without cortical surface on the right..... 59
Figure 25 Fragments with pits and/or grooves above, fragments without any pits on the bottom60
Figure 26 Impact pits indicated by the arrows..... 62
Figure 27 Percussion pits indicated by the arrows..... 62
Figure 28 Impact groove..... 63
Figure 29 Percussion groove..... 64
Figure 30 Impact striations 65
Figure 31 Percussion striations..... 66
Figure 32 Hackle marks on cave roof fall created fragment..... 67
Figure 33 Ribs on a cave roof fall created fragment..... 68
Figure 34 Hackle marks on a hammerstone-on-anvil created fragment..... 68
Figure 35 Ribs on a hammerstone-on-anvil created fragment..... 69
Figure 36 Digital caliper used to measure fragments longitudinally..... 70
Figure 37 Tape measure used to measure large fragments longitudinally..... 71
Figure 38 Example of fragments under 2 cm from a cave roof fall assemblage 72
Figure 39 Example of fragments between 4 and 4.99 cm from a cave roof fall..... 72

Figure 40 Proximal epiphysial element 75
Figure 41 Distal epiphysial element with a fused metaphysis 76
Figure 42 Distal epiphysial element with an unfused metaphysis 77
Figure 43 Distal epiphysial element without an epiphysis 78
Figure 44 Figure shows notch measurements 79
Figure 45 Normally distributed variables. 92
Figure 46 Histogram of left skewed data 92
Figure 47 Anatomy of a violin plot 93
Figure 48 Fragment size distribution in relation to the assemblage 94
Figure 49 Violin plots of all significant variables 99
Figure 50 Fragment count 129
Figure 51 Incipient flake count 129
Figure 52 Flake count 130
Figure 53 Notch count 130
Figure 54 Pit count 131
Figure 55 Groove count 131
Figure 56 Striation count 132
Figure 57 Fragments less than 2 cm count 132
Figure 58 Fragments 2-2.99 cm count 133
Figure 59 Fragments 3-3.99 cm count 133
Figure 60 Fragments 4-4.99 cm count 134
Figure 61 Fragments 5-5.99 cm count 134
Figure 62 Fragments 6-6.99 cm count 135
Figure 63 Fragments 7-7.99 cm count 135
Figure 64 Fragments 8-8.99 cm count 136
Figure 65 Fragments 9-9.99 cm count 136
Figure 66 Fragments more than 10 cm count 137
Figure 67 Distal element length in centimeters 137
Figure 68 Proximal element length in centimeters 138
Figure 69 Fragments that preserve cortical surface count 138
Figure 70 Fragments that exhibit at least one pit and/or groove count 139
Figure 71 Fragments that exhibit at least one notch 139
Figure 72 Percentage of cortical fragments with pits and grooves 140
Figure 73 Percentage of cortical fragments with notches 140
Figure 74 Pseudo-notch count 141
Figure 75 Ratio of pseudo-notches to notches 141
Figure 76 Ratio of notch breadth to notch depth 142
Figure 77 Ratio of notch breadth to notch depth 142
Figure 78 Notch release angle 143
Figure 79 Fragment count 144
Figure 80 Incipient flake count 144
Figure 81 Flake count 145
Figure 82 Notch count 145
Figure 83 Pit count 146
Figure 84 Groove count 146
Figure 85 Striation count 147

Figure 86 Fragments less than 2 cm count 147
Figure 87 Fragments 2-2.99 cm count 148
Figure 88 Fragments 3-3.99 cm count 148
Figure 89 Fragments 4-4.99 cm count 149
Figure 90 Fragments 5-5.99 cm count 149
Figure 91 Fragments 6-6.99 cm count 150
Figure 92 Fragments 7-7.99 cm count 150
Figure 93 Fragments 8-8.99 cm count 151
Figure 94 Fragments 9-9.99 cm count 151
Figure 95 Fragments larger than 10 cm count 152
Figure 96 Distal element length in cm 152
Figure 97 Proximal element length in cm 153
Figure 98 Cortical fragment count 153
Figure 99 Cortical fragments with a pit and/or groove count 154
Figure 100 Cortical fragments with at least one notch 154
Figure 101 Percentage of fragments with pits and/or grooves 155
Figure 102 Percentage of fragments with at least one notch 155
Figure 103 Pseudo-notch count 156
Figure 104 Ratio of pseudo-notches to notches 156
Figure 105 Ratio of notch breadth to notch depth 157
Figure 106 Ratio of flake scar breadth to notch depth 157
Figure 107 Release angle in degrees 158
Figure 108 Scatter plot of fragments smaller than 2 cm from both actors 159
Figure 109 Scatter plot of fragments between 2 and 2.99 cm from both actors 159
Figure 110 Scatter plot of fragments between 3 and 3.99 cm from both actors 160
Figure 111 Scatter plot of fragments between 4 and 4.99 cm from both actors 160
Figure 112 Scatter plot of fragments between 5 and 5.99 cm from both actors 161
Figure 113 Scatter plot of fragments between 6 and 6.99 cm from both actors 161
Figure 114 Scatter plot of fragments between 7 and 7.99 cm from both actors 162
Figure 115 Scatter plot of fragments between 8 and 8.99 cm from both actors 162
Figure 116 Scatter plot of fragments between 9 and 9.99 cm from both actors 163
Figure 117 Scatter plot of fragments larger than 10 cm 163

CHAPTER I: INTRODUCTION

Fractured bones are a common component of many archaeological assemblages associated with hominins from the Pliocene, Pleistocene, and Holocene records (Blumenschine, 1995; Bunn et al., 1986; Morlan, 1994). Bone fracture is defined as the breakage of the diaphyseal cortical surface into the medullary cavity of the bone, creating two large bone fragments along with smaller fragments (Johnson, 1985). While most archaeological sites preserve fractured bone, the process of fracturing is not exclusively an anthropogenic or hominin phenomenon (Gifford-Gonzalez, 2018c; R. L. Lyman, 1984; Myers et al., 1980; Oliver, 1989). Carnivore made assemblages of fractured bone have been created in laboratory settings and have been recovered from time periods that predate hominins. (Blumenschine, 1995; Coil et al., 2017; Haynes, 1983; Myers et al., 1980; White et al., 1991). Herbivores can induce bone fragmentation through trampling suggesting that bone fragmentation is not a carnivore or hominin exclusive phenomenon. Bone fragmentation is not just a biotic phenomenon but can also have abiotic causes. Abiotic vectors of fragmentation include but are not limited to soil compaction, diagenetic processes, weathering, impact following free fall, and roof fall (Behrensmeyer, 1978; Denys, 2002; R. L. Lyman, 1984; Oliver, 1989; Villa & Mahieu, 1991).

Research into causes of bone fragmentation has largely favored hominin and carnivores as the main accumulators of broken bone assemblages (Binford, 1981c; Bunn et al., 1986; Capaldo & Blumenschine, 1994; Coil et al., 2017; Haynes, 1983; Johnson, 1985). This is understandable because both hominins and carnivores are active accumulators, meaning the accumulation is done with intent. This intent is nutritional, with each feeding episode expanding the assemblage. By studying these accumulations, anthropologists can piece together an understanding of hominin feeding behavior by separating hominin generated assemblages from

carnivores created assemblages (Binford, 1981d; Blumenschine, 1995; Blumenschine & Selvaggio, 1988; Capaldo & Blumenschine, 1994; Gifford-Gonzalez, 1991; Johnson, 1985). Feeding behavior can be used as a proxy for hominin habitation and presence at a site. Further research into more complex hominin behaviors cam be conducted once a hominin presence has been firmly established.

The focus on biotic accumulators has produced a substantial collection of literature, dwarfing the sizable literature on abiotic causes of bone fragmentation (Andrews & Whybrow, 2005; Kos, 2003; Mann & Monge, 2006; Oliver, 1989). This gap in research is detrimental to the narratives that are created about hominin feeding behavior and more complex behaviors. This is because while abiotic causes of bone fragmentation are not intentional, they can still contribute to the understanding of hominin feeding behavior and more complex behaviors derived from established hominin sites (Binford, 1981a; Griggo et al., 2019; Haynes, 2015; R. L. Lyman, 1984; Oliver, 1989; Olsen & Shipman, 1988; Trinkaus, 1985). Hominin involvement as an accumulator of bones at a site can be overturned or diminished if abiotic accumulators are shown to have played a part in the accumulation seen at the site (Binford, 1981a; Mann & Monge, 2006; Oliver, 1989; Trinkaus, 1985). Emil Bächler's interpretation of the Drachenlock assemblage, and the overturn of this interpretation by Bjorn Kurten is an example of where hominin involvement was overturned.

The cave bear cult has its origins in Bächler's interpretation of cave bear remains at Drachenlock cave (Switzerland, Upper Paleolithic) (Chase, 1987; Pacher & Rabeder, 2016). Bächler's excavations unearthed a cave bear faunal assemblage, which included a cave bear limb bone thrust through the eye socket of a cave bear skull, and four bear skulls encased in a crypt (Kurtén, 1995). Hominin tools or other hominin traces were not found among the cave bear

assemblage at Drachenlock cave (Wunn, 2001). He interpreted these cave bear anomalies as evidence that Neanderthals manipulated the bones and skull as part of a religious rite (Chase, 1987). This interpretation created and popularized the idea of the cave bear cult (Kurtén, 1995). Later this interpretation was challenged and overturned on the basis that hominin created tools or other traces of hominin habitation were not associated with the cave bear assemblage (Wunn, 2001). Kurten (1995) building on the work of other suggested that a combination of cave bear tramping and geologic activity through cave roof fall are responsible from manipulating the bones to their discovered positions.

While the "Cave Bear Cult" is an example where hominin action was overturned, the highly fragmented Neandertal remains and faunal assemblage from Krapina Cave is still poorly understood. The Krapina rock shelter (Croatia, 130 kya) is one of the oldest and largest caches of Neanderthal remains ever discovered (Gorjanović-Kramberger, 1906). The fact that the collection is also highly fragmented has been the source of speculation for multiple generations of paleoanthropologists. Some of the literature credits Neanderthals as the accumulators through cannibalistic behaviors (Ullrich, 2005; Villa, 1992). Others suggest cave roof fall as the primary agent of bone fragmentation at Krapina (Mann & Monge, 2006; Trinkaus, 1985). If cave roof fall can be distinguished from hammerstone-on-anvil percussion through actualistic experiments, this knowledge can be applied to solve the equifinality between the actors and end the debate over the culpable actor at Krapina and other sites with uncertain actor involvement.

1.1 Research Question and Theoretical Framework

The research question that is at the center of this experiment is whether the taphonomic signature of roof fall is different from the taphonomic signature of hammerstone-on-anvil percussion. The reasoning behind this question is the blind spot in the taphonomic literature

concerning cave roof fall. This is seen in the prevalence of cave roof fall events described in archaeological sites, however sparse research has been done to characterize the taphonomic pattern left by cave roof fall on bone assemblages. This lack of research is seen in the sparse actualistic studies and descriptions of cave roof fall in the taphonomic literature (Dixon, 1984; Karr & Outram, 2012a; Oliver, 1989).

To investigate if the taphonomic signature of cave roof fall is different from the taphonomic signature of hammerstone-on-anvil percussion the following hypotheses were developed:

H_0: All variables collected indicate that the taphonomic pattern of cave roof fall is not different from that of hammerstone-on-anvil percussion.

The null hypothesis (H_0) will be considered if all the variables collected prove not to be significant in differentiating between cave roof fall and hammerstone-on-anvil percussion.

H_1: All variables collected are indicative of a difference between cave roof fall and hammerstone-on-anvil percussion.

The condition under which the first alternative hypothesis (H_1) will become viable is if all the variables collected point towards a difference between the taphonomic pattern of cave roof fall from hammerstone-on-anvil percussion.

H_2: Some of the variables collected are different in the taphonomic patterns of cave roof fall compared to hammerstone-on-anvil percussion.

This second alternative hypothesis (H_2) will be evident if one or more variables but not all variables, are different between the taphonomic pattern of cave roof fall and hammerstone-on-anvil percussion.

It is the aim of this thesis to utilize an actualistic experiment to infer the taphonomic signature of cave roof fall. This is achieved by simulating cave roof fall using various weights and heights on a sample of bison bones. After the experiment was executed, multiple variables were collected from the broken bones and compared to the same variables collected from sample of bones that were primarily modified by hammerstone-on-anvil percussion in a laboratory setting. If no variables stand out as being significantly different between the two actors, then the equifinality remains between the two actors. An equifinality is when two actors are indistinguishable because they leave the same trace pattern (R. Lyman, 1987). This means that other avenues must be used to solve the overlap between the two actors. If some variables do prove to be significant different between the two actors, then the equifinality between the two actors can be further explored. This means the variables that are found significant could be applied to the archaeological record to refine the hominin taphonomic signature by removing any uncertainties brought up by cave roof fall.

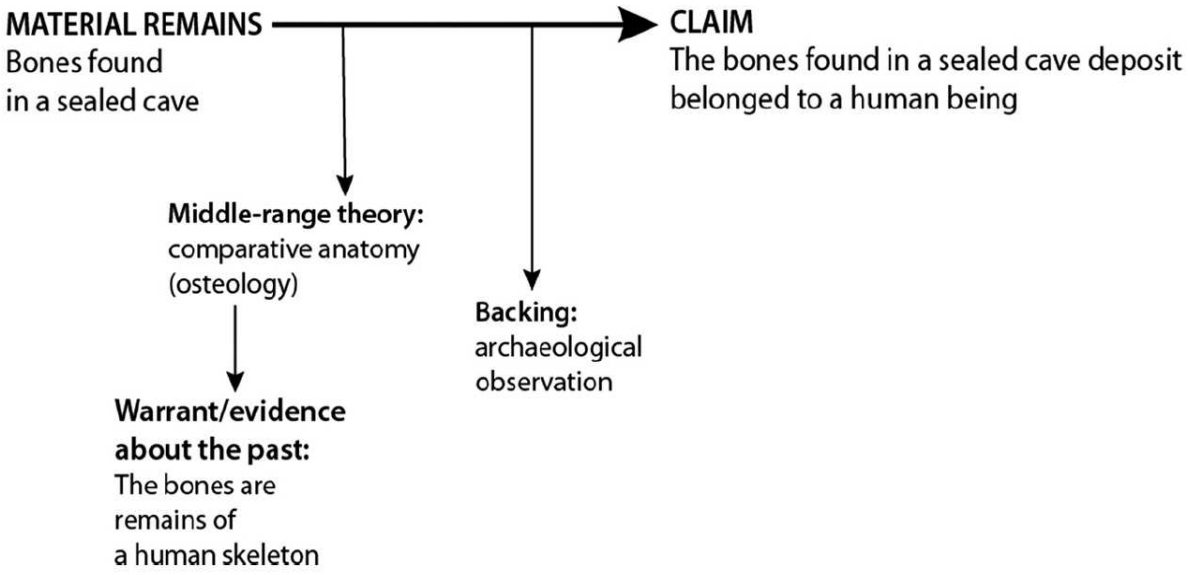

Figure 1 An illustration of the processes that encompass middle-range theory and middle-range research. From "Warrants, Middle-Range Theories, and Inferential Scaffolding in Archaeological Interpretation", by K. Kokkov, 2019, Perspectives on Science, 27(2), p. 183. Copyright 2019 by The Massachusetts Institute of Technology.

The theoretical framework that allows this experiment to be valid is primarily middle-range theory and actualistic studies. Binford (1981b) developed middle-range theory to verify traces made in the past by recreating the traces in the present as seen in Figure 1. As he points out an archaeological assemblage is static and devoid of energy. This means that the taphonomic history of the assemblage, which includes all actors that partook in the creation of the assemblage, is all superimposed on the assemblage eliminating time and causal relationships, leaving only traces. In order to correctly link the trace with the actor Binford (1981b) proposes actualistic experiments as a bridge between the past and the present. These experiments seek to recreate the traces seen in the past by mimicking a suspected actor.

Actualistic experiments in turn depend on the assumption of uniformitarianism, which states that the processes today are the same as processes in the past. Actualistic experiments link traces in the present to traces in the past through relational analogies. The links created by actualistic experiments in turn can be applied through inductive reasoning to the archaeological

record to verify that traces seen at a site can be linked to an actor as seen in Figure 1. By successfully applying the findings of an actualistic study to an archaeological assemblage the taphonomic history of the assemblage can be better understood enabling archaeologists to link traces with actors. Once all traces have been securely linked to their respective actors, the actors of interest can be refined and studied.

1.2 Summary of Chapters

Following this chapter will be Chapter II the Background chapter that will explore and define the concepts necessary to contextualize the research questions presented in this chapter. Chapter III Materials and Methods will detail the materials that were used in this actualistic experiment, and the methodology to carry out the experiment, gather data, and analyze the data. Chapter IV, the Results chapter will present the findings of this experiment and any variables that were found to be significant in differentiating between cave roof fall and hammerstone-on-anvil percussion. Chapter V is the Discussion chapter in which the driving forces behind the significant variable will be explored, and the insignificant variables will be discussed, and any untested variables will be explained. The final chapter will be Chapter VI Conclusion which will summarize the findings and provide some directions for future research and the expansion of this research.

CHAPTER II: BACKGROUND

2.1 Taphonomy and Paleoanthropology

Taphonomy can be described as the science of death and fossilization (Gifford, 1981). It was defined by Ivan Efremov who sought to investigate and decipher the fossilization process (Efremov, 1940). Taphonomy borrows concepts from geology, paleontology, and ecology (Gifford, 1981). Taphonomy as a science can be divided into three parts, necrology, biostratinomy, and diagenesis. These parts together document an organism's journey from death to discovery (Grupe & Harbeck, 2014). Necrology explores the death of an organism, which could be from predation or other environmental factors, such as mass die-offs during droughts (Grupe & Harbeck, 2014). Biostratinomy is the interaction between the carcass and the biosphere until burial occurs, which includes interactions with scavengers, disarticulation, and transport by biotic and abiotic actors (Gifford, 1981). Lastly, if the assemblage is buried it becomes subject to diagenetic processes, like microbial attack and calcium leaching which are examples of biotic and abiotic actors that affect the assemblage until its discovery (Grupe & Harbeck, 2014).

The principles of taphonomy have wide applications across disciplines interested in ancient biota (Gifford, 1981). The addition of taphonomy was an important milestone in the maturation of paleoanthropology as a discipline because it employs faunal remains as one of the criteria to separate a hominin signature from the "white noise" present at sites. Properly attributing faunal remains as hominin altered is crucial in correctly interpreting hominin behavior (Gifford-Gonzalez, 1991). The incorrect assessment of altered faunal remains can lead to false interpretations of hominin behavior. These incorrect interpretations can lead to an incorrect understanding of hominin behavior as seen in the Cave Bear Cult inferred from the Drachenlock cave in Switzerland by Emil Bächler (Kurtén, 1995; Pacher & Rabeder, 2016). Bächler jumped

to the conclusion that Neanderthals were worshiping cave bears because of what he interpreted as crypts where cave bear skulls were supposedly stashed by Neanderthals. After this site was reevaluated using taphonomy it was found that the crypts were created by natural forces (Gargett et al., 1989). Taphonomy is a vital tool for interpretation in paleoanthropology because it helps accurately decipher the actor responsible for producing a site. Taphonomy is necessary for interpreting site remains and must be used along-side a theoretical framework for well-rounded interpretations (Gifford-Gonzalez, 1991). Taphonomy and its accompanying theoretical application, middle-range research, need to work in tandem to provide a proper site interoperation. Taphonomy is the practical part of site interpretation, where trace patterns are recorded. Middle-range research in turn connects and verifies the trace patterns recorded at a site with the responsible actors through experimentation in the present. Together taphonomy and middle-range research provide a framework to properly interpret the taphonomic history of a site.

Similarly to how paleoanthropology imported taphonomy from paleontology to understand the actors present in an assemblage, middle range theory was appropriated from archaeology to provide the theoretical framework for taphonomy (Binford, 1981b; Gifford, 1981). Middle-range theory links the past with the present by validating actors responsible for assemblages in the past through actualistic experiments in the present (Binford, 1981b). The linkage of the past and present is possible through the assumption of uniformitarianism. Uniformitarianism was developed by James Hutton as one of the pillars of geology. It states that processes in the past and present are the same and operate the same way (Hutton, 1788). In a paleoanthropological sense, this means that processes in the past are assumed to have left the same kind of pattern as they do in the present (Binford, 1981b). An example of this would be the traces left on bone by hammerstone-on-anvil percussion in archaeological sites and the

hammerstone-on-anvil percussion traces generated during an experiment, both are assumed to leave the same trace (Binford, 1981b). Uniformitarianism and middle-range theory provides the link between the past and the present and thus traces left by processes can be assumed as constant, the processes themselves just need to be isolated which can be done through actualistic experiments (Gifford-Gonzalez, 1991).

The necessity of actualistic experiments is illustrated by Binford (1981b), when he describes archaeological assemblages as inert, with indistinguishable patterns from all processes that contributed to the assemblage. Linking patterns to processes solely based on the archaeological sites leads to circular reasoning, which then gets applied to other sites, and eventually metastasizes into myths. (Binford, 1981a). An example of this is the case of the Guattari Cave (Italy, 52 kya) skull (Piperno & Giacobini, 1990). The Neanderthal skull was recovered from an faunal assemblage on the cave floor by Alberto Claro Blanc in 1939 (White et al., 1991). Blanc noticed that the base of the Neanderthal skull was missing, which he interpreted as headhunting and skull worship behavior (Wunn, 2000). This interpretation was based on traces interpreted as cut marks left on the skull and on the Neanderthal's skull superficial similarity to a museum collection of head hunter modified skulls (White et al., 1991). The association of two concepts based on superficial similarities is called a formal analogy (Gifford-Gonzalez, 1991). Following Blanc's interpretation Neanderthals were thought to possess a rudimentary skull cult and engage in head hunting (Wunn, 2000). Later the skull was reevaluated through data gathered from actualistic experiments which overturned Blanc's interpretation. The "cut marks" were properly identified as tooth marks and the damage at the base of the skull was attributed to a hyena accessing the brain cavity (White et al., 1991). Actualistic experiments are modern-day experiments that seek to recreate the pattern of one

process seen in the past. Actualistic experiments allow control to be exerted on one process so that the pattern and process can be unequivocally associated (Binford, 1981b). Once the actualistic experiment is carried out and a reference collection created, the pattern and process have a relational analogy (Binford, 1981a; Blumenschine, 1995). This relationship can then be applied to the archaeological record facilitating the identification of a responsible actor in the assemblage (Binford, 1981b). While middle-range theory does have other uses for this thesis its main use is to facilitate actor differentiation. Through actualistic experiments and uniformitarianism, middle-range theory breaks the cycle of mythmaking and provides the means to analyze an archaeological site with an objective methodology (Binford, 1981a). While middle-range theory and uniformitarianism provide the theoretical backbone for taphonomy, relational analogies provide the connective tissue for a taphonomic analysis (Gifford-Gonzalez, 1991).

Relational analogies are the means through which middle-range research can be applied to a taphonomic interpretation of an archaeological site. Relational analogies link two concepts through a causal link, where process A produces only B (Gifford-Gonzalez, 1991). For example, using a stone tool to strip flesh from bone will leave cut marks on the bone. The two concepts, cut marks on bone and cutting meat off bone with a stone tool are linked through a relational analogy where cutting meat from a bone with a stone tool produces cut marks on bone. Relational analogies are at the core of actualistic studies, where traces created in the present can be causally linked to actors because the causal interaction between the actor and the trace is observed. The relational analogies created in the present can then be exported into the past through the assumption of uniformitarianism. Much the same way that uniformitarianism assumes that processes in the past are the same as processes in the present, relation analogies can also be applied from the present to the past. To invoke the earlier example, if cut marks can be

causally linked to butchering with stone tool in the present, then this link between the two can be assumed to have happened in the past as well. Hominins using a stone tool to butcher a carcass in the past would leave similar traces to those produced during an actualistic experiment in the present (Binford, 1981b). This assumption can be made because in both instances a cutting motion is used to strip the meat off the bone using a stone tool. Thus, the present and the past can be connected through relationships created during actualistic experiments in the present and transferred to the past through relational analogies and the assumption of uniformitarianism.

Relational analogies are used in middle-range theory and taphonomy to act as bridges of inference between a known concept and an inferred one (Gifford, 1981). Gifford-Gonzalez (1991) creating a nestled hierarchy of necessary steps as seen in Figure 2 to help build a proper interpretation of an archaeological site. This is necessary because as Binford (1981b) pointed out an archaeological site is an inert entity, with all forces and processes involved in creating the site already spent and gone. What is left is an amalgamation of signatures and traces without the actor and effector present. To prevent misinterpretations through formal analogies, the most basic and empirical evidence must be considered first (Binford, 1981a).

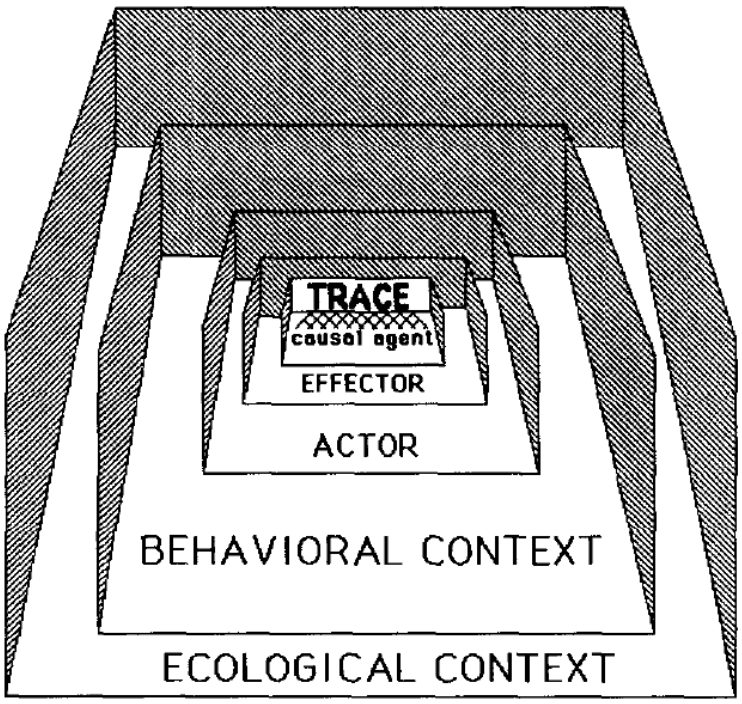

Figure 2 Nestled hierarchy of steps necessary to build a proper network of inferences between steps. From "Bones Are Not Enough: Analogous, Knowledge, and Interpretive Strategies in Zooarchaeology" by D. Gifford-Gonzalez, 1991, Journal of Anthropological Archaeology, 10(3), p. 229. Copyright 1991 by the Journal of Anthropological Archaeology.

Traces are the outcome of an effector interacting with a bone (Gifford-Gonzalez, 1991). These traces can be cutmarks, percussion marks, or chop marks associated with hominins (Fisher, 1995) or toothmarks, tooth furrows, or tooth pits associated with carnivores (Fisher, 1995). Abrasions and defoliation are associated with various abiotic processes (Fisher, 1995). Collectively traces left on bone can be referred to as bone surface modification (BSMs). Through the interaction of the effector with the bone, traces are imprinted on the bone, and as long as those traces remain, they are the most empirical and tangible evidence, and are at the center of the nested hierarchy as seen in Figure 2 (Behrensmeyer, 1978; Gifford-Gonzalez, 1991). Once these traces are identified they can be linked to an actor through a causal agent (Gifford-Gonzalez, 1991).

From traces, the next step is the identification of the causal agent which addresses the processes of how the traces were created (Gifford-Gonzalez, 1991). For example, a cutmark and a toothmark are created through slightly different means, with one involving an interaction between a lithic tool and bone, while the other is an interaction between two organic entities, which ultimately will leave different traces (Shipman, 1981). These causal agents interact with the bone using different types of force. For example, cutmarks are left on bone following the application of force in a scraping motion, while percussion marks are left following the application of energy during a dynamic loading episode (Johnson, 1985). For this thesis, only loading types will be explored since it is the only kind of force relevant to the research question.

Loading can be divided into two categories, dynamic and static (Johnson, 1985). The difference between the two is in the way that force is applied. Dynamic loading is characterized by a concentrated delivery of force to a small surface area (Johnson, 1985). In terms of lithics, dynamic loading is employed during percussion flaking (Johnson, 1985). Similarly dynamic loading is associated with hominins and the use of hammerstone-on-anvil percussion to fracture bones (Capaldo & Blumenschine, 1994). Static loading is the application of constant pressure over a surface area and is seen during pressure flaking in lithics (Johnson, 1985). Within paleoanthropology, static loading has been associated with carnivore interaction with bones (Capaldo & Blumenschine, 1994). Carnivore teeth eventually crack bones through structural fatigue by applying constant localized pressure on the diaphysis of the bone (Johnson, 1985). Dynamic and static loading are the two main casual agents that are involved in bone fracture (Johnson, 1985).

Traces and causal agents describe the way that an effector interacts with bone, which leads to the next inference step, the effector (Gifford-Gonzalez, 1991). While the causal agent

describes the physics behind the creation of traces, the effector refers to the actual object that interacts with bone and creates the trace (Gifford-Gonzalez, 2018c). An effector can be connected to a biotic process as seen with carnivore jaws and teeth, hammerstone-on-anvil percussion used by hominins, grains of sand interacting with bone during trampling by herbivores, or related to abiotic processes, as shown by a rock hitting bone during a roof fall event, or sediment pressure as part of deposition among others (Capaldo & Blumenschine, 1994; Oliver, 1989; Olsen & Shipman, 1988). The effector is the catalyst through which the causal agent interacts with bone.

The actor is a conceptual level above the effector (Figure 2) and requires an inferential bridge to associate it with the effector (Gifford-Gonzalez, 1991). The actor is the individual or process that employed the effector (Gifford-Gonzalez, 2018a). This relationship is easy to understand in a biotic context, as a hominin actor employs the hammerstone (effector) to fracture the shaft of the bone leaving a trace, or that a carnivore actor employs its jaws and teeth as effectors to fracture the diaphysis of a bone leaving a trace (Gifford-Gonzalez, 1991; Johnson, 1985). These connections are clear to interpret because they are intentional, however unintentional employment of an effector by an actor is also possible. An example of this is trampling done by an animal that causes the grains of sand to abrade the diaphysis of the bone, or a roof fall event where a falling piece of bedrock fractures a bone on the cave floor. These are both events without any intention or purpose (Fisher, 1995). Actors link traces, causal agent and, effectors to a behavioral and ecological context. (Gifford-Gonzalez, 1991).

The behavioral context is the penultimate level in the hierarchy as seen in Figure 2 and describes why actors engage in certain behaviors and is informed by all lower levels (Gifford-Gonzalez, 1991). With biotic actors the behavioral context might involve nutrient acquisition or

tool production. The behavioral context can also help to describe assemblage formation as there is an intention behind the bone accumulation (Gifford-Gonzalez, 1991). Although abiotic actors do not process bones for a purpose, they can still provide important criteria used to identify intentionally processed bones (Oliver, 1989; Olsen & Shipman, 1988). From the reconstruction of the behavioral context, it is possible to infer why and how the assemblage was created.

At the top of the hierarchy as seen in Figure 2 is the ecological context (Gifford-Gonzalez, 1991). The ecological context is dependent on properly constructed inference connections between the lower steps (Gifford-Gonzalez, 2018a). The purpose of the ecological context is to determine a biotic actor's role within the surrounding environment (Gifford-Gonzalez, 2018a). This can involve the role of hominins as hunters and/or scavengers, the carnivore guild present in area, or even the kind of vegetation cover present at a site (Blumenschine et al., 1994). The ecological context can also be extended to abiotic actors. Fast deposition of soil over bones leading to sedimentary overburden action on bones could be indicative of a wet environment. Likewise, rapid fluctuations in in climate can lead to intensive weathering of bedrock on a cave roof which would promote the frequency of roof fall episodes within a given period, increasing the likelihood of an interaction between roof fall debris and bones, if bones are present in the cave (Mann & Monge, 2006). As the final step of the hierarchy, the ecological context is the most susceptible to incorrect interpretation (Gifford-Gonzalez, 1991). This vulnerability can be seen in the ongoing debate on the role of hominins as hunters or scavengers(Blumenschine, 1995; Gifford-Gonzalez, 2018d).

Lastly, equifinality is the final core concept within bone assemblage analysis. Lyman (1987) defines equifinality as two different processes creating the same pattern. In this context equifinality would be two actors creating the same trace making it impossible to determine the

responsible actor (Gifford-Gonzalez, 1991). This, for example, could be carnivores gnawing and hominin percussion producing spiral fractures, or roof fall and hominin percussion leaving similar traces on modified bone (Johnson, 1985; Oliver, 1989). Though some equifinalities can be solved by using other variables, others cannot be solved without external means (Capaldo & Blumenschine, 1994; Oliver, 1989). Actualistic experiments are the most effective way to determine if there are other ways to differentiate the correct actor or if it truly is an equifinality (Binford, 1981b; Karr & Outram, 2012a)

Poor inferences can compromise the information that is gained from studying traces and leads to faulty conclusions. (Binford, 1981a; Gifford-Gonzalez, 1991). A famous example of poor site interpretations is Raymond Dart's proposal of the osteodentokeratic industry unearth at Makapansgat Cave (South Africa, 3-2.6 mya, Herries et al., 2013). Dart began excavations at Makapansgat following his chance encounter with the Taung child (*Australopithecus africanus*) fossil excavated at Taung quarry in South Africa (Derricourt, 2009). Makaganscat yielded a large fragmented faunal assemblage intermixed with hominin bones that was dominated by spiral fractures (Langdon, 2016). Dart interpreted the presence of spirally fractured limb bones as proof that the assemblage was created by hominins based on the idea that hominins were the only specie able to produce spiral fractures through the "crack and twist" technique (Brain, 1983). Dart further interpreted the fractured hominin limb bones as signs of violence and cannibalism perpetrated by the local hominins against their own kind by using animal bones as a pre-lithic industry called osteodentokeratic industry (Langdon, 2016). From there on Dart weaved a "myth" narrative that our ancestors were hyper-violent apes that aggressively hunted and engaged in violence and cannibalism to explain the horrors and brutality seen throughout human history and showcased in World War 2, thus creating the "Killer Ape Hypothesis" (Binford,

1981a; Kover, 2017). This interpretation was later challenged and overturned by Charles K. Brain, who pointed out that spiral fractures can be created by carnivores as well, falsifying Dart's osteodentokeratic hypothesis and providing evidence of carnivore involvement by matching punctures on an australopithecine to the jaws of a carnivore (Brain, 1983; Dart, 1957).

2.2 Traces and Taphonomic Site Interpretation

Middle-range theory and research integrated smoothly within taphonomy in the second half of the 20th century. This integration enabled the revision of previously faulty interpretations by questioning the degree of human involvement and offering more grounded explanations. As the taphonomic history was revised at some sites, African sites became of interest. This interest was grounded in the pursuit to understand when hominins began to modify and exploit carcasses. This led to an increase in middle-range research by paleoanthropologists to understand the taphonomic signature left by hominins, separate it from the signature of other actors and refine it, to gain a better understanding of hominin feeding behavior.

Dart (1957) first proposed fracture pattern analysis to identify hominin involvement within a site. He proposed that the crack and twist method which was part of the osteodentokeratic industry hypothesis was the only way to produce spiral fractures, making spiral fractures diagnostic of hominin involvement (Dart, 1957). These claims were later rebutted through actualistic experiments and observations of carnivore bone modification (Haynes, 1983). Brain pointed out that carnivores were the main accumulators by matching perforations on a hominin skull to the teeth of a carnivore jaw (Brain, 1983). Actualistic experiments and observations also supported the claim that carnivores have the capability to produce spiral fractures (Johnson, 1985). Furthermore, Myers et al. (1980) pointed to spiral fractures within paleontological sites in North America long before the dispersal of hominins out of Africa. All

these pieces of evidence point to spiral fractures by themselves are a poor indicator of hominin involvement (Behrensmeyer, 1987).

To produce spiral fractures, dynamic and static loading need to operate on fresh bone (Johnson, 1985). Spiral fractures form when the structural integrity of green bone fails under stress, either by carnivore jaw or percussion, causing fragmentation as a way for the bone to release the energy (Capaldo & Blumenschine, 1994). The fracture follows collagen fibers that are spirally organized on the longitudinal axis of the bone shaft, leading to spiral fractures (Johnson, 1985). Green bone produces spiral fractures when loaded by dynamic or static processes. This association between fracture type and loading highlights the importance of bone freshness. When bone dries out microfractures form along the diaphysis encouraging fractures to occur through these weakened sections creating transverse fractures (Johnson, 1985). This biomechanical property of bone can be used to infer the overall condition of bone when it was fractured (Villa & Mahieu, 1991). The nutritive phase of a bone is when it is still fresh and hominins and carnivores can extract nutrients from it (Marean et al., 2000). The non-nutritive phase of a bone is when it is not appealing to carnivores or hominins anymore (Marean et al., 2000). Spiral fractures are associated with the nutritive phase of bone, while other fracture patterns like transverse and stepped are associated with the non-nutritive phase of the bone (Johnson, 1985).

Spiral fractures by themselves are not a good indicator of hominin behavior. Dynamic loading, however, can be associated with hominins (Johnson, 1985). Dynamic loading leaves a different pattern on bone, compared to static loading, due to the differential in energy release by the bone. Hackle marks and ribs are created as the energy from the hammerstone blow travels through the bone and dissipates (Capaldo & Blumenschine, 1994; Oliver, 1989). Hackle marks

can be described as imprints of radiating energy traveling through bone and leaving traces in the process as a means of stress relief (Fisher, 1995). Ribs are stress relief traces created when energy waves travel through the diaphysis in a straight line, leaving serrations in their wake (Johnson, 1985). A better way to visualize the difference between the two traces would be to imagine a water ripple as analogues hackle marks while a wave would best describe the traces left by ribs. Static loading does not exhibit this trace pattern; thus, hackle marks and ribs can be safely associated with dynamic loading (Johnson, 1985). .

The identification and analysis of bone surface modifications (BSMs) on faunal assemblages became commonplace as taphomonical considerations were integrated into paleoanthropological research (Gifford-Gonzalez, 2018d). They have been used in conjunction with skeletal part profiles and mortality profiles as auxiliary evidence. Because a growing body of scholarship indicated that skeletal part and mortality profiles did not reliably distinguish between actors, BSMs became the preferred method of analysis (Blumenschine, 1995). These marks can be subdivided into two general categories, BSMs linked to bone fragmentation and those created by the act of defleshing a bone (Fisher, 1995).

BSMs generated by bone defleshing are created by both hominins and carnivores (Blumenschine et al., 1996). Butchery BSMs are cutmarks, scrape marks and chop marks, while tooth marks and gnaw marks are BSMs associated with carnivores (Fisher, 1995). Both actors have analogous BSMs produced through a similar action, however tooth marks and cutmarks have been the most extensively studied and described (Shipman, 1981). Tooth marks are analogous to cutmarks since both are used to remove flesh from bone (Fisher, 1995). Cutmarks however tend to be parallel to the long axis of the bone, accompanied by microstriations, deep and V-shaped in cross section and usually have a “shoulder effect” where bone material is

displaced by the tool (Olsen & Shipman, 1988). Tooth marks are usually superficial, curved, V to U shaped in profile, and sometimes can have a shoulder (Shipman, 1981). While there is an overlap between mammalian toothmarks and cutmarks, with training the two can be distinguished with some certainty (Blumenschine et al., 1996; but see Njau & Blumenschine, 2006). Actualistic studies have provided evidence that tooth marks segregated to the epiphysis and occurring in about 20% of the assemblage is indicative of hominin action (Blumenschine, 1995).

The other category of BSMs is related to bone fragmentation. BSMs like peeling, flake creation, and heavy fragmentation are associated with bone fragmentation. The BSM that could be the most diagnostic in differentiating between carnivore and hominin involvement are bone flakes. Bone flakes share a similar creation process with lithic flakes (Vettese et al., 2020). Just like lithic flakes, bone flakes can be created when the loading on the bone is dynamic like a percussive blow dealt to the diaphysis of the bone (Fisher, 1995). Additionally, bone flakes can also be created through static loading as in pressure flaking, not dissimilar to lithic pressure flakes (Johnson, 1985). Percussion flakes can exhibit a platform and a bulb (Fisher, 1995), stress marks (hackle marks and ribs) (Fisher, 1995), greater breath than length (Vettese et al., 2020) and an absence or reduction in cortical bone (Vettese et al., 2020), however as indicated by Fisher (1995) some of the bone flake characteristics can be missing. However these traces are often erased by carnivores during bone fragmentation, leading to an overlap between hominin induced fragmentation, and an equifinality (Vettese et al., 2020).

Percussion notches and percussion marks have been shown to be diagnostic in distinguishing hominin created traces form carnivore generated traces (Blumenschine & Selvaggio, 1988; Capaldo & Blumenschine, 1994). Percussion notches are “semicircular to

arcuate indentations of the fracture edge of a long bone that are produced by a dynamic or static loading on cortical surfaces…leaving a negative flake scar that extends through the entire thickness of the bone and onto the medullary surface" (Capaldo & Blumenschine, 1994, p. 730). Percussion marks are described as pits and grooves present on the cortical bone surface, accompanied by microstriations present within the pits and grooves or emanating out of them (Blumenschine & Selvaggio, 1988). Percussion pits are rounded depressions present on the cortical surface of bone along the fracture edge (Blumenschine & Selvaggio, 1988). They are created by the natural protrusions present on the hammerstone and the anvil (Blumenschine & Selvaggio, 1988). Percussion grooves are like percussion pits but more oblong and are created by the hammerstone or anvil sliding and gouging along the bone surface as opposed to imprinting into the cortical surface (Blumenschine & Selvaggio, 1988). A good illustration would be to think of pits as depressions made by a stick in the sand, while grooves are lines created by skilling the tip of a stick along the sand. In addition to percussion pits and grooves percussions marks can also encompass striation patches. A key distinction between striation patches and pits and grooves is the size and depth of the striations (Vettese et al., 2020). Striations exhibit as long, parallel and superficial bone surface modification traces, while pits and grooves are smaller and deeper (Vettese et al., 2020), although striations often accompany pits and grooves (Blumenschine, 1995). Perhaps a good analogy might be to think of pits and grooves as points and broken lines drawn into the sand, while striations are more akin to a stick being dragged along the sand. Percussions pits and percussion notches appear at a frequency of about 38% in hominin modified assemblage (Blumenschine, 1995).

Capaldo & Blumenschine (1994) work on percussion and carnivore notches showed that notch dimension ratios and release angles were able to distinguish between carnivore and

hominin modified limb bones in size 1 and 2 animals, but not in size 3. Notch dimensions were defined as notch breath, notch depth and flake scar breadth. The ratios created attempted to quantitatively describe the notch shape and the flake dimensions. Notch breadth to notch depth describe the notch shape. Carnivores create more deeper notches while percussion creates more shallower notches. Flake scar breadth to notch depth describe the dimensions of the missing flake. Thicker flakes are created by carnivores and thinner flakes are produced by percussion. This actualistic research provides the means to differentiate between carnivore and hominin modified bones with some limitations. While notches might be irrelevant past size 3 animal bones, percussion marks are still diagnostic of hominin feeding behavior due to the presence of microstriations (Blumenschine & Selvaggio, 1988; Fisher, 1995).

Other actors besides hominins and carnivores have been investigated in open air site settings. Herbivores and rodents have been known to modify bone (Gifford-Gonzalez, 2018c). Herbivores usually engage with bones due to a calcium deficiency, however their taphonomic signature is minimal at best (Gifford-Gonzalez, 2018b). Rodents like porcupine accumulate bones and use them to file down their incisors (Fisher, 1995). Porcupines prefer dry bone so their tooth marks are usually on dry or permineralized bone which is easily identified (Gifford-Gonzalez, 2018b). Trampling is another biotic modification to bone without intent, which involves stepping on and kicking bones that are present on the ground (Olsen & Shipman, 1988). Trampled bones can be broken if weathered enough, and the act of trampling can cause cutmark like trample marks by scraping the bone on sand particles (L. A. Borrero, 1990; Olsen & Shipman, 1988). These pseudo-cutmarks have random orientations, random lengths, and do not correspond to any muscle attachment sites on the bone (Olsen & Shipman, 1988). Trampled fragments also tend to be pushed perpendicularly into the ground (Blasco et al., 2008).

Actualistic studies have attributed notches on the cortical edge of bone fragments to trampling (Blasco et al., 2008).

Abiotic processes have also been investigated as actors of bone fragmentation. Weathering is the exposure of bones to the environment (Behrensmeyer, 1978). This causes bones to dry out and overtime lose integrity through exfoliation (Karr & Outram, 2015). Weathering can eventually cause bone fracture like the fracture patterns seen in dry bone (Fisher, 1995). Finally, sediment pressure has been known to fracture bone (Villa & Mahieu, 1991). Due to the predictable nature of sedimentation seen in open air sites, sediment pressure builds up slowly on the bone, allowing diagenetic processes to act on the microscopic structure of bone, replacing or leaching out calcium and weakening the overall structure of the bone (Grupe & Harbeck, 2014). By the time that the sediment pressure is enough to break the bone, the fracture pattern is consistent with dry bone (Villa & Mahieu, 1991).

Many actors contribute to the BSM observable in faunal assemblages from open air sites. Carnivore and hominin are identified most frequently as the actors responsible for much of the taphonomic processes that impact the paleoanthropological record. However other less studied actors do contribute to the formation of open air assemblages. To get a holistic view of bone accumulations all actors need to be investigated and accounted for, before the taphonomic pattern associated with hominins can be fully understood.

2.3 Traces and Cave Site Taphonomy

Caves have been of archaeological interest because of their use by hominins for shelter and storage. Caves offer protection from the elements and the vagaries of seasonal temperature change. For those reasons, caves often preserve the archaeological record better than open air sites (Gargett, 1999). However, caves also present interesting challenges to taphonomic analyses.

Caves are uniquely created by forces that hollow out a cavity in the bedrock thus giving each cave a unique environment (Gargett et al., 1989). This uniqueness extends to the types of possible actors that can interact with a bone assemblage such as cave roof fall, the rate of deposition and the overall humidity of the cave. Deposition can also be fast and unpredictable. Roof fall events quickly add a depositional layer, modifying any bones present on the cave floor, or bones that are partially buried (Gargett, 1999). Underground streams can completely erase the depositional history of the cave by eroding away the cave floor and leave a sink hole (Gargett et al., 1989). All these forces need to be taken into consideration when applying methodologies developed for open air site taphonomy to cave taphonomy.

Animals have used caves for a multitude of reasons. Carnivores made use of caves as burrows and food cache locations promoting the accumulation of bones within caves as accumulators and eventually as part of the assemblage upon their death in the cave (de Ruiter & Berger, 2000; Kurtén, 1995). Hominins have used caves for shelter and homes especially in the Middle and Late Pleistocene acting as accumulators of animal bones, and upon their death becoming part of the assemblage (J. Richter, 2006; Sala et al., 2016). However, carnivores and Pleistocene hominins are not the only groups that use caves. Herbivores have been known to use caves for shelter or as sources of water and food (Gargett et al., 1989). Chimpanzees use of caves as shelter or for food has been recorded (Boyer Ontl & Pruetz, 2020). This chimpanzee behavior hints at Pliocene hominins engaging in cave use prior to hominin dispersal out of Africa. Cave use by animals implies that at times they died in caves as well making caves productive sites of bone accumulation.

As a unique environment, caves require innovative methodologies to explore the taphonomic history of a bone assemblage. Much of the methodologies and theory created for

testing the taphonomic history of open air sites can be applied to caves. The nestled hierarchy seen in Figure 2 can still be used to link a trace to a causal agent and so on until an actor is identified (Gifford-Gonzalez, 1991). Similarly traces left by hominins and carnivores in caves are the same as the traces left on bone within an open air site. In this regard a cutmark in a savannah setting is the same as a cutmark in a cave setting (Binford, 1981b). Open air sites and caves do share some depositional and erosional forces like wind, water, and mass earth movements (Gargett, 1999; Gargett et al., 1989) Differences between the two settings arise from the unique environments seen in caves and the depositional forces unique to caves such as cave roof fall.

Table 1 Archaeological and Paleontological Cave Sites with Evidence of Cave Roof Fall

Site	Country	Site Type	Time period (kya)	Roof fall fragment size (m) or description	Weight in kg (if provided)	Reference
Contrebandiers	Morocco	Archaeological	120-90	0.05-0.5	NA	(Dibble et al., 2012)
Blombos	South Africa	Archaeological	140	Small and large blocks	NA	(Jacobs et al., 2006)
Lang Rongrien	Thailand	Archaeological	43 – 27	Up to 0.08, gravel to boulder	NA	(Anderson, 1997)
Zhoukoudian	China	Archaeological	669-224	0.01-4.9	NA	(Goldberg et al., 2001)
Roc De Marsal	France	Archaeological	50	0.01->1	NA	(Aldeias et al., 2012; Goldberg et al., 2017, 2018)
Misliya	Israel	Archaeological	270-170	Huge boulders	NA	(Mina et al., 2010)
Shield Trap	USA	Paleontological	9.2-.62	Boulders	NA	(Oliver, 1989)
Krapina	Croatia	Archaeological	130	1	NA	(Trinkaus, 1985)
Pod Hradem	Czech Republic	Archaeological	71-57	Pebbles to boulders	NA	(Nejman et al., 2018)

Porcupine River	USA	Paleontological	21-3.4	Large blocks	400-500	(Dixon, 1984)
Natural Trap	USA	Paleontological	8-7	Gravel	NA	(Martin & Gilbert, 1978)
Victoria Fossil	Australia	Paleontological	206-76	Boulder	NA	(Fraser & Wells, 2006; Reed, 2006)
Mezmaiskaya	Russia	Archaeological	65-55	Large angular fragments	NA	(Baryshnikov et al., 1996)
Timpanogos	USA	N/A	Modern	0.05-<1	NA	(Harp et al., 2011)
Bois Roche	Italy	Paleontological	130-57	Granules to decimeter size	NA	(Marra et al., 2004)
Kebara	Israel	Archaeological	60	0.01-1	NA	(Goldberg & Bar-Yosef, 2002)
Hayonim	Israel	Archaeological	220-115	0.01-1	NA	(Goldberg & Bar-Yosef, 2002)
Jerf'Ajla	Syria	Archaeological	33	0.01-0.1	NA	(Goldberg & Bar-Yosef, 2002; D. Richter et al., 2001)
Yabrud I	Syria	Archaeological	195	0.01-0.1	NA	(Bar-Yosef et al., 1992; Goldberg & Bar-Yosef, 2002)
Tabun	Israel	Archaeological	350	0.01-0.1	NA	(Goldberg & Bar-Yosef, 2002, 2019)
Qafzeh	Israel	Archaeological	114-95	0.01-0.1	NA	(Goldberg & Bar-Yosef, 2002, 2019)
Amud	Israel	Archaeological	113-53	0.01-0.1	NA	(Goldberg & Bar-Yosef, 2002; Rink et al., 2001)
Skhul	Israel	Archaeological	120-90	0.01-0.1	NA	(Goldberg & Bar-Yosef, 2002; Hershkovitz et al., 2018)

La Ferrassie	France	Archaeological	130-82	Centimeter to decimeter	NA	(Talamo et al., 2020)
Sima de los Huesos	Spain	Archaeological	1200-1	Decimeter to meter	NA	(Aranburu et al., 2017)
Die Kelders	South Africa	Archaeological	50-25	Small pieces to large blocks	NA	(Marean et al., 2000)
Shanidar	Iraq	Archaeological	70-60	Large blocks	NA	(Pomeroy et al., 2020; Trinkaus, 1983)

Rock fragment categories and associated sizes.
Granule- rock fragment with a diameter between 0.2 and 0.4 cm (Hill, 2003)
Pebble- rock fragment with a diameter between 0.4 and 6.4 cm (Hill, 2003)
Cobble- rock fragment with a diameter between 6.4 and 25.6 cm (Hill, 2003)
Boulder- rock fragment with a diameter larger than 25.6 cm (Hill, 2003)
Gravel- lose of unconsolidated deposit of pebbles, cobbles or boulders (Hill, 2003)

The average bedrock fragment size was between 7 cm and >770 cm. The minimum average rock fragment size was calculated by picking the smallest reported value, or quantifiable size description (e.g 0.4 cm for a pebble). Boulder values were set at 25.7 cm in diameter. The maximum average rock fragment size was calculated by picking the largest reported value, or quantifiable size description. Boulders were not included in the average because they do not have a maximum value. To compensate for tis a greater than sign was placed in front of the maximum average value to indicate that the actual maximum size of a rock fragment is larger than reported here.

In the past much of the research done on bone fragmentation actors have been relegated to hominins and carnivores, since both are intentional actors seeking the nutritive qualities of fresh bone (Johnson, 1985). While this focus has provided criteria to distinguish the two, other actors of bone fragmentation have not been as extensively researched. Roof fall is one of these actors, with a paucity of research done on roof fall even though its presence is seen at many cave sites (L. Borrero et al., 2007; Goldberg et al., 2018; Solecki, 1957). Roof fall is the weathering of bedrock until a piece decouples from the bedrock and is pulled by gravity towards the cave floor (Gargett, 1999). The weathering of the bedrock can be due to water, or due to temperature fluctuations (Mann & Monge, 2006). The size of the chunk of rock depends largely on the bedrock composition and on the intensity of weathering but can range from pebbles to pieces the size of cars or larger (Gargett et al., 1989). Large roof fall events are maintained in the stratigraphic record of the cave as slabs and serve as clear indicators of a roof fall event. These

can be seen in cave sites like Pech IV (France, 99-45 kya), Shanidar (Iraq, 70-60 kya), Misliya (Israel, 260-170 kya) (Goldberg et al., 2018; Mina et al., 2010; Trinkaus, 1983). However smaller pieces of bedrock can detach, interact with bone assemblages, and disappear from the record through fragmentation, weathering, or displacement as seen in Table 1 (Mann & Monge, 2006; Oliver, 1989). The interaction between smaller pieces of bedrock and bone assemblages could create spiral fractures and masquerade as a hominin created spiral fracture (Dixon, 1984; Griggo et al., 2019; Oliver, 1989).

Spiral fractures paired with stress relief traces (hackle marks and ribs) are informative of the moisture content of bone (Johnson, 1985). These traces are associated with the fracture of fresh green bone due to its ductile properties (Karr & Outram, 2012b). Fragmentation of dried bone produces transverse and stepped fractures due to the loss of ductile properties associated with green bone (Johnson, 1985). In open air sites bones are exposed to the full brunt of the elements, which cause bones to lose moisture, drying out the bone in the process at an accelerated rate (Behrensmeyer, 1978). Caves can mitigate moisture loss due to their enclosed nature extending the green state of bone past what has been recorded in an open air site (Gargett, 1999). Since cave environments promote the retention of moisture within bone, extending its green qualities it is possible for roof fall to interact with bone and create spiral fractures similar to those created by hominins causing an equifinality (Dixon, 1984; Gifford-Gonzalez, 1991; Johnson, 1985; Oliver, 1989).

Table 2 Traces of Dynamic Loading on Bones Modified By Hominins at Open Air Sites and Roof Fall at Cave Sites

Dynamic Loading at Hominin Open Air Sites	Dynamic Loading at Cave Sites with Roof Fall
Percussion notches (Blumenschine, 1988)	Percussion Notches (Oliver, 1989)
Percussion marks (Blumenschine, 1995)	Percussion marks (Oliver, 1989)
Bone flakes (Blumenschine, 1988)	Bone flakes (Oliver, 1989)
Stress relief traces (hackle marks and ribs) (Johnson, 1985)	Stress relief traces (hackle marks and ribs) (Oliver, 1989)

Research into roof fall as an actor is minimal when compared to the research in hominin or carnivore bone modification patterns, however the research done has provided some definition to roof fall. Oliver (1989) points out that roof fall does operate through dynamic loading by investigating the assemblage created within the Shield Trap cave (USA, between 9.2 to .62 kya). The Shield Trap cave assemblage was created independent of hominin intervention, and credits roof fall with the fragmentation observed (Oliver, 1989). Traces linked to dynamic impact are seen in the assemblage manifesting as stress relief traces (hackle marks and ribs) (Johnson, 1985; Oliver, 1989). Additionally, percussion notches and percussion marks are identified, providing evidence that roof fall can mimic hominin percussion as seen in Table 2 (Griggo et al., 2019; Oliver, 1989). Mann and Monge (2006) present evidence of a sliver of roof fall interacted with the skull of a Neanderthal in Krapina. After they rule out all interpersonal conflict and other types of traumas on the morphology of the trauma seen on the parietal bone, they concluded that roof fall is the likely culprit (Mann & Monge, 2006). Mann and Monge (2006) provide further evidence that a small sliver of roof fall can detach for the bedrock, alter bone, and then disappear from the record. Dixon (1984) presents evidence that carnivores and roof fall can interact on the same assemblage. He points out that at Porcupine River Caves (USA, between 21 to 3.4 kya) roof fall is evident in blocks preserved on the cave floor and as pseudo-cultural traces left on bone, hinting at interactions between bone and bedrock particles, followed by carnivore ravaging

(Dixon, 1984). This interaction could mimic human and carnivore modification of bones, where roof fall fractures the diaphysis exposing bone marrow, followed by carnivores extracting the bone marrow and deleting the epiphysis, leaving behind a pattern observed by Blumenschine (1995) in the hammerstone to carnivore assemblage. This scenario is further supported by actualistic research done by Karr and Outram (2012). After subjecting bones to multiple episodes of simulated roof fall events they found that roof fall has an inverse relationship to density mediated attrition seen within carnivore assemblages (Karr & Outram, 2012a). Due to the spongy nature of epiphysial ends allows the articular ends to remain intact following contact with roof fall events, whereas the diaphysis gets deleted due to its rigid nature (Karr & Outram, 2012a). All these examples show that roof fall has the potential to modify bones in a similar manner to hominin percussion and disappear from the record, thus producing a pseudo-archaeological site, which can be interpreted as human modified with or without the input of carnivore actors.

The lack of data and research on roof fall is the focus of this thesis. One goal of the experiment that is at the core of this thesis is to create a roof fall reference collection through an actualistic experiment. Even though the roof fall reference collection is small (n=16), it is a first step towards understanding the taphonomic pattern of roof fall. The other goal is to compare the pattern left by roof fall to the pattern generated by hammerstone-on-anvil percussion. This is crucial because as Oliver (1989) indicates that both actors leave similar traces, operate through the same causal agent and effector which leads to a possible equifinality (Gifford-Gonzalez, 1991). The roof fall reference collection will be used to attempt to solve this equifinality with the goal being to provide the necessary criteria to recognize roof fall as an actor and separate it from hominin generated assemblages.

CHAPTER III: MATERIALS AND METHODS

3.1 Materials

For a comprehensive list of materials, see Table 18 in the Appendix.

3.2 Methodology

Setup for cave roof fall actualistic study

Sixteen (n=16) bison bones were broken during the cave roof fall actualistic study. The age of the slaughtered bison is approximated to older than four and a half years but younger than five and a half years. This estimate was based on the complete fusion of the distal tibial epiphysis and the lack of fusion of the proximal tibial epiphysis (Koch, 1935). The sex of the slaughtered bison was unknown. Both left and right tibiae were used without any preference. According to Meagher (1986), the age bracket of four and a half and five and a half would categorize all animals as mature regardless of sex. Mature bison weigh between 318 kg to 907 kg (Meagher, 1986), placing the slaughtered bison in a size 4 category (Blumenschine, 1986; Diez et al., 1999). The tibiae assigned to the cave roof fall actualistic study were received frozen due to weather delays caused by a blizzard and other snowy conditions. The bones were thawed when they were broken.

Bone condition (e.g., frozen, refrigerated, or thawed) was considered because of its effect on bone freshness and fracture mechanics (Grunwald. 2016, Outram and Karr, 2015). Outram and Karr (2015) remark that refrigerated bones maintain their freshness longer than thawed bones. To maintain refrigeration temperature ice and salt were used respectively to keep the tibiae cool during warm temperatures and prevent the tibiae from freezing during colder temperatures. Freezing was discouraged to prevent the freeze thaw cycle from further alerting the microstructure of the diaphysis (Grunwald, 2016).

Bone freshness was a condition that was controlled for. Fracture patterns produced by dry bone can be distinguished from fracture patterns on fresh bone (Johnson, 1985). This means that a cave roof fall event on dry bone can be distinguished from fresh bones percussed by hominins through the resulting fracture patterns (Karr & Outram, 2012b). However, if a cave roof fall occurs on a living animal or fresh bones, the fracture patterns produced by this event would be comparable to hammerstone-on-anvil percussion. This is because both actors are believed to leave the same traces, utilize the same causal agent and use the same effectors (Gifford-Gonzalez, 1991; Oliver, 1989). To investigate this the bones were broken fresh and thawed to mimic bone condition that would be desirable to a hominin.

Table 3: Measurements of boulders used in the cave roof fall simulation

Assigned number	Type	Weight (kg)	Length (cm)	Width (cm)	Diameter (cm)
1	Sandstone	6.8	22.9	12.7	26.2
2	Sandstone	13.6	33	15.2	36.3
3	Sandstone	6.8	22.9	20.3	30.6
4	Sandstone	13.6	33	22.9	40.2

Rock fragment categories and associated sizes.
Granule- rock fragment with a diameter between .2 and .4 cm (Hill, 2003)
Pebble- rock fragment with a diameter between .4 and 6.4 cm (Hill, 2003)
Cobble- rock fragment with a diameter between 6.4 and 25.6 cm (Hill, 2003)
Boulder- rock fragment with a diameter larger than 25.6 cm (Hill, 2003)
Gravel- lose of unconsolidated deposit of pebbles, cobbles or boulders (Hill, 2003)

Figure 3 Boulder number 1 (6.8 kg)

Figure 4 Boulder number 2 (13.6 kg)

Figure 5 Boulder number 3 (6.8 kg)

Four sandstone boulders were procured for the cave roof fall actualistic study. The boulders weights and dimensions were settled upon after conducting a survey of the literature as seen in Table 1. The average range of cave roof fall fragments falls between 7 and >770 cm. Boulder sized bedrock particles have been described at most cave sites with reported cave roof fall. The selected rocks fall within this average and have a diameter that can be described as boulder as seen in Table 3. A more conservative diameter (e.g., closer to 25.7 cm) was picked to test if a more conservative sized rock can damage bones. The only reported weight of roof fall blocks was between 400 and 500 kg as seen in Table 1, which would have not been feasible for this experiment (Dixon, 1984). A more feasible weight of 6.8 kg and 13.6 kg boulders was settled upon. These weights were selected because this experiment relies on an individual powered pulley system to hoist up a boulder up using a pulley system. The weights suggested by the literature are not attainable without machinery. Two boulders of each weight were procured as a contingency if one of the boulders broke or became damaged beyond use. The dimensions of the impact face and weight of all four boulders are summarized in Table 3. The boulders that were used in the experiments can be seen in Figure 1-3.

Table 4: Pleistocene Archaeological Rock Shelter Sites with Cave Heights

Cave	Country	Time Period (kya)	Height (m)	Source
Pod Hradem	Czech Republic	57-29	1.5-7	(Lisiecki & Raymo, 2005; Nejman et al., 2018)
Kobeh	Iran	250-35	more than 3.2	(Marean & Kim, 1998)
Bisitun	Iran	243-57	4	(Lisiecki & Raymo, 2005; Trinkaus & Biglari, 2006)
Jarama VI	Spain	~50	4	(Kehl et al., 2013)
Veternica	Croatia	96-82	4	(Karavanić et al., 2017; Lisiecki & Raymo, 2005)
Zhoukoudian Upper Cave	China	38.3-33.5	4-8	(Li et al., 2018; Norton & Gao, 2008)
Spy	Belgium	36	More than 4.5	(Fernández-Jalvo & Andrews, 2019; Toussaint & Pirson, 2006))
Cro-Magnon	France	30	5	(Henry-Gambier et al., 2013)
Scladina	Belgium	80	6	(Pirson et al., 2018)
Moula-Guercy	France	191-71	8	(Lisiecki & Raymo, 2005; Valensi et al., 2012)
Velika Pecina	Croatia	191- 14	8	(Karavanić & Smith, 1998; Lisiecki & Raymo, 2005)
Vindija	Croatia	114-28	10	(Wolpoff et al., 1981)
La Naulette	Belgium	Pleistocene	11	(Toussaint & Pirson, 2006)
Krapina	Croatia	130	12	(Trinkaus, 1985)
Shanidar	Iraq	70-60	13.7	(Reynolds et al., 2018; Solecki, 1957)
Gran Dolina	Spain	730-244	18	(Blasco et al., 2010)

The average of all cave heights is between 7.3 m and >12.3 m. The minimum was calculating by averaging the minimal cave heights provided, while the maximum was calculated by averaging the maximum cave height provided. Cave heights that did not have a reported maximum (e.g Marean & Kim, 1998) were not included in the maximum average. To compensate for this a greater than sign was used to indicate that the actual maximum cave height might be larger than the one calculated.

The heights, from which the sandstone boulders were dropped, were selected by surveying the literature for Pleistocene cave sites in Europe, the Levant region and Asia (see

Table 4) and then simplifying them to make it feasible to conduct the experiment. Some measurements are from the entrance or mouth of the cave, while others are from the internal chamber of the cave. This was also done because some of the literature only provided cave heights at the mouth of the cave or did not specify if the measurements were from the mouth or the internal chamber. Where the cave height measurements are from is not important, because a cave roof fall event can happen anywhere in the cave, from the entrance to the inner chamber. This is because bones can be transported to the cave's mouth or to the inner chamber of the cave by carnivore, hominin, or abiotic actors (Gifford-Gonzalez, 1991; R. L. Lyman, 1994; Marra et al., 2004; Oliver, 1989). This means that a falling bedrock fragment has just as much of a chance to impact a bone at the mouth of a cave as it does in the inner chamber. The heights presented in Table 4 range from 1.5 m to 18 m with an average cave height between 7.3 m and >12.3 m. While heights from 1.5 m to about 3 m can be achieved using a ladder, heights above 3 m becomes progressively harder to accomplish without heavy machinery or an accessible structure, such as a tree or a building. Due to the novelty of this experiment and the lack of drop height standardization, drop height increments needed to be generated. The drop height maximum of 7.6 m was selected because it was an achievable height by using tree branches. Additionally, the drop height of 7.6 m surpasses, or is close to most cave heights listed in Table 4 and is within the average range. This allows the maximum drop height of 7.6 m to become an analog for the height of an average cave. The drop height of 4.6 m was selected because it is within a 3 m increment of the maximum drop height of 7.6 m. This heigh is representative of the lower range cave height. A height of 4.6 m was also picked to investigate if a more conservative cave height could modify bones. The larger drop height is representative of an average cave, while the smaller drop height could be representative of smaller caves.

The necessary boulder drop heights were identified using rope and markers. For the drop heights of 4.6 m and 7.6 m, a tree branch pulley system was employed to reach the desired drop heights. The boulder drop heights were verified by marking a rope at 9.2 m and 15.2 m, looping the rope around a promising branch, and then aligning the beginning of the rope or zero, with either 9.2 m, for 4.6 m or 15.2 m for 7.6 m on the ground. If the two markers aligned, then the branch was selected.

Figure 6 Tibia positioned on tarp underneath the boulder

A tarp was placed on the grass underneath the hoisted block of sandstone. In preparation for the drop, a tibia was placed on top of the tarp as seen in Figure 6. The purpose of the tarp was to enable the easy identification and recovery of bone fragments and prevent any bone fragments from getting lost in the grass.

Cave roof fall actualistic study

The 16 tibiae used in the cave roof fall actualistic study were equally divided into four experiments. Each experiment was assigned a height value of either 4.6 m or 7.6 m. This would be the height from which the boulder would be dropped on a tibia. These heights, 4.6 m and 7.6 m are an artificial stand-in for cave height. Each experiment was also assigned a boulder that

weighed either 6.8 kg or 13.6 kg. This would be a stand-in for a bed rock fragment coming loose from the cave wall. The purpose of multiple drop heights and boulder weights was to investigate if drop height and boulder weight have any influence on bone modification. Each boulder would simulate a bedrock fragment coming loose from the cave roof and impacting a bone located on the cave floor.

Figure 7 Rock fastened with string

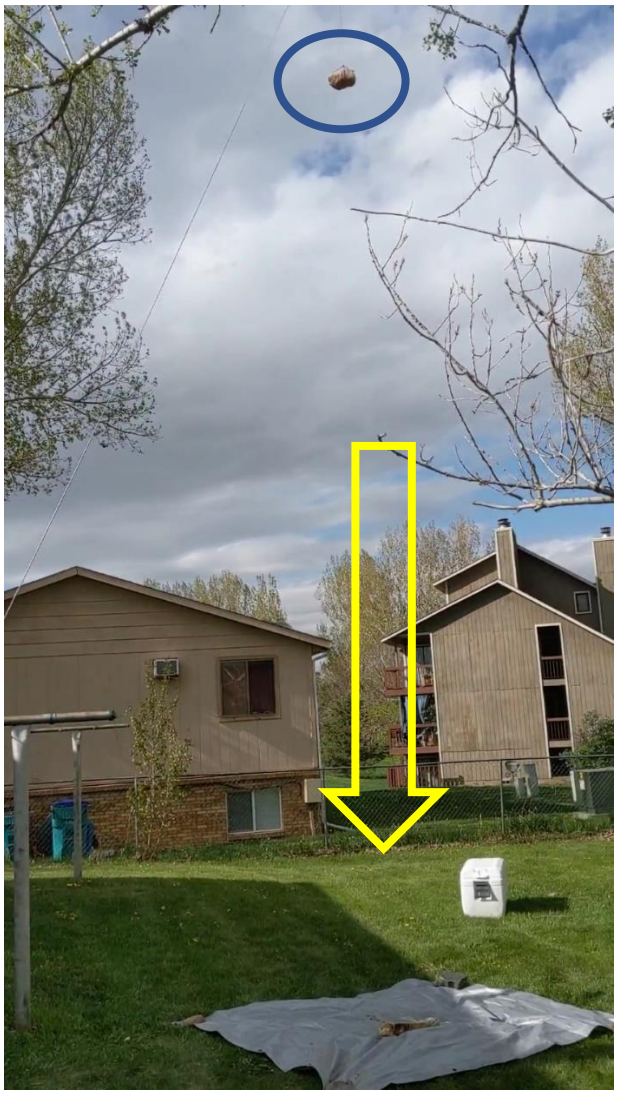

Figure 8 Cave roof fall simulation

To simulate a cave roof fall event the following protocol was developed. A tarp was placed on grass to prevent any bone fragments from getting lost (Figure 6). The tibiae were placed on the tarp one at a time with the medial side facing upwards. There was one exception which is discussed below. At this point the tibiae were thawed and did not freeze again. The boulder was secured with rope, positioned above the middle of the diaphysis of each tibia and then lifted to the desired drop height by pulley action as seen in Figure 7. Care was taken to not allow the rock to contact the tibia before the drop to prevent the creation of any bone surface modifications on the bone. Because the desired drop height was the height of a branch, the

boulder was at the appropriate drop height when it was adjacent to tree branch. After a countdown the boulder was released to fall on the bone. If the boulder contacted the bone, the tibia was inspected for breakage. If the diaphysis of the bone was split open, this was considered breakage. If the diaphysis was not clearly broken, the bone was twisted. This action was done because the periosteum was not removed from the bone, which can hold a bone together even if the diaphysis is broken (Pickering & Egeland, 2006). The bone twisting was done by grabbing the epiphysis and applying torsional force to the bone. If the tibia was easily twisted apart, the bone was considered broken. Once the bone was considered broken it was placed in a plastic bag. A number from one to sixteen, starting with the first bone, was assigned to each bag. If the tibia did not look broken, or was not easily twisted apart, the bone was placed back on the ground. The boulder was then reset for another drop. Each drop represents a cave roof fall event and was considered one trial. This reset was done to account for the possibility that a previously impacted bone could be subjected to another cave roof fall event. This design does not account for bones that are not broken by a roof fall event prior to their burial, however as presented by Oliver (1989) and Dixon (1984) roof fall events do fracture impacted bones. This could be a blind spot for this experiment, however breakage was part of the experimental design, to create a cave roof fall assemblage as close to a hominin created assemblage as possible. A drop was considered a trial regardless of whether the boulder contacted the bone. If the bone failed to break after the tenth trial the experiment ended. The ten trials cut off point was arbitrary but grounded in reason. The number of necessary roof fall events to cover and protect a bone from further roof fall damage is unknown. This is because variables like the diameter of the bedrock fragment, the friability of the parent material, the contact angle of impact among other factors are either unknown or unpredictable. With that amount of unpredictability, it was assumed that ten

cave roof fall events would be enough to cover and shield the bone from further roof fall damage.

Table 5 Cave Roof Fall Simulation Summary with Defined Drop Height and Boulder Weight For Each Experiemnt

Bone Number	Bone Side	Experiment Number	Drop Height (m)	Boulder number	Boulder Weight (kg)	Bone ID
1	Left	1	7.6	2	13.6	ASH-T-001
2	Right	1	7.6	2	13.6	ASH-T-002
3	Right	1	7.6	2	13.6	ASH-T-003
4	Left	1	7.6	2	13.6	ASH-T-004
5	Left	2	7.6	1*/3	6.8	ASH-T-005
6	Right	2	7.6	3	6.8	ASH-T-006
7	Left	2	7.6	3	6.8	ASH-T-007
8	Right	2	7.6	3	6.8	ASH-T-008
9	Right	3	4.6	3	6.8	ASH-T-009
10	Left	3	4.6	3	6.8	ASH-T-010
11	Right	3	4.6	3	6.8	ASH-T-011
12	Right	3	4.6	3	6.8	ASH-T-012
13	Right	4	4.6	2	13.6	ASH-T-013
14	Left	4	4.6	2	13.6	ASH-T-014
15	Left	4	4.6	2	13.6	ASH-T-015
16	Right	4	4.6	2	13.6	ASH-T-016

*Rock(riprap) #1 only used for one drop because it broke upon impact. Rock #3 used for remainder of experiment
Lateral side of bone number 5 used due to the presence of cut marks from butchering on the medial side

The cave roof fall actualistic experiment was broken down into four experiments. Each experiment paired a drop height with a boulder weight to simulate a cave roof fall event as seen in Table 5. Four tibiae were assigned to each experiment. Each tibia was subjected to the cave roof fall simulation individually as described above. The tibia placed on the tarp with the medial side facing up. The only exception was bone 5 which was placed with the lateral side facing up due to butcher marks present on the medial side. This was done to prevent the butcher marks from confounding the expression of bone surface modifications that were collected later.

After all experiments were carried out a pattern became apparent. All four experiments produced bone fragmentation. Once all the experiments were completed the bagged bones were stored in a cooler without ice to await processing. Ice was not used to chill the bones because the condition of the bones was no longer of importance, though care was taken to make sure that the temperature of the bones did not get too extreme. Bone condition became irrelevant because fracture patterns and BSMs which are dependent on bone condition, are present and imprinted on the bone and cannot be erased if the bone loses moisture or becomes frozen.

Figure 9 Bone in canning pot

Bone Processing

The next step was fully defleshing and degreasing the bone fragments through simmering. All fragments from a bag were placed together in one of two large enamel canning pots as seen in Figure 9. Care was taken to boil the contents of one bag in one pot at a time. Water was added until the fragments were submerged, with an additional 2.5 cm of water added on top. One cup or 0.25L of 20 Mule Team borax and 0.25L of odorless and clear Ecos Plus Liquid Laundry Detergent with enzymes was added to each pot. Ecos Plus Liquid Laundry Detergent was selected because this plant-based detergent with enzymes does not damage the bone during simmering. Additionally, the enzymes help breakdown grease more efficiently. Borax was used to boost the cleaning and degreasing power of the plant-based detergent. Like the detergent borax does not damage the bones. The water was heated on high with the canning pot covered until boiling and then left to simmer for approximately eight hours on medium heat with the canning pot partly covered. The number that was assigned to each bone bag was written on a piece of paper, which stayed with the pot throughout the process. Simmering the bones guaranteed that any remaining flesh was removed, and fat in the bone, including the bone marrow was extracted. After the bone fragments were boiled for a minimum of eight hours, large bone fragments were removed, rinsed and the pots were emptied in a sink with a 1 cm mesh over the drain. Any fragment that was caught in the mesh was collected, cleaned, and placed with their respective bone number. The number written down at the beginning of the simmering process accompanied the bone fragments throughout the cleaning process. The tibial fragments were left to dry indoors overnight. The following day the bone fragments were placed in a paper bag, with their respective number stabled to the bag, and left to dry outside in a plastic bin for two days. The plastic bin had small holes drilled into it that allowed airflow and dissipated any

humidity. The holes were small enough to prevent any animals from attacking or modifying the bone fragments. After the bones were left to dry outside for two days the bags were brought indoors and left to dry further for an additional two days.

Once all the tibial fragments were boiled and left to dry outside in a perforated plastic bin for two days and indoors for at least two days, the bone fragments were given a 12% hydrogen peroxide bath. This step ensured that the bones were sterilized and ensured against any future mold assaults. This step was taken so the bones could be safely stored within the 3D imaging and analysis laboratory at Colorado State University. After the bones were soaked in the 12% hydrogen peroxide solution, they were left to fully dry indoors for at least two days. Once the bones fully dried, they were accessioned.

During the experiment the bones were numbered from one to sixteen. After the bones were fully processed, they were given an accession number (Bone ID). The accession number started with "ASH-T-" followed by one to sixteen as seen in Table 5, which corresponded to the number that was initially given to each bone during the simulation. The same accession number was placed on large bone fragments, and any fragments that could accommodate an accession number without covering any vital marks. Smaller bone fragments were placed together in a small plastic bag with the appropriate accession number written on it. To ensure that the accession number will not be removed by other means, a coat of clear nail polish was applied to each fragment, in a discreet place, after which the proper accession number was written on the nail polish strip using a fine point sharpie. A second layer was applied on top of the accession number to seal it. Once all the bone fragments were accessioned, they were transferred to a plastic bag, with the proper accession number written on it.

Percussion Sample

Sixteen bison tibiae (n=16) broken by hammerstone, and anvil percussion were randomly selected from a collection of percussed tibiae and femurs currently residing at the 3D imaging and analysis laboratory at Colorado State University. This set of bones fragments are representative of the hominin percussion sample. Only tibiae were selected from the collection in order to eliminate bone density as a possible confounding variable in bone surface modification expression (Lam et al., 1998). A sample size of sixteen percussed tibiae was picked to match the number of tibiae broken by cave roof fall and to reduce any confounding variables that could promote the over-expression of bone surface modifications in the percussion sample. The bones were broken by students as part of a previous experiment. The hammerstone and anvil used in these experiments was a metamorphic rock. The hammerstone could be described as cobble size. These bones were processed in the same manner as the cave roof fall bones. The tibiae are catalogued under Robert Kaplan with accession numbers beginning in RSK. The similarity in processing manner is crucial because it means that there is the same quality of bone surface to observe bone surface modifications.

3.3 Data Collection from Fractured Bones

Variables were collected from all bone fragments generated by the cave roof fall actualistic experiment and on the sample selected from the percussed bone collection. As seen in Table 6 collected variables were broken down into three major categories: visual, measured, and composite.

Table 6: Variables Collected from Fractured Bison Bones

			Variables Collected
Collection Method	Visual	No Magnification	Fragment count Flake count Incipient notches Notches Fragments with cortical surface Fragment with a notch Fragments with a pit and/or groove Pseudo-notches
		Magnification 3x and 10 x	Pits Grooves Striations
		Presence/Absence	Ribs Hackle marks
	Measurements	Linear Measurements (cm)	Fragment size (in 1 cm categories)[1] Epiphyseal element length[1] Notch breadth[2] Notch depth[2] Flake scar breadth[2]
		Goniometer (°)	Release Angle
	Composite		Percentage of cortical fragments with pits and/or grooves Percentage of cortical fragments with notches Pseudo-notch to notch Notch breadth to notch depth Flake scar breadth to notch breadth

[1]Fragments were measured longitudinally. Epiphyseal elements were measured longitudinally from the metaphysis to farthest fracture edge.
[2]Measurements obtained using reusable molding material. Used only for ratios.

Visual variables are further broken down into variables that required no magnification, variables that required magnification and present/absent features as seen in Table 6. Variables that required no magnification to collect such a fragment count, flake count, and fragments with a cortical surface were collected without any visual aid. Magnification of 3x (magnifying glass) and 10x (hand lens) were used to collect variables that required magnification to identify, which were pits, grooves, and striations. The last subcategory of visual variables was presence/absence

variables, which marked the presence or absence of stress relief traces (hackle marks and ribs) in both assemblages.

Measured variables were gathered using the aid of a digital caliper, tape measure or goniometer as seen in Table 6. A digital caliper was used for linear measurements of fragment length, epiphysial element length, notch breadth and depth, and flake scar breadth, however if the length of the fragment exceeded the caliper a tape measure was employed. A goniometer was used to measure the notch release angle.

Composite variables consist of ratios build from count or measured variables. Ratios as seen in Table 6 were used to investigate the relationships between two variables. This was done to "flatten" two variables into one and expose if the relationship between them is significant.

The experimental categories created during the cave roof fall actualistic study were maintained throughout data collection. Collected data within one experiment was not combined with other experiments. This precaution was taken to preserve any variations generated by a difference in boulder drop height or boulder size.

Cave Roof Fall and Hammerstone-on-Anvil Variable Labeling

A different way of labeling each of the assemblages was use to easily and clearly identify between bone surface modifications recorded in the cave roof fall assemblage from those in the hammerstone-on-anvil assemblage. Variables recorded from the cave roof fall experiment have the descriptor of "impact" attached to them (e.g., impact grooves, impact pits, impact notches). Variables gathered from the hammerstone-on-anvil percussion sample were given the descriptor of "percussion" (e.g., percussion grooves, percussion pits and percussion notches). This labeling convention is purely semantic to clearly identify traces created by one actor from the other. Identification wise the same criteria was used to for each collected BSM variable with

Blumenschine & Selvaggio (1988) used for percussion marks, White (1992) and Pickering & Egeland (2006) were employed to identify pits and striations, Capaldo & Blumenschine (1994) was applied to define notches, incipient notches, and pseudo notches, Vettese et al. (2020) was utilized for grooves, and bone flakes were identified using Fisher (1995) and Vettese et al. (2020).

3.3.1 Visual-No Magnification

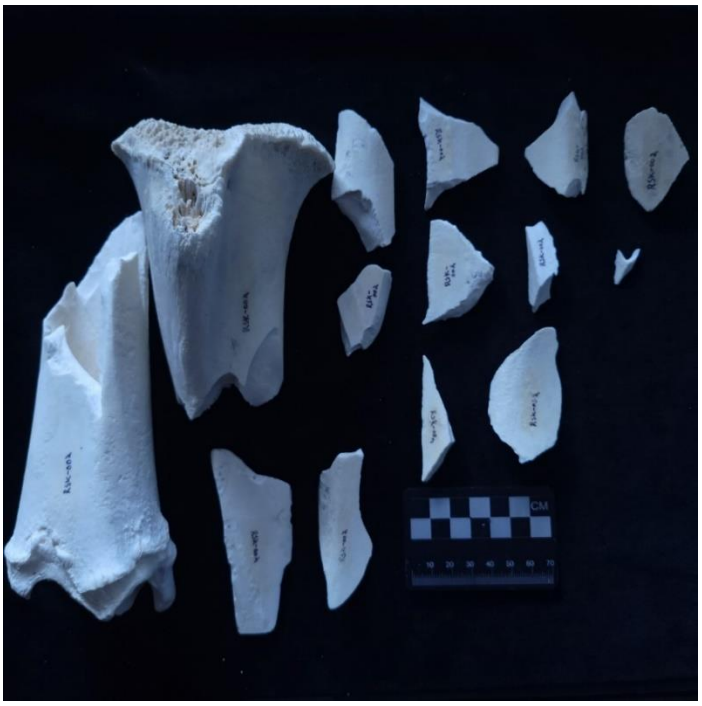

Figure 10 Hammerstone-on-anvil fragments

Figure 11 Cave roof fall created fragments

Fragment Count

A bone fragmentation count was carried out on both samples. Each bag was emptied out on a foam surface along with any other smaller bags that were inside the larger bag. All fragments including the epiphyseal elements were counted. Cave roof fall experiments were counted separately from each other. Figure 10 shows an example of a fragmented assemblage created actualistically by hammerstone-on-anvil percussion. Figure 11 shows an example of a fragmented assemblage from the actualistic cave roof fall experiment.

Bone Flakes

Bone flakes can exhibit a platform and a bulb (Fisher, 1995), stress relief marks (Fisher, 1995), greater breath than length (Vettese et al., 2020) and an absence or reduction in cortical bone (Vettese et al., 2020), however as indicated by Fisher (1995) some of the bone flake characteristics can be missing. Both assemblages were surveyed for bone flakes using an incandescent lightbulb. Figure 12 shows typical bone flakes produced by cave roof fall, while

Figure 13 shows bone flakes produced by hammerstone-on-anvil percsion. Each bag was emptied on a foam piece. Any small bags inside of the larger bags were emptied out as well. The criteria used to identify bone flakes from each assemblage was described above and modelled after Fisher (1995) and Vettese et al. (2020). All identified bone flakes that were counted.

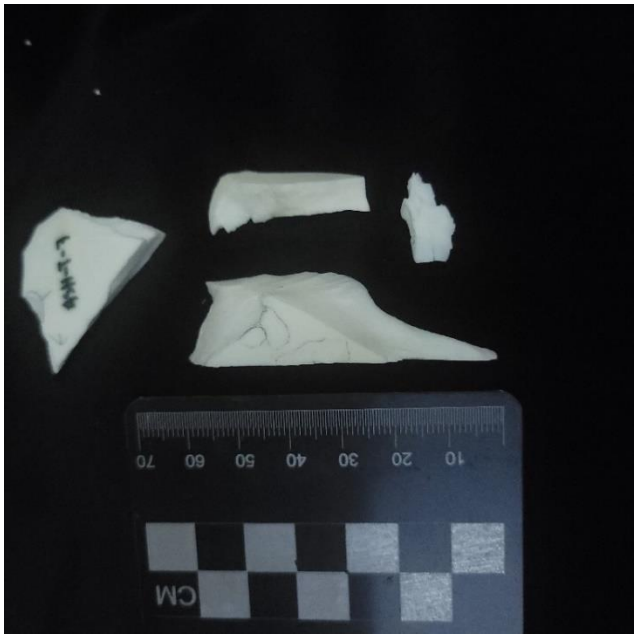

Figure 12 Bone flakes created by cave roof fall

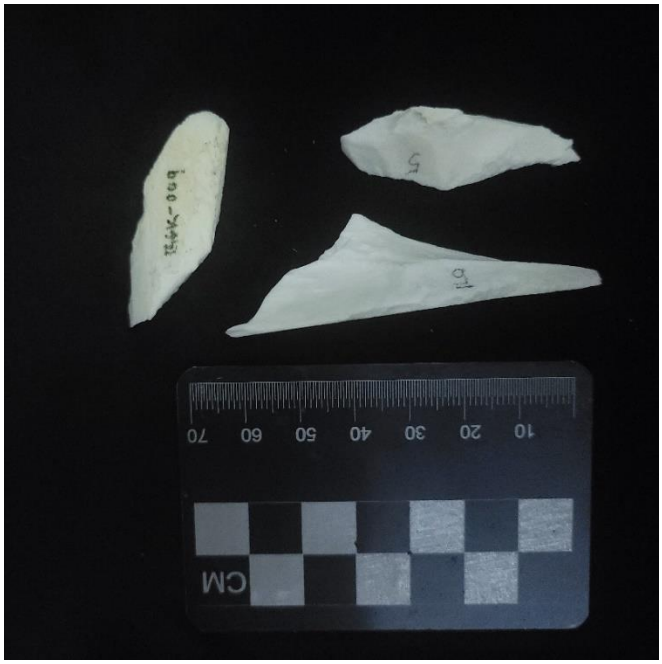

Figure 13 Bone flakes created by hammerstone-on anvil percussion

Incipient notches, Notches, and Pseudo-Notches

Table 7: Notch Variations and Pseudo Notches Definitions

Class	Notch Type	Description	Measurements possible	Source
Notch	Complete	Notch has two inflection points present and no overlapping flake scar	All	(Capaldo & Blumenschine, 1994)
Notch	Incomplete Type A	Notch is missing one or both inflection points	Notch Depth (Usually) Platform Angle	
Notch	Incomplete Type B	Notch is missing the flake scar	Notch Breadth (Occasionally)	
Notch	Incomplete Type C	Notch has an overlapping flake scar with another notch	Notch Breadth Notch Depth Platform Angle (Usually)	
Notch	Incipient/ Adherent notch	Notch still has an attached flake or multiple flakes	Notch Breadth Notch Depth	(Capaldo & Blumenschine, 1994; Vettese et al., 2020)
Notch	Biface	Flake scar is present on both cortical and medullary surface	Notch Breadth (Usually) Flake Scar Breadth	(Capaldo & Blumenschine, 1994)
Pseudo notch	Inverse Flake Scar	Flake scar is present on cortical surface only	N/A	
Pseudo notch	Incomplete Type D	Notch is limited to the cortical surface of the bone		
Pseudo notch	Micro	Miniature notches present on the cortical surface. Can be clustered together.		(Capaldo & Blumenschine, 1994; Vettese et al., 2020)

Definitions adapted from Capaldo & Blumenschine (1994) and augmented with definitions from Vettese et al. (2020)

Figure 14 Incipient notch created by cave roof fall

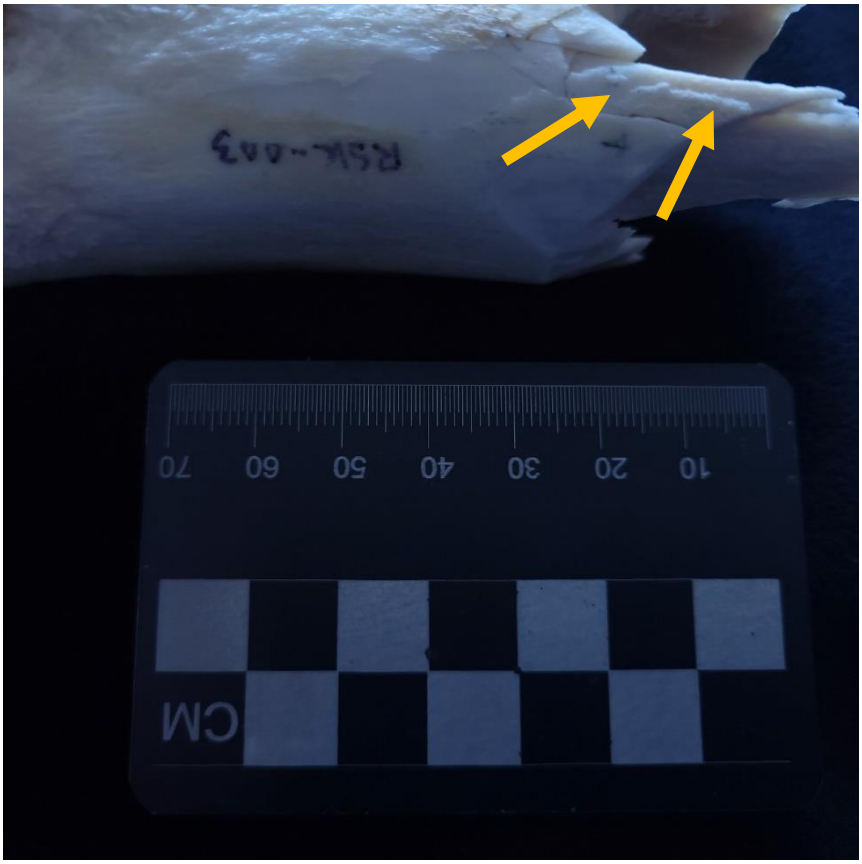

Figure 15 Incipient notch created by hammerstone-on-anvil percussion

Incipient flakes and notches can be described as having a similar arcuate shape as normal notches, but with an incomplete or superficial fracture front and a flake that is still attached to the bone shaft (Vettese et al., 2020). Figure 14 shows an example of an incipient notch in a cave roof fall assemblage, while Figure 15 shows an example of an incipient notch in the hammerstone-on-anvil assemblage. All bone fragments from both assemblages were surveyed for incipient notches underneath an incandescent lightbulb. Individual bags were emptied on foam mats. Smaller fragment bags that were inside a larger bag were emptied as well. When an incipient notch was found it was marked with an arrow pointing away from the incipient notch. These BSM were then numbered with a "N1" for the first one, "N2" for the next one and so on. This numbering convention was reset for each bone surveyed.

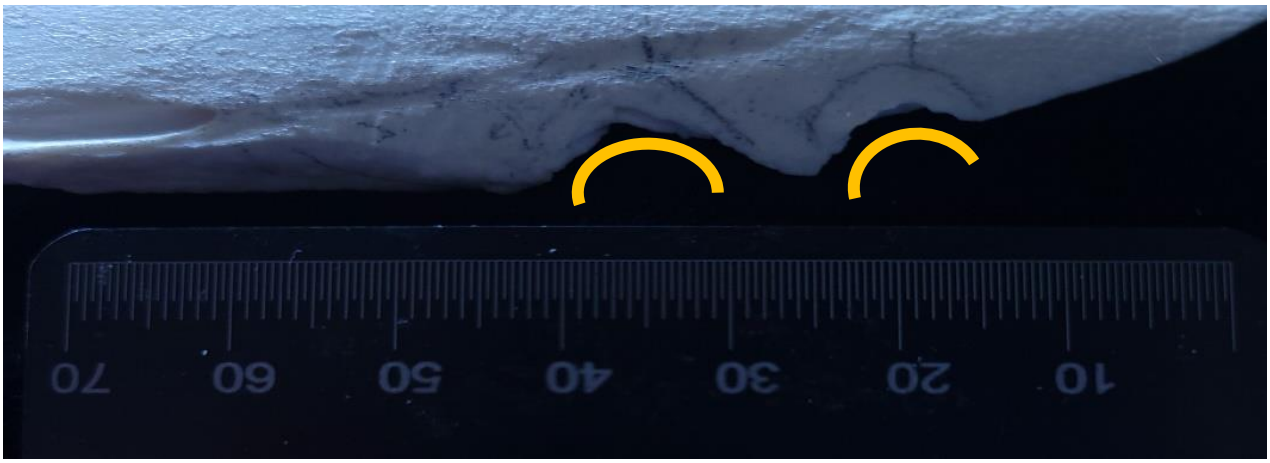

Figure 16 Percussion notch on the cortical side of the fragment

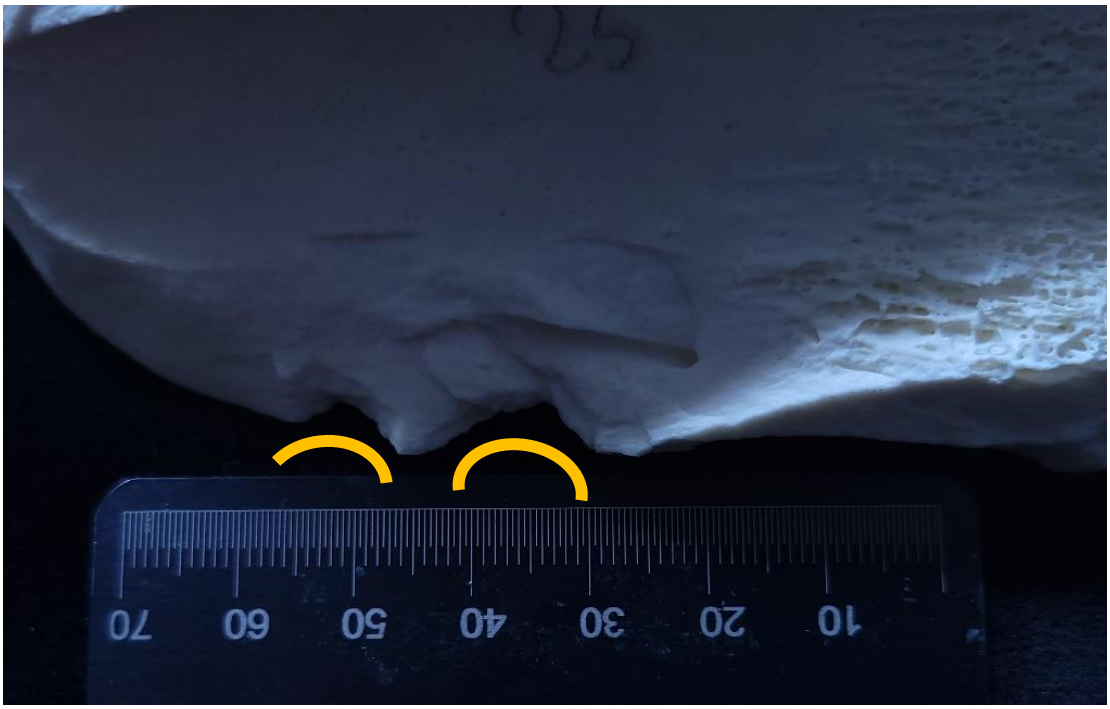

Figure 17 Percussion notch on the medullary side of the fragment

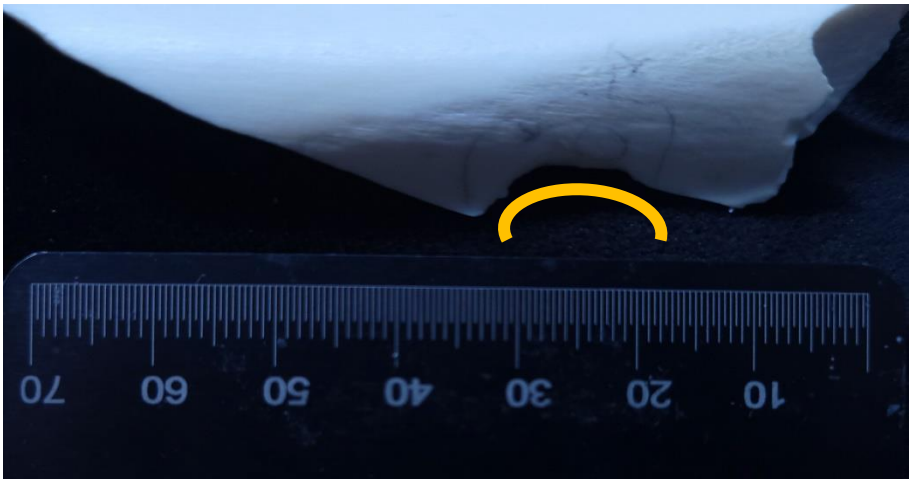

Figure 18 Impact notch on the cortical side of the fragment

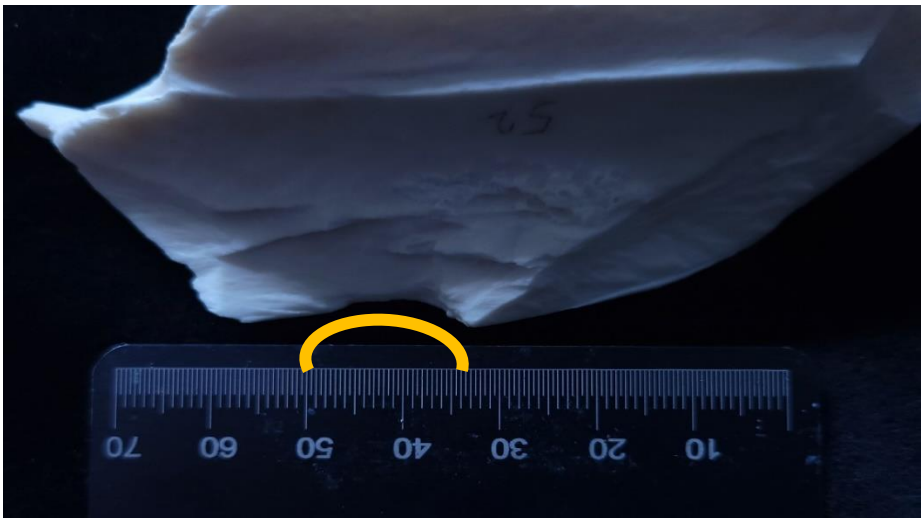

Figure 19 Impact notch on the medullary side of the fragment

Notches are a form of bone surface modification trace that was recorded (see Gifford-Gonzalez, 1991). The criteria used to identify notches is as follows: notches need to be arcuate or semi-lunar, (Vettese et al., 2020), both inflection points need to be present, and the notch needs to penetrate the medullar cavity (Capaldo & Blumenschine, 1994). A count of all notches in each assemblage was carried out. All fragments were emptied out of a single bag. If a smaller bag was inside of a larger bag, the smaller bag was emptied as well. All fragments were surveyed for notches using an incandescent lightbulb as suggested by Blumenschine et al. (1996). Figures 16 and 17 show an example of a percussion notch from both the cortical side of the fragment and the medullary side of the fragment. Figures 18 and 19 show examples of an impact notch from both the cortical side and the medullary side of a fragment. When a notch was found it was marked by a semi-circle. A roman numeral was assigned to the first notch that was identified. The numbering system was reset for each bone.

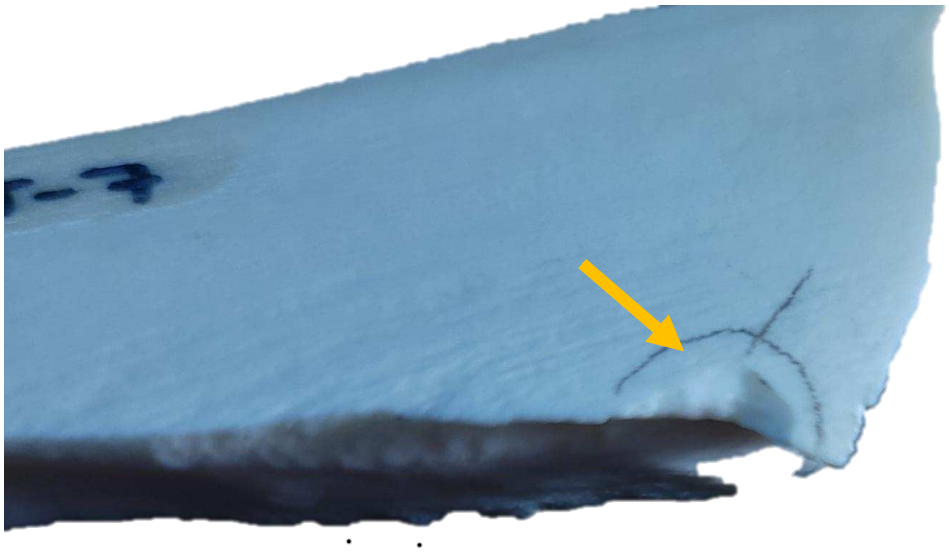

Figure 20 Pseudo-notch on the cortical side of a cave roof fall fragment

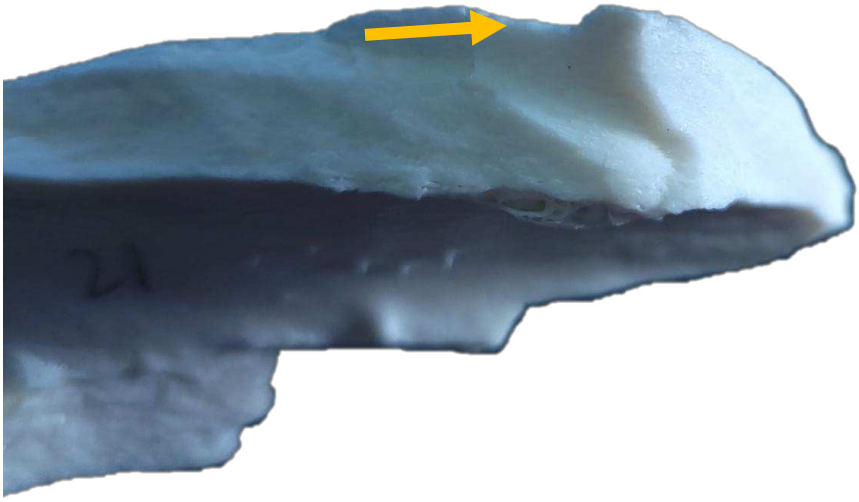

Figure 21 Pseudo-notch on the internal part of a cave roof fall fragment. Note: The pseudo-notch does not penetrate the medullary cavity.

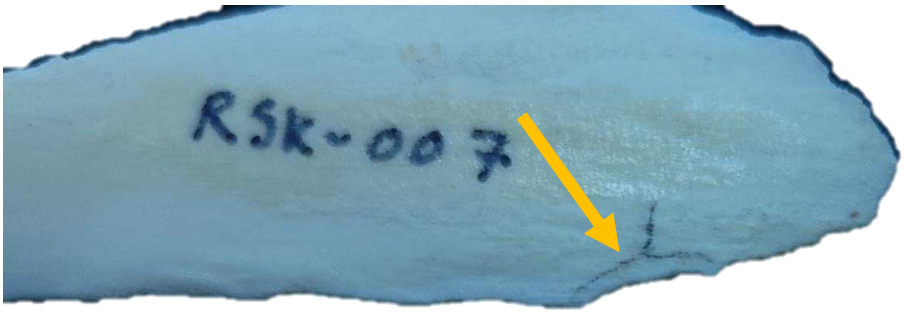

Figure 22 Pseudo-notch on the cortical side of a hammerstone-on-anvil fragment

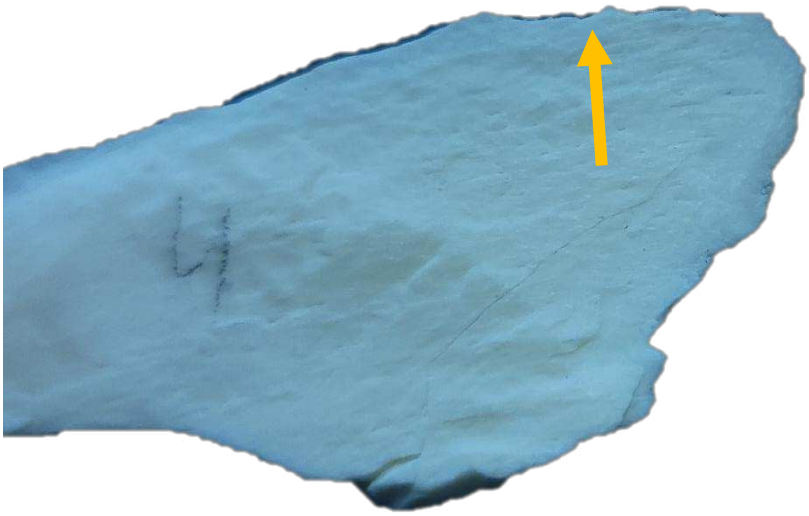

Figure 23 Pseudo-notch on the medullary side of hammerstone-on-anvil fragment

Pseudo-notches appear like notches but do not exhibit any of the criteria applied to notches. Pseudo-notches were counted and placed as a separate variable. All fragments were emptied out of a single bag. If a smaller bag was inside of a larger bag, the smaller bag was emptied as well. All fragments were surveyed for pseudo-notches using an incandescent lightbulb as suggested by Blumenschine et al. (1996). When identified pseudo-notches were marked with a semicircle with a dash in the middle. Figures 20-23 show examples of pseudo-notches on the cortical and medullary sides of fragments in both samples. Table 7 provides a summary of notch types and pseudo-notch types.

Fragments with cortical surface

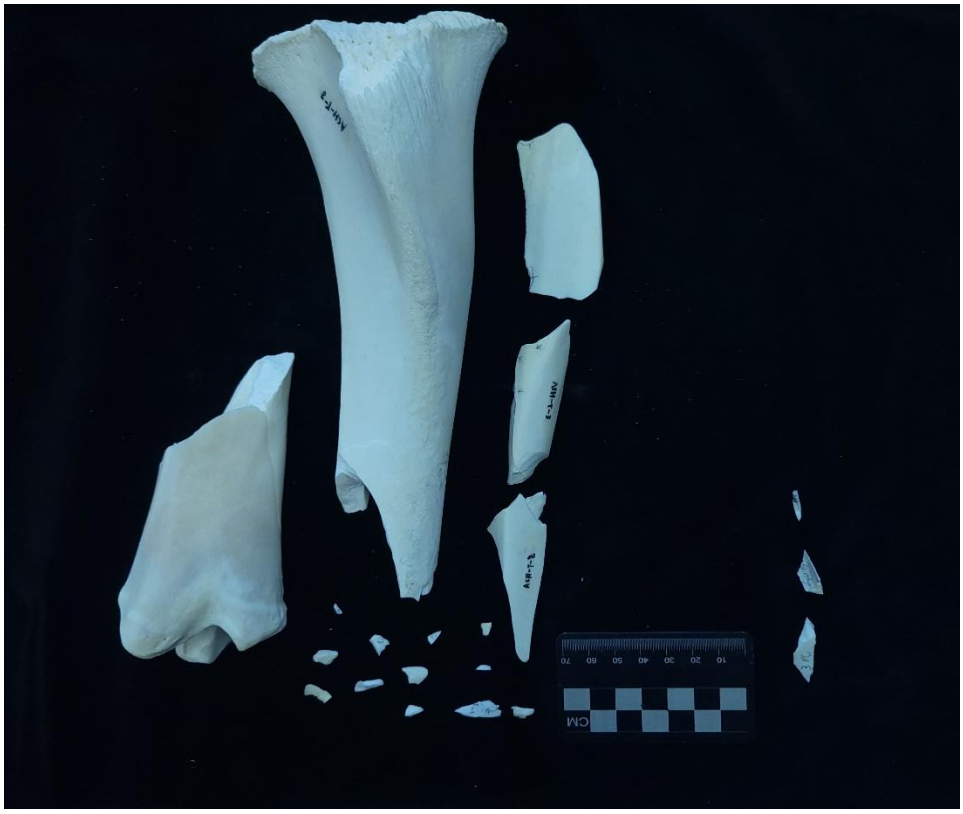

Figure 24 Fragments with a cortical surface on the left, fragments without cortical surface on the right

Fragments with cortical surface can be defined as pieces of bone that still have the tough durable outer layer of bone. The cortical layer on bone fragments is also important because BSMs are imprinted and persevered on it (Blumenschine & Selvaggio, 1988; Capaldo & Blumenschine, 1994). A count of fragments with an intact cortical surface was carried for both assemblages. All fragments were emptied out of a single bag on a foam pad to be surveyed. If a smaller bag was inside of a larger bag, the smaller bag was emptied as well. Fragments that have a cortical layer, but not a medullary cavity were still grouped with the fragments that had both. Fragments that did not have any cortical layer left were excluded and not counted. Figure 24 indicates this division, with fragments that do preserve a cortical surface on the left and fragments that do not preserve a cortical surface on the right. This distinction was made because

counting fragments that do not have an intact cortical layer would inflate the overall number of possible fragments that could have a BSM.

Fragments with pits and grooves

Figure 25 Fragments with pits and/or grooves above, fragments without any pits on the bottom

This count is the number of bone fragments that exhibit at least a pit, a groove or both. Pits and grooves were put in the same category in this regard because they are created by similar processes, and could be indicative of the same effector (Blumenschine & Selvaggio, 1988; Vettese et al., 2020). A visual survey was carried out on all bone fragments from both assemblages underneath an incandescent light. All bone fragments belonging to a bag were emptied out on a foam pad. If a smaller bag was present in the larger bag, it was emptied out as well. All fragments that exhibited a pit and/or groove were separated and then counted for a total.

Figure 25 shows this division, with fragments that exhibit a pit and/or groove on top, and fragments that do not exhibit a BSM on the bottom.

Fragments with notches

The number of fragments with notches is a count that recorded the number of bone fragments that exhibit at least one notch. All bone fragments from the cave roof fall and hammerstone-on-anvil assemblage were surveyed. The bone fragments belonging to a specific bag were emptied out on a foam mat. If a smaller fragment bag was present in the larger bag, it was emptied out as well. If a at least one notch was identified on a fragment, it put aside. Any additional afflicted fragments from the same bag were also placed in the same group. A count of fragments afflicted by notches was then carried out. All bone fragments were surveyed underneath an incandescent lightbulb.

3.3.2 Visual - With Magnification

Percussion marks as described in Blumenschine & Selvaggio (1988) were identified using magnification. To investigate the relationship between percussion marks left by hammerstone-on-anvil percussion and the analogous traces left by cave roof fall, percussion marks were split into pits, grooves and striations as described in White (1992). This separation was also carried out for the analogous traces left by cave roof fall. The decoupling of pits, grooves and striations from percussion pits is done with the understanding that these traces are created through similar processes and are part of the same trace complex (Pickering & Egeland, 2006).

Pits

Figure 26 Impact pits indicated by the arrows

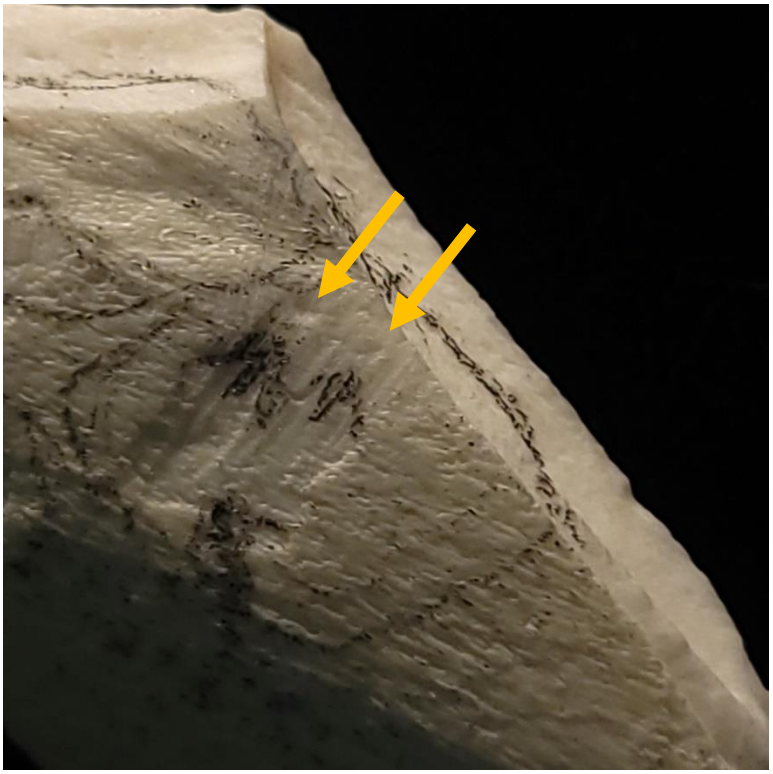

Figure 27 Percussion pits indicated by the arrows

A survey of all bone fragments in both assemblages was carried out using an incandescent light a 3x magnifying glass and a 10x hand lens as described in Blumenschine et al. (1996). All bone fragments were emptied out of a single bag. Smaller bags that were within the large bag were emptied out as well. The fragments were placed on a foam mat. Pits were counted if they conformed to the following criteria: pits had to be imprinted in the cortical layer of the bone (Blumenschine & Selvaggio, 1988), pits had to be deep, round and either exhibit microstriations or radiate microstriations (Blumenschine & Selvaggio, 1988). When an impact pit (Figure 26) or percussion pit (Figure 27) was identified an arrow was drawn pointing to the pit.

Grooves

Figure 28 Impact groove

Figure 29 Percussion groove

Grooves are a BSM that was recorded (see Gifford-Gonzalez, 1991). Grooves can be described as a pit that has been stretched out. The criteria by which grooves were selected was as follows: the groove had to be located on the cortical surface of the bone (Blumenschine et al., 1996), the groove had to be elongated (Vettese et al., 2020) and the groove had to exhibit microstriations or radiate microstriations (Blumenschine & Selvaggio, 1988). All bones from the cave roof fall assemblage and the hammerstone-on-anvil percussion assemblage were surveyed. The fragments were each taken out of their bag and placed on a foam mat. If smaller bags were within the larger bag, the smaller bags were emptied out as well. All bone fragments were surveyed using a 3x magnifying glass 10x magnifying hand lens and an incandescent light bulb as instructed by Blumenschine et al. (1996). All impact grooves (Figure 28) and percussion grooves (Figure 29) that were identified were marked with an arrow that had a dash through it.

Striations

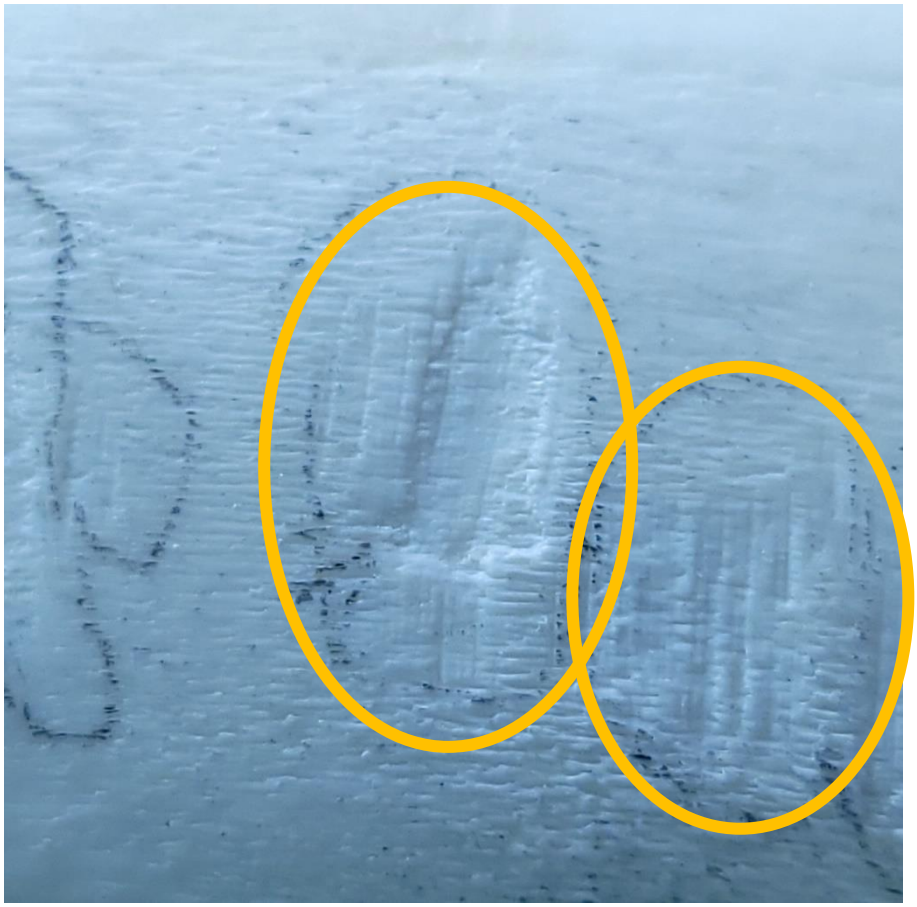

Figure 30 Impact striations

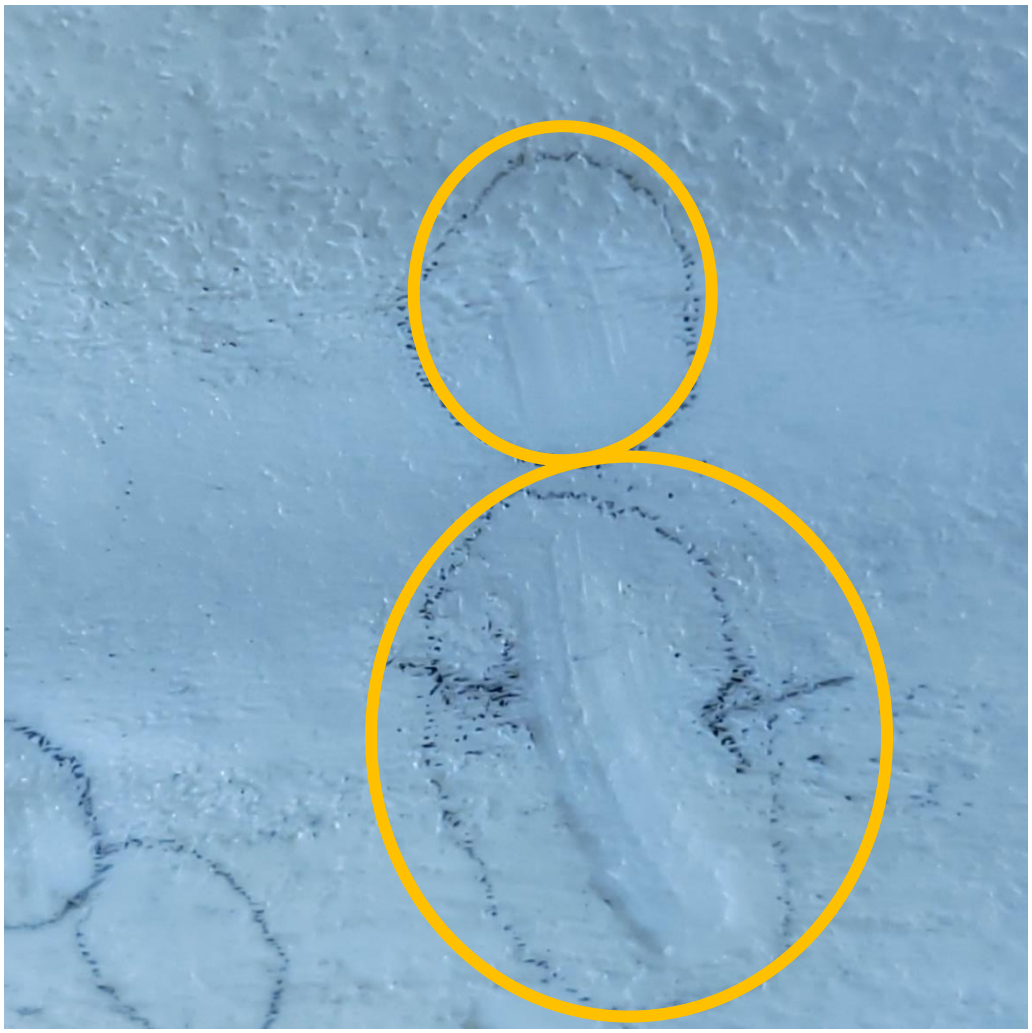

Figure 31 Percussion striations

Striations are a BSM that was recorded. Striations can be described as parallel superficial scratches on the cortical surface of the bone that appear in patches (Blumenschine & Selvaggio, 1988). Examples of both striations created by both actors can be seen in Figure 28 and 29. All bone fragments in the cave roof fall assemblage and in the hammerstone-on-anvil assemblage were visually surveyed. All bone fragments belonging to a bag were emptied out on a foam pad. If a smaller bag was inside the larger bag, the smaller bag was emptied out as well. Striations were identified using a 3x magnifying glass for a general survey, a 10x hand lens for proper identification and an incandescent light bulb as described in Blumenschine et al. (1996). When

striations were found a circle was drawn around the striations. After all striations were identified a count was carried out for a total.

3.3.3 Presence/Absence

Hackle marks and Ribs

Hackle marks and ribs are traces associated with dynamic loading. Hackle marks can be seen in Figure 32 and Figure 34 while ribs are in Figure 33 and Figure 35. Both traces were treated as separate variables and given individual columns. All the bone assemblages were surveyed for hackle marks and ribs. A simple absence/presence observation was used per assemblage. If one fragment exhibited hackle marks then the whole bone assemblage was marked with a "Yes". If no hackle marks were found the whole bone assemblage was marked with a "No". A similar technique was employed for ribs, with a "Yes" assigned to a whole bone assemblage if a rib was found on a fragment, and a "No" assigned if no ribs were found on any fragments within a bone assemblage.

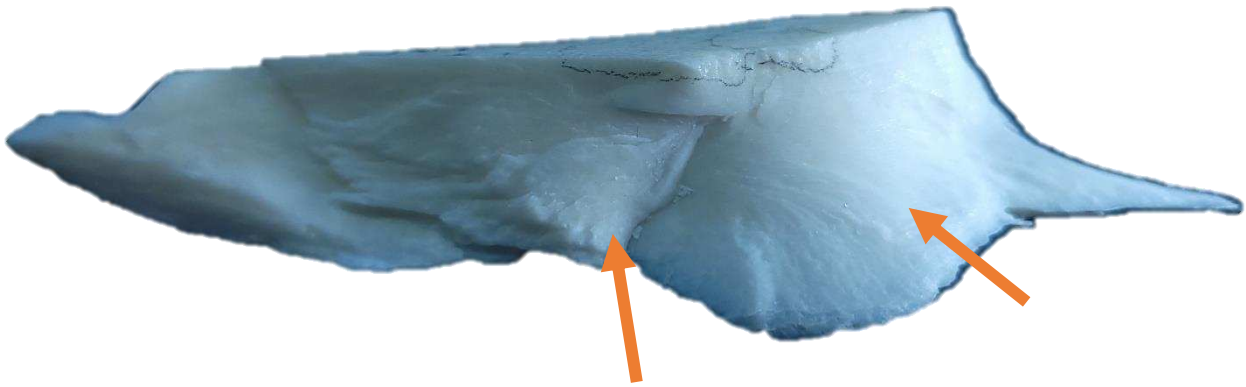

Figure 32 Hackle marks on cave roof fall created fragment

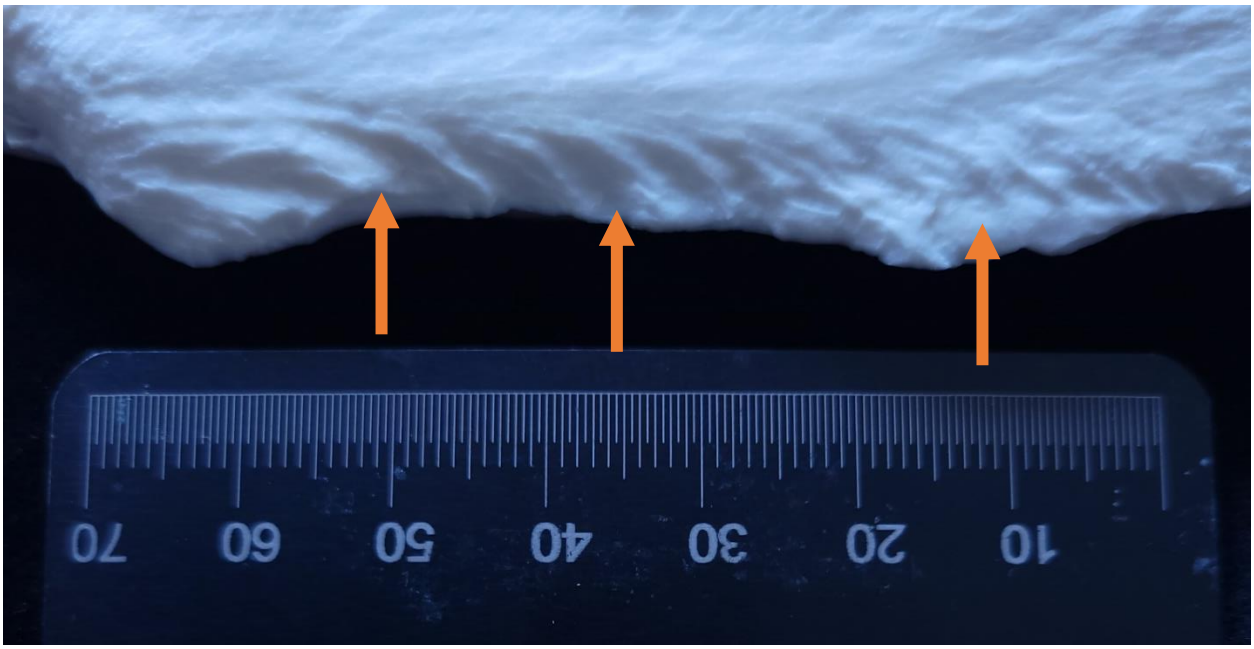

Figure 33 Ribs on a cave roof fall created fragment

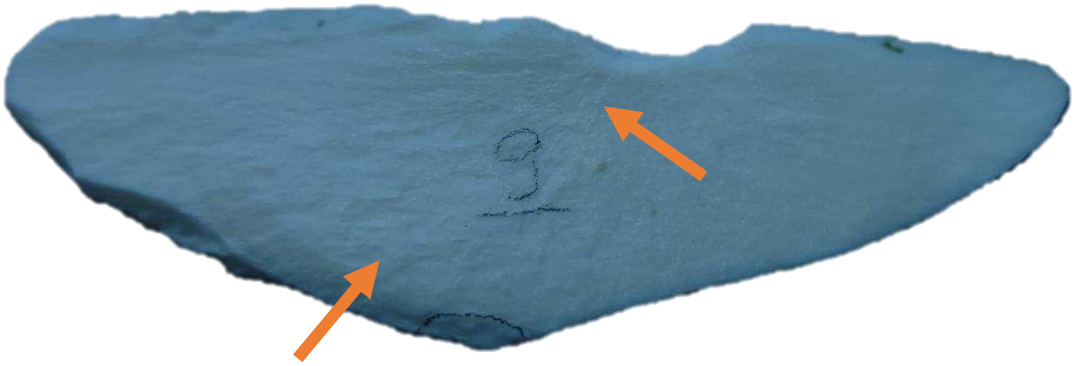

Figure 34 Hackle marks on a hammerstone-on-anvil created fragment

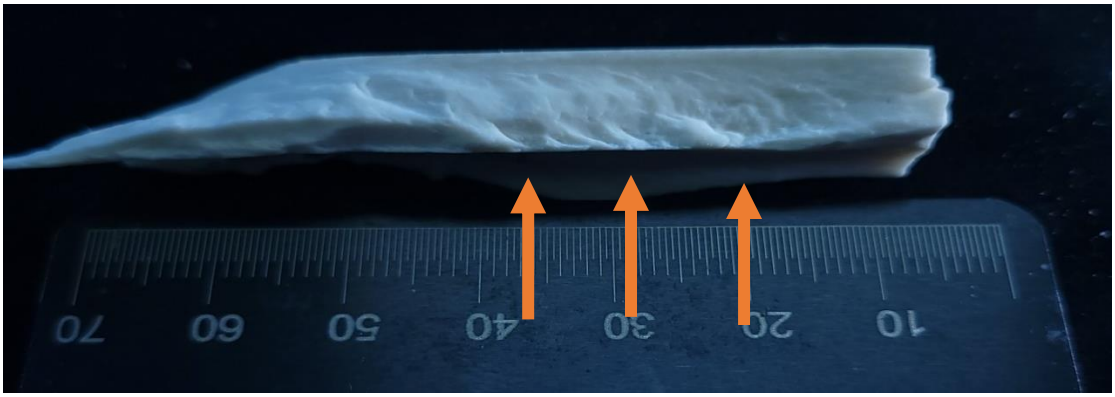

Figure 35 Ribs on a hammerstone-on-anvil created fragment

Hackle marks and ribs were recorded to verify that dynamic impact is the causal agent for both cave roof fall and hammerstone-on-anvil percussion (Gifford-Gonzalez, 1991). If the cave roof fall assemblages exhibit hackle marks and ribs on at least one bone in each assemblage then it can be inferred that cave roof fall ruptures the diaphysis through dynamic loading like hammerstone-on-anvil percussion. If only some of the cave roof fall bone assemblages exhibit hackle marks and ribs then doubt is cast on dynamic impact as the causal agent for cave roof fall.

3.3.4 Measurements

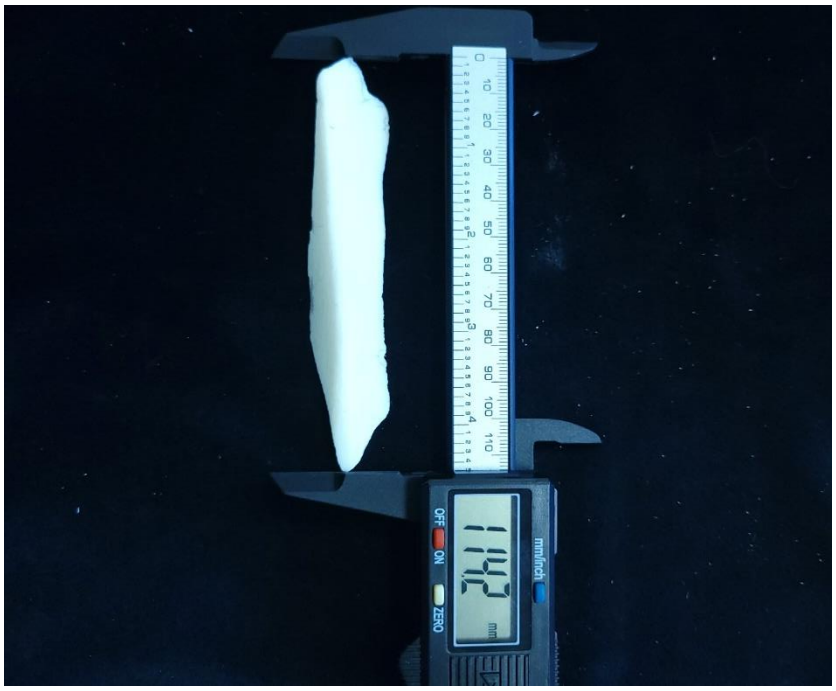

Figure 36 Digital caliper used to measure fragments longitudinally

Linear measurements were done in centimeters using a caliper as seen in Figure 36 and a measuring tape for larger fragments as seen in Figure 37. Fragment size and epiphysial element length was measured in both assemblages. Linear measurements were taken longitudinally to the long axis of the bone. For fragments that detached from the shaft the long axis of the bone was established by observing the general orientation of the cortical bone, which is longitudinally oriented. Notch dimensions were obtained in centimeters by using a caliper to measure molds pressed into notches to form the missing flake. Release angle was measured in degrees using a goniometer.

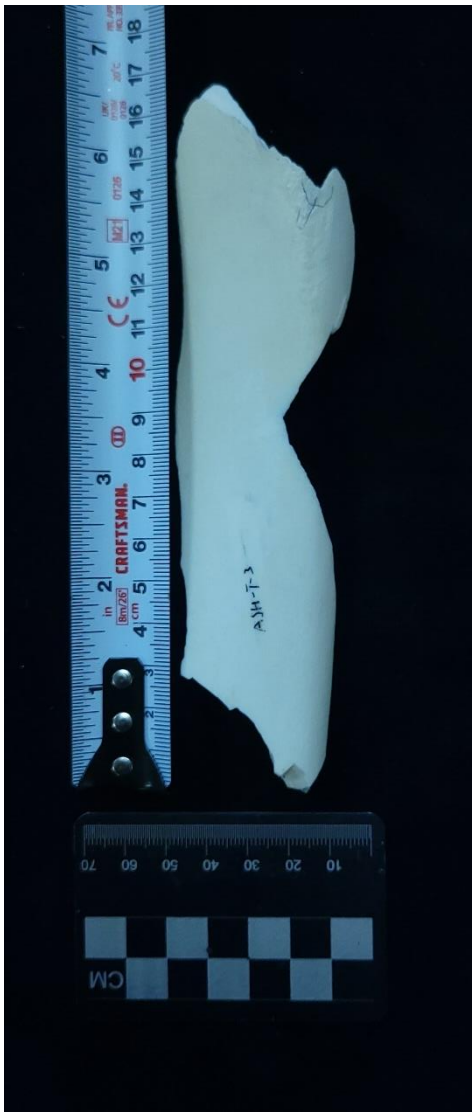

Figure 37 Tape measure used to measure large fragments longitudinally

Fragment size categories

Figure 38 Example of fragments under 2 cm from a cave roof fall assemblage

Figure 39 Example of fragments between 4 and 4.99 cm from a cave roof fall

Ten size categories were created to accommodate the variety of fragments that are produced during shaft fragmentation with some examples illustrated in Figure 38 and 39. The

size categories are fragments smaller than 2 cm, 2-2.99 cm, 3-3.99 cm 4-4.99 cm, 5-5.99 cm, 6-6.99 cm, 7-7.99 cm, 8-8.99 cm, 9-9.99 cm and larger than 10 cm. The bone fragments were not presented as individual measurements because the individual dimensions of the bone fragments would be less informative than the number of fragments in each dimension category. The measurement intervals were created based on the example provided by Capaldo & Blumenschine (1994). Fragments smaller than 2 cm represents small fragments, such as chips, and some flakes. Fragments in between 2 cm and 9.99 cm represent medium sized fragments, like some flakes, or complete parts of the diaphysis. Fragments larger than 10 cm are usually large fragments that survived fragmentation such as epiphyseal elements and intact shaft fragments.

All bone fragments including epiphyseal elements, were measured, and then placed in their respective category. This was done for both assemblages. A bag containing the fragments of one bone assemblage was emptied out on a foam pad. If a smaller bag was inside the larger bag, the smaller bag was emptied out as well. A caliper was used to measure fragments that were of appropriate size. The caliper was extended past the size of the fragment, and then the adjustable part was pushed until it contacted the fragment as seen in Figure 34. The measurements were produced in millimeters but were recorded in centimeters. After the measurement was recorded, the adjustable part was pushed back to zero and the caliper was reset to prevent mismeasurements. If a measurement exceeded the capabilities of the caliper, a tape measure was used. The tape measure was unfurled and the fragment was placed adjacent to the metric scale. Measurements were recorded in centimeters, with millimeters to the nearest tens decimal point. To obtain the percentage that a size category contributed to the overall fragment number of an actor, a size category was summed up and then divided by the total fragment number. The quotient was then multiplied by 100 (see Appendix Table 24).

Epiphyseal Element Measurements

Epiphyseal element length was recorded. Epiphysial elements are the articular ends of a bone usually made up of trabecular bone. In the case of the tibial bones used, the proximal epiphysial element connected to the distal epiphysial end of the femur, and the distal epiphyseal element of the tibia connected to the astragalus bone (talus in humans). All epiphysial elements from both assemblages were visually surveyed and measured. Measurements were split into two categories, the distal epiphyseal element, and the proximal epiphyseal element. Measurements were done using a digital caliper or a measuring tape. Measurements were taken from the metaphyseal line to the longest part of the fragment as indicated by the orange lines in Figures 40-43. The metaphyseal line was used as a measuring point instead of the actual epiphysis because of the following reasons. For almost all bones in both samples the proximal epiphysis was removed. This either happened during boiling as part of bone processing, or it was removed to curb mold and bacterial growth as seen in Figure 40. The other reason for the use of the metaphysis over the epiphysis as a measurement point was because in the hammerstone-on-anvil sample the distal epiphysis became detached as well as seen in Figure 43. Measurements would be inconsistent if the distal epiphysis was present for some elements and not others.

Figure 40 Proximal epiphysial element

Figure 41 Distal epiphysial element with a fused metaphysis

Figure 42 Distal epiphysial element with an unfused metaphysis

Figure 43 Distal epiphysial element without an epiphysis

Notch dimensions

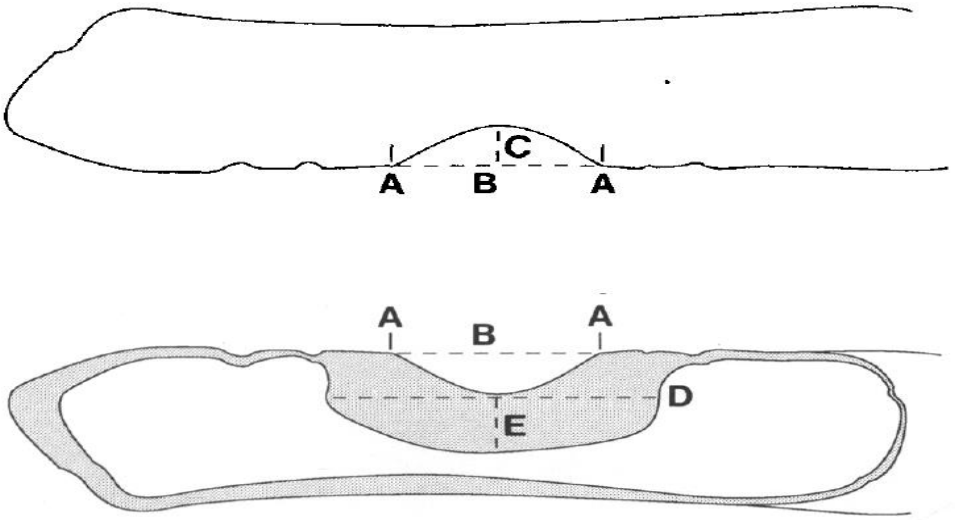

Figure 44 Figure shows notch breadth (A), halfway point of notch breadth (B), notch depth (C), flake scar breadth (D) and flake scar depth (E). From A Quantitative Diagnosis of Notches Made by Hammerstone Percussion and Carnivore Gnawing on Bovid Long Bones by S. D. Capaldo, & R. J Blumenschine, 1994. American Antiquity, 59(4), p. 733. Copyright 1994 by the Society for American Archaeology.

Notch measurements follows the methodology laid out by Capaldo & Blumenschine (1994). This methodology involves the use of molding putty applied to the percussion notch to recreate the dimensions of the flake and to help define the dimensions of the percussion notch (Capaldo & Blumenschine 1994). The measurements are as follows: maximum notch breadth (Figure 44 A), maximum notch depth (Figure 44 C), maximum flake scar breadth (Figure 44 D), maximum flake depth (Figure 44 E), and platform angle. Maximum notch breadth was measured by marking the inflection points of the notch on the cortical side of the fragment on the putty and then measuring the distance between the two points. The breadth also informed the measurement of the maximum notch depth, which was measured from the middle of the notch breadth towards the cortical bone. The flake scar breadth and flake depth were gathered from the medullary part of the mold, with the flake scar breath measured at the widest part after the cortical surface, and

the flake depth was measured form the beginning of the cortical bone to the beginning of the medullary cavity.

Impressive putty© was used to created molds of the identified notches in both the cave roof fall sample and in the hammerstone-on-anvil sample. The molding material was heated up in a microwave to make it malleable. After it was kneaded chunks of the putty were pressed into the notches to create a notch mold. Care was taken to spread the molding material fully between inflection points and to completely cover the flake scar. After the molding material was set the bone was left in a refrigerator for 15 minutes for the molding material to harden. Once 15 minutes elapsed the bone was taken out and the molding material was measured. A line was drawn on the hardened molding material connecting the two inflection points delineating the notch breadth as seen in Figure 44 A. A ruler was used to find the middle of the notch breadth as seen in Figure 44 B. From this middle point a straight line was drawn towards the notch, which would be the notch depth as indicated by Figure 44 C. Both notch breadth and notch depth were measured using digital calipers. Notch breadth and notch depth were also measured from incipient flakes in a similar manner, but without using putty, since the flake itself was still present. Once notch breadth and notch depth were measured the molded flake was removed to measure flake scar breadth as shown in Figure 44 D. Flake scar breadth was measured using a digital caliper. Flake scar breadth was not collected from incipient flakes because the body of the flake prevented such measurement. The roman numerals assigned for each notch were transferred to the notch measurements. As indicated by Capaldo & Blumenschine (1994) these measurements are not diagnostic of notch qualities, but rather the ratios build from these variables are descriptive of notch qualities.

Release angle

Release angle of the platform angle is defined as the angle at which the flake detached from the diaphysis forming a notch (Capaldo & Blumenschine, 1994). To measure the release angle a goniometer was used. After gathering the notch dimensions from the molds created from impressive putty© one arm of the goniometer was placed on the "cortical" top of the mold where notch breadth and notch depth was measured. The other arm of the goniometer was brought towards the "medullary" side of the mold that had the flake scar breadth until it met the farthest part of the medullary mold. The roman numerals assigned for each notch were transferred to the release angle measurements.

3.3.5 Composite Variables

BSM Ratios

Percentage of Cortical Fragments with a Pit or a Groove

The percentage of cortical fragments with a pit or a groove was derived by dividing the number of fragments that exhibit pits or grooves by the total number of fragments that still preserve a cortical surface. Following this division, the ratio was multiplied by 100 to get a percentage. This variable was used to "flatten" two variables, in this case fragments with pits and notches and fragments with a cortical surface into one variable and expose the relationship between the two.

Percentage of Cortical Fragments with Notches

The percentage of cortical fragments with notches was derived by dividing the number of fragments that have a notch by the total number of fragments that still preserve a cortical surface. Following this division, the ratio was multiplied by 100 to get a percentage. This variable was

used to “flatten” two variables, in this case fragments with notches and unaffected fragments with a cortical surface into one variable and expose the relationship between the two.

Pseudo-Notch to Notch Ratio

The ratio of pseudo-notch to notch ratio was calculated by dividing the number of pseudo-notches in each bone assemblage by the number of identified notches. This was done to generate a “collapsed” variable that portrays the relationship between the two variables.

Notch Ratios

Capaldo & Blumenschine (1994) used notch breadth, maximum notch depth and flake breadth to form the following ratios: notch breadth : maximum notch depth and flake scar breadth : maximum notch depth. Notch shape was described by notch breadth : maximum notch depth. Flake shape was described by flake scar breath: maximum notch depth. These same ratios were employed to describe the general notch shape and flake shape of impact notches and percussion notches. Notch shape (notch breadth : maximum notch depth) data gathered from incipient notches was combined with the notch shape data recovered from notches.

3.4 Hypothesis Testing and Statistics

Intra Actor

Throughout the experiment the four trials were kept separate to pick up any differences between the different boulder weights and boulder drop heights. Unfortunately, this is not possible due to the small sample size of 4 bones that was assigned per group. Furthermore, some of variables of interest had fewer than 4 observations due to the lack of data. To remedy this all trials were collapsed into one experiment, cave roof fall. While this action does erase any difference that might have existed between trials, it does introduce variation within the new cave roof fall sample (M. Glantz & M. Pante, personal communication, 2022).

Inter Actor

Summary Statistics and Graphs

Mean, median, standard deviation were calculated as summary statistics for the twenty nine testable variables collected form the cave roof fall sample and the hammerstone-on-anvil percussion sample. Histograms were created in R Studio for each testable variable in both samples. Violin plots in the vioplot R package were used instead of box plots for better data visualization. Violin plots were utilized because they combine the summary statistics provided by box plots with a visualization of data distribution. Scatter plots were created to visualize variables tested with Spearman's rank order correlation.

Statistical Tests

Mann-Whitney U test, Spearman's rank correlation and Fisher's exact test were used to evaluate the relationship between variables collected from the cave roof fall and hammerstone-on-anvil percussion samples. These three tests were used to accommodate the different types of data and hypotheses derived from the data. All tested variables and statistical tests that were used are summarized in Table 8. The alpha for all tests was set at 0.05.

The Fisher's exact test (FET) was employed to test the binary response of incipient notches and notches between the cave roof fall sample and the hammerstone-on-anvil sample. This is done by testing the association between each binary response and actor through a contingency table. These two variables were tested using FET because cave roof fall had less than the minimum of 5 observations needed to carry out a Mann-Whitney U test.

Fragment size categories were assessed using Spearman's rank correlation. This test was picked to test if fragment size categories produced by each actors have a monotonic relationship and if so if the correlation is positive or negative. A monotonic relationship between two

variables is when one variable increases the other either decreases or increase as well. The degree to which the variables correlate is provided by the correlation coefficient (between -1 and 1).

All other variables except for fragment count were tested using the Mann-Whitney U test. Fragment count was not tested because bone fragmentation is sensitive to influence from other actors (e.g., sediment pressure, trampling, diagenetic fragmentation) and cannot be applied to archaeological sites. The Mann-Whitney U tests was used because of its versatility to handle multiple types of data (measured, ratios and counts) and because the normality of the data set was called into question by the numerous skewed histograms (see Appendix). This test was used to test for a difference between the cave roof fall and hammerstone-on-anvil percussion. Any variable that had less than 5 observations in any sample was either tested using a different tests (FET or Spearman's rank correlation) or were not tested. This was done because any variable with less than 5 observations per sample will always return a p-value larger than 0.05 (A. Hess, personal communication, 2021).

Table 8 Statistical Tests with Assigned Variables from Both Assemblages

Variable	Test
Notch count	Fisher's exact test
Incipient notch count	
Fragment size categories	Spearman's rank order correlation
Flake count	Mann-Whitney U test
Pit count	
Groove count	
Striation count	
Distal element length	
Proximal element length	
Percentage of fragments with a pit and/or groove	
Percentage of fragments with a notch	
Pseudo-notch count	
Pseudo-notch : notch	
Notch breadth : maximum notch depth	
Flake scar breadth : maximum notch depth	
Fragments with a cortical surface	
Fragments with a pit and/or grooves	
Fragments with a notch	
Release angle	

Hypotheses and Predictions

For each test employed a pair of hypotheses were created to test each assigned variable. Prediction (see Table 9) were made to about each variable, how each variable might interact with each actor and why.

***Fisher's Exact Test*:**

H_0: The binary response of this variable is not different for both samples

The null hypothesis will be considered if there is no difference (p-value > 0.05) in the variable binary response for the cave roof fall and hammerstone-on-anvil percussion sample.

H_1: The binary response of this variable is different for both samples

The alternative hypothesis will be viable if there is a significant difference (p-value < 0.05) in the variable binary response for both samples.

Spearman's rank correlation:

H_0: The relationship between these two variables is not monotonic.

The null hypothesis will be feasible if the compared variables from each actor are not monotonic (p-value > 0.05).

H_1: The relationship between these two variables is monotonic.

The alternative hypothesis will be considered if there is enough significant evidence (p-value < 0.05) that the variables are monotonic.

Mann-Whitney U test:

H_0: There is no difference between cave roof fall and hammerstone-on-anvil percussion.

The null hypothesis will be viable if the variable tested does not point to a significant difference (p-value > 0.05) between cave roof fall and hammerstone-on-anvil percussion.

H_1: There is a difference between cave roof fall and hammerstone-on-anvil percussion.

The alternative hypothesis will be considered if the tested variable point towards a significant difference (p-value < 0.05) between cave roof fall and hammerstone-on-anvil percussion.

Table 9 Predictions for the Outcome of each Tested Variable for Each Actor

Variable	Prediction
Visual	
Flake count	-Higher energy transfer into the diaphysis by roof fall impact creates more impact flakes -Wider blow distribution along the diaphysis by hammerstone-on-anvil percussion creates more percussion flakes
Incipient notch count	-More energy radiating from roof fall impact site through the diaphysis creates more impact Incipient notches -Smaller diaphyseal surface area affected by roof fall creates less impact incipient notches -Wider blow distribution along the diaphysis by hammerstone-on-anvil percussion creates more percussion incipient notches
Notches	-Higher energy transfer to the diaphysis from roof fall impact creates more impact notches -Smaller diaphyseal surface area affected by roof fall creates less impact notches -Wider blow distribution along the diaphysis by hammerstone-on-anvil percussion creates more percussion notches

Fragments with cortical surface	-Higher energy transferred into the diaphysis by roof fall impact creates less fragments with cortical surface -Lower energy transferred into the diaphysis by hammerstone-on-anvil percussion creates more fragments with cortical surface
Fragments with a notch	-Smaller diaphyseal surface area affected by roof fall impact creates less fragments with impact notches -Wider blow distribution along the diaphysis by hammerstone-on-anvil percussion creates more fragments with percussion notches
Fragments with a pit and/or groove	-Smaller diaphyseal surface area affected by roof fall impact creates less fragments with impact pits and/or grooves -Larger impact surface of the boulder creates more fragments with impact pits and/or grooves -More fragments with percussion pits and/or grooves are created due to the dual action of the hammerstone and anvil
Pseudo-notches	-Higher amount of energy radiating through the bone creates more impact pseudo-notches -Smaller affected diaphyseal surface area by roof fall creates less impact pseudo-notches -Wider blow distribution along the diaphysis by hammerstone-on-anvil percussion creates more percussion pseudo-notches
Pits	-Smaller diaphyseal surface area affected by roof fall causes fewer impact pits -Larger impact surface area of the boulder creates more impact pits - More percussion pits are created due to the dual action of the anvil and hammerstone
Grooves	-More impact grooves are created due to the random sliding action of the boulder following impact -Less percussion grooves are created because of the control exerted on the bone by the intentional fracture of the bone
Striations	-More impact striations are created by the larger impact face of the roof fall boulder -More percussion striations are created by the dual action of the hammerstone and anvil
Hackle marks	-Hackle marks will be present on at least one bone fragment in every roof fall assemblage because the effector is dynamic loading
Ribs	-Ribs are present on at least one bone fragment in every roof fall assemblage because the effector is dynamic loading
Measured	
Fragment size	-Cave roof fall will produce more fragments in the small sized categories (under 2 cm, to 3-3.99 cm) due to higher impact force transferred into the diaphysis, less fragments in the medium sized categories (4-4.99 cm to 8-8.99 cm) because of less impacts to fracture the diaphysis, and more fragments in the large sized category (9-9.99 cm and larger than 10 cm) caused by less damage done to the diaphysis by less blows. -Hammerstone-on-anvil percussion will produce more small sized fragments (under 2 cm to 3-3.99 cm), more medium sized fragments (4-4.99cm to 8-8.99 cm), and less fragments in the large sized category (9-9.99 cm and larger than 10 cm) because of a wider blow distribution along the diaphysis.
Epiphyseal element length	-Cave roof fall will produce epiphyseal element lengths of random lengths due to the randomness of the boulder impact site on the shaft

	-Hammerstone-on-anvil percussion will produce more uniform epiphyseal element lengths because bone fracture was done through intentional and methodological means
Release angle	-Cave roof fall will produce release angles closer to 90° because of the direct impact from the boulder on the tibial shaft -Hammerstone-on-anvil percussion will produce more variable angles due to the varied angle of each blow
Composite	
Percentage of fragments with a pit and/or groove	-Cave roof fall will produce less fragments with pits and/or grooves causing the percentage of affected fragments to be smaller -Hammerstone-on-anvil percussion will produce more fragments with pits and/or grooves making the percentage of affected fragments larger
Percentage fragments with notches	-Cave roof fall will produce fewer notches causing the percentage of fragments with notches to be smaller -Hammerstone-on-anvil percussion will produce more fragments with notches making the percentage of fragments with notches will be larger
Pseudo-notch : Notch	-Cave roof fall will produce more pseudo-notches than notches, making the ratio larger -Hammerstone-on-anvil percussion will produce less pseudo-notches than notches, causing the ratio to be smaller
Notch breadth : Maximum notch depth	-Cave roof fall will create “hyper” arcuate notches with a higher notch breadth to notch depth ratio than those created by hammerstone-on-anvil percussion
Flake scar breadth : Maximum notch depth	-Cave roof fall will create thinner flakes with a larger flake scar breadth to notch depth ratio than those created by hammerstone-on-anvil percussion

CHAPTER IV: RESULTS

The purpose of this actualistic experiment is to differentiate between cave roof fall and hammerstone-on-anvil percussion. The need for a differentiation between the two actors has been brought up by multiple researchers (Capaldo & Blumenschine, 1994; Dixon, 1984; Oliver, 1989). However, despite this need, only Karr & Outram (2012) have looked at cave roof fall from an actualistic perspective. The lack of research into cave roof fall as a modifier of bones has created a hole in the taphonomic literature and the appearance of an equifinality between the actors. The results from the cave roof fall experiment and its comparison with hammerstone-on-anvil percussion will be presented here. Before the results are presented, the research question with accompanying hypotheses will be restated as a refresher, along with the tests used to answer this research question and their supporting hypotheses as seen in table 10.

Table 10 Reaserch Question with Hypotheses and Statistical Tests with Hypotheses

Research question: Is the taphonomic signature different from the taphonomic signature of hammerstone-on-anvil percussion? H_0: All variables collected indicate that the taphonomic pattern of cave roof fall is not different from that of hammerstone-on-anvil percussion. H_1: All variables collected are indicative of a difference between cave roof fall and hammerstone-on-anvil percussion. H_2: Some of the variables collected are different in the taphonomic pattern of cave roof fall comparted to hammerstone-on-anvil percussion.
Fisher's Exact Test: H_0: The binary response of this variable is not different in both samples H_1: The binary response of this variable is different in both samples
Spearman's rank correlation: H_0: The relationship between these two variables is not monotonic. H_1: The relationship between these two variables is monotonic.
Mann-Whitney U test: H_0: There is no difference between cave roof fall and hammerstone-on-anvil percussion. H_1: There is a difference between cave roof fall and hammerstone-on-anvil percussion.

4.1 Experimental Results

Table 11 Summary Statistics for Number of Blows Attributed to Cave Roof Fall to Fracture the Bison Tibiae

	Number of blows for bone fracture
Mean	1.75
SD	1
Median	1

All sixteen bison tibiae were broken during the experiments. This means that a rock that weights at least 6.8 kg that is dropped from 4.6 m will likely produce bone breakage. On average 1.75 blows were needed to fracture the diaphysis of the bison tibiae. This average only considers the times the boulder contacted bone as opposed to the number of overall trials. The standard deviation is 1, while the median is 1. The summary statistics of the cave roof fall experiments can be seen in Table 11. A more detailed table can be found in the Appendix. Three of the four rocks used survived the experiment. Rock 1 fractured as soon as it impacted the bone. To carry on the experiment Rock 3 was used as a replacement. Rock 3 was the same weight as Rock 1 and of similar shape and dimensions.

Table 12 Summary Statistics for Number of Blows Attributed to HAP to Fracture the Bison Tibiae

	Total number of blows for bone fragmentation
Mean	21.9
SD	5.5
Median	23.5

Source: A GIS based approach to long bone breakage patterns derived from marrow extraction, by T. Stavrova el al., PLoS ONE 14(5): e0216733, p. 12. Copyright 2019 by Stavrova et al.

The data associated with the creation of the hammerstone-on-anvil sample was unavailable. To compensate Stavrova et al. (2019) was used as a proxy for the hammerstone-on-anvil data. The study uses ten tibiae, which while less than the sixteen tibiae selected from the assemblage, is still informative about the blows necessary to fracture the diaphysis. As summarized in Table 12, the mean blows necessary to break the diaphysis is 21.9. The standard deviation of the hammerstone-on-anvil sample is 5.5 and the median is 23.5. Overall cave roof fall breaks the tibial epiphysis with less blows than hammerstone-on-anvil percussion.

4.2 Data Distribution and Summary Statistics

The data for all collected variables is depicted as histograms in the Appendix under Histograms. This was done to illustrate the distribution of each variable. Some of the histograms that diverge from the normal distribution will be presented here. Most of the variables tend to skew right. The tendency of the data to skew to the right is related to the abundance of zeros generated by using counting as a data-gathering technique. A few variables have closer to a normal distribution, as seen in Figure 45. Of the Hammerstone-on-anvil percussion (HAP) variables the fragments count, distal element length, fragments with percussion pit count, and cave roof fall striation count are closer to a normal distribution. These variables likely have a more normal distribution because the data collected does not have many zeros and is more evenly spaced out, as opposed to aggregating around specific values as seen in left and right skewed data.

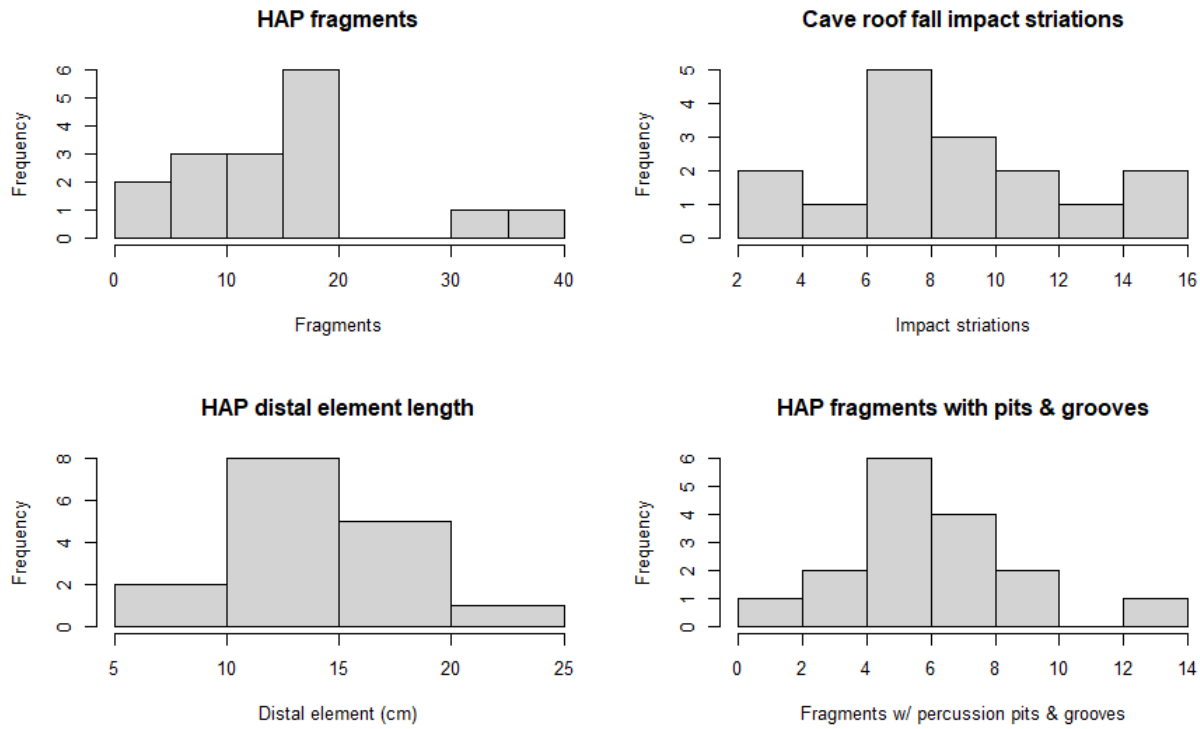

Figure 45 Normally distributed variables. HAP is hammerstone-on-anvil percussion

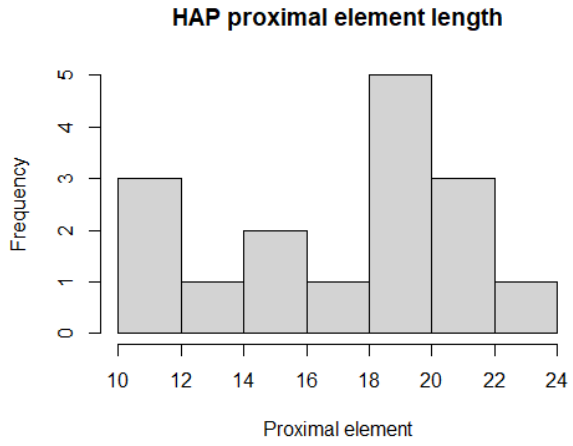

Figure 46 Histogram of left skewed data

Hammerstone-on-anvil percussion proximal element length is the only variable that is skewed left (see Figure 46). This skew might be an artifact and related to the direction of percussion blows. If the first blow started roughly in the middle of the diaphysis and then traveled towards the distal end of the bone then the proximal end would be larger. This is supported by the somewhat normal distribution seen in the distal element histogram in Figure 45. A normal distribution means that there is a wider range of values which implies that the values are not clustering around a specific value as seen in Figure 46.

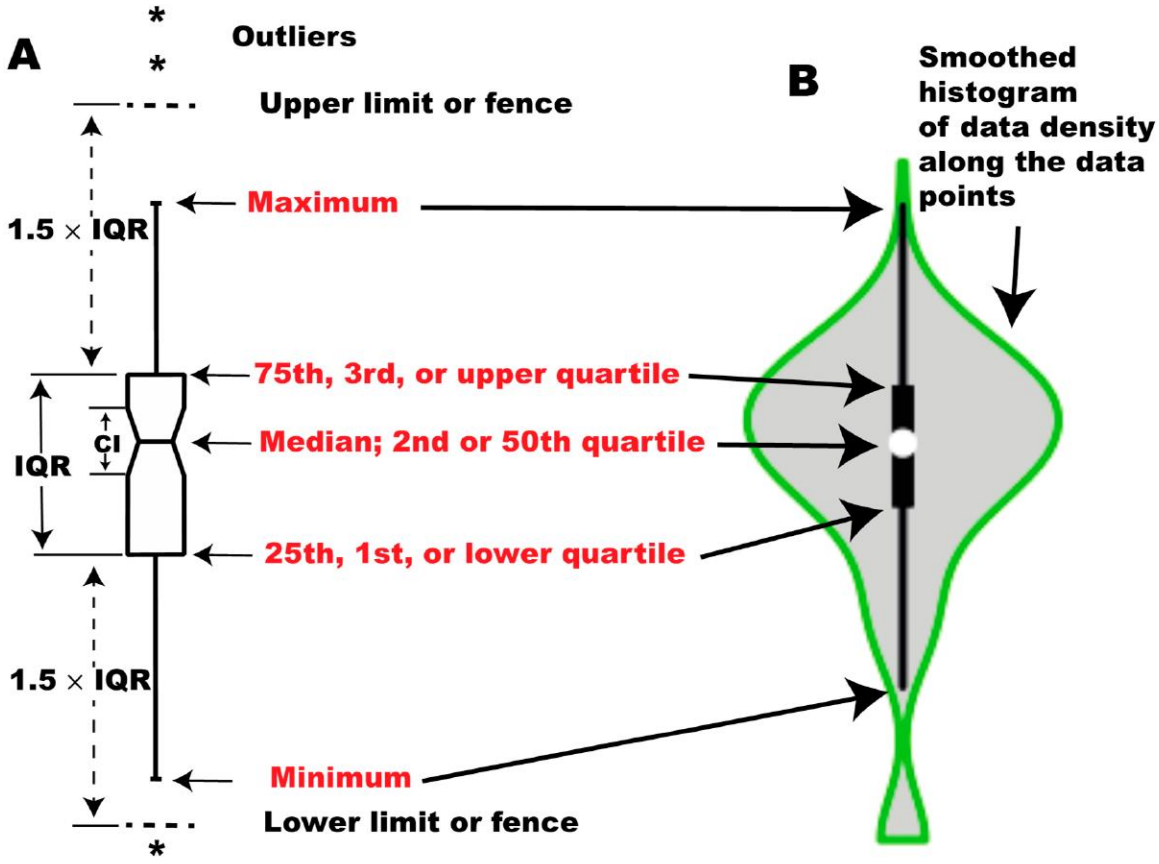

Figure 47 Anatomy of a violin plot. Source: " Become Competent within One Day in Generating Boxplots and Violin Plots for a Novice without Prior R Experience" by K. Hu, 2020 The Methods and Protocols, 64(3), p. 3. Copyright 2020 by the author

Violin plots were used to visually represent the information from Table 13 and provide a side by side comparison of the two actors. As seen in Figure 47, violin plots depict the median, the quartile range, the range, and the general density of values. The violin plots for all the variables can be found in the Appendix under Violin Plots. Most of the variables in both data sets are shown to have overlapping medians upper/lower adjacent values. Violin plots of variables that proved to be statistically different will be presented in the result section. The summary statistics presented in Table 13 are the mean, standard deviation (SD) and median.

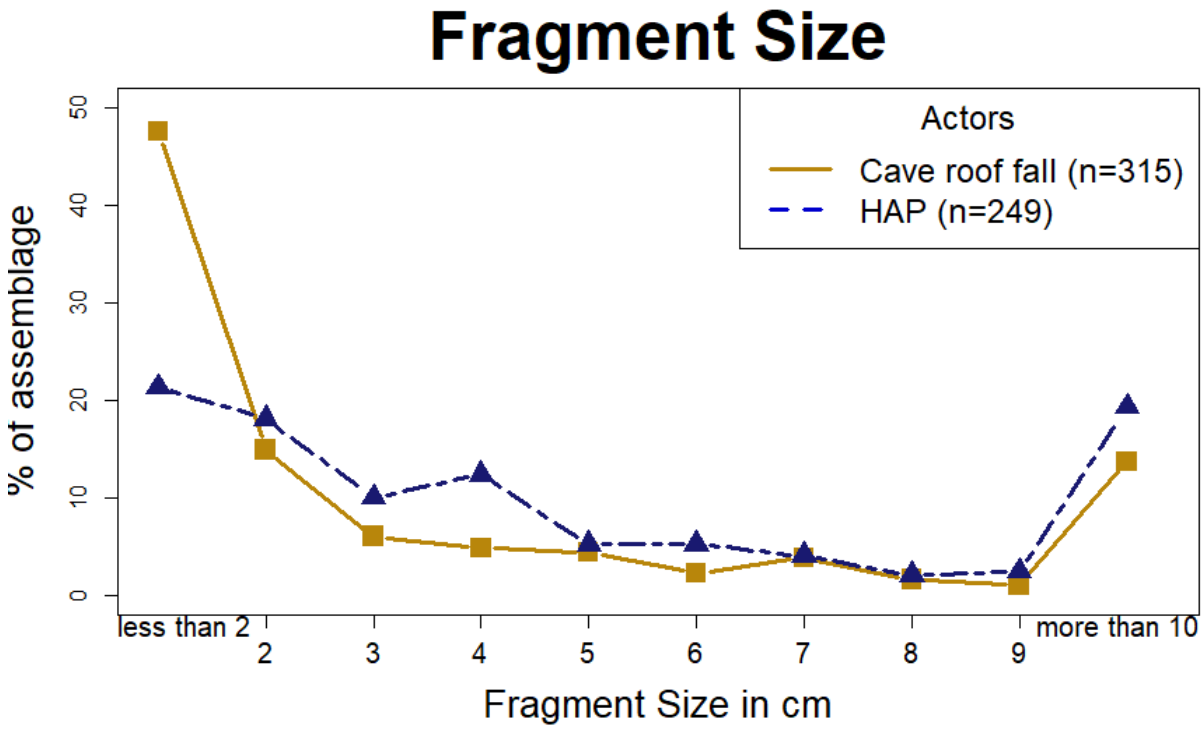

Figure 48 Fragment size distribution in relation to the assemblage

Table 13 Summary Statistics for Each Collected Variable

Actor		Fragment count	Incipient notch count	Flake count	Notch count	Pit count	Groove count	Striation count	Fragments <2 cm	Fragment 2-2.99 cm	Fragment 3-3.99 cm	Fragment 4-4.99 cm	Fragment 5-5.99 cm	Fragment 6-6.99 cm	Fragment 7-7.99 cm	Fragment 8-8.99 cm	
Roof Fall	Mean	19.7	0.1	10.0	0.2	11.75	1.5	9.2	9.4	2.9	1.19	0.9	0.9	0.4	0.8	0.3	
	SD	13.2	0.3	6.9	0.5	7.9	1.6	3.9	7.2	2.9	1.11	1.1	1.0	0.7	0.9	0.7	
	Median	17.5	0.0	9.5	0.0	10.0	1.0	8.5	9.0	1.5	1.00	1.0	1.0	0.0	1.0	0.0	
Hammerstone-on-anvil percussion	Mean	15.6	0.4	4.9	0.7	22.4	2.2	7.4	3.3	2.8	1.56	1.9	0.8	0.8	0.6	0.3	
	SD	9.3	0.6	3.3	1.3	9.5	1.5	5.4	5.7	3.2	1.59	1.2	1.0	0.9	0.7	0.5	
	Median	15.0	0.0	4.5	0.0	22.0	2.0	6.0	1.0	1.5	1.50	2.0	0.5	1.0	0.5	0.0	
Actor		Fragment 9-9.99 cm	Fragment > 10 cm	Distal epiphyseal element (cm)	Proximal epiphyseal element (cm)	Fragments with cortical surface	Fragments with pits and grooves	Fragments with notches	Percent cortical fragments with pits and grooves	Percent cortical fragments with notches	Pseudo-notch count	Pseudo-notch to notch ratio	Notch breadth to notch depth ratio	Flake scar breadth to notch depth ratio	Release angle(°)	Ribs	Hackle Marks
Roof Fall	Mean	0.2	2.7	15.4	16.2	16.5	4.6	0.1	0.3	0.0	2.6	0.4	5.3	8.42	34.7	Yes (100%)	Yes (100%)
	SD	0.4	1.0	6.1	4.6	10.9	2.8	0.3	0.1	0.0	1.5	1.3	0.8	3.54	1.5		
	Median	0.0	2.5	15.7	15.7	13.5	4.5	0.0	0.3	0.0	2.0	0.0	5.4	6.64	35.0		
Hammerstone-on-anvil percussion	Mean	0.4	3.0	13.6	17.0	13.8	6.6	0.7	0.5	0.0	3.2	0.7	4.6	6.06	37.1	Yes (100%)	Yes (100%)
	SD	0.5	1.2	4.1	4.1	6.9	2.9	0.8	0.2	0.1	1.4	1.4	1.8	2.33	4.7		
	Median	0.0	3.0	13.4	18.8	14.0	6.0	0.5	0.5	0.0	3.5	0.0	4.4	6.81	36.0		

4.3 Statistical Test Results and P-values

The results from all tests are reported here. The combined results from each statistical test are presented individually with all tested variables.

Fisher's Exact Test

Table 14 P-values from Fisher's Exact Test for Notch and Incipient Notch Presence

Variable	P-value
Notch presence	0.22
Incipient notch presence	0.39

Variables tested using Fisher's exact test, which are notch presence (p-value=0.22) and incipient notch presence (p-value= 0.39), did not show a significance difference in their presence. This means that notch presence and incipient notch presence were not significantly different between the cave roof fall assemblage and the hammerstone on anvil assemblage. FET p-values are summarized in Table 14.

Spearman's rank correlation

Table 15 P-values and Correlation Coefficients From Spearman's Rank Order on Fragemnt Size Categories Between both Actors

Fragment size (cm)	P-value	Rho coefficient
Under 2	0.09915	0.4268647
2-2.99	0.4766	0.191865
3-3.99	0.6631	0.1181229
4-4.99	0.5408	0.1652486
5-5.99	0.7867	0.07350524
6-6.99	0.3672	0.2416661
7-7.99	0.7047	-0.1028395
8-8.99	0.8744	0.04297722
9-9.99	0.8792	-0.04134491
Over 10	0.1293	0.3956787

Variables tested using Spearman's rank correlation were fragment size categories (see Table 8). Each fragment size variable was tested by investigating if a monotonic relationship

exists between fragment size categories produced by both actors. The p-value of all fragment size variables came back as not significant (p-value > 0.05) as seen in Table 15. This indicates that a monotonic relationship does not exists in fragment categories created by both actors. The overall distribution of each actor's fragment size, in relation to the overall fragment count can be seen in Figure 48.

Mann-Whitney U Test

Table 16 P-values for All Variables Testes Using the Mann-Whitney U Test

Variable	**P-value**
Flake count	0.016*
Pit count	0.0024*
Groove count	0.10
Striation count	0.13
Distal epiphyseal element length (cm)	0.32
Proximal epiphyseal element length (cm)	0.46
Fragments with cortical surface	0.73
Fragments with pits and/or grooves	0.073
Percent cortical fragments with pits and/or grooves	0.000094*
Pseudo-notch count	0.30
Notch breadth to notch depth ratio	0.26

Three variables of the eleven variables tested showed a significant difference as seen in Table 16. Significant variables are differentiated from insignificant variables by red and a star. Flake count (p-value=0.016), pit count (p-value=0.002), and percent cortical fragments with pits or grooves (p-value=0.00009) were all variables that pointed towards a difference between cave roof fall from hammerstone-on-anvil percussion.

Eight variables were not significant in differentiating between cave roof fall and hammerstone-on-anvil percussion. The variables that are not significant are summarized in Table

16. Significant variables are differentiated from insignificant variables by red and a star. Most of the insignificant values have p-values above 0.1 which are all well outside of the necessary 0.05 threshold. One exception is fragments with pits and grooves which has a P-value of 0.073 which is close to threshold. This p-value might be due to the small sample size used in this experiment.

Presence/absence

Both assemblages had BSMs related to dynamic impact stress relief which are ribs and hackle marks (Fisher, 1995; Johnson, 1985). Ribs were observed on at least one fragment in each bone assemblage. Hackle marks were observed on at least one fragment in both bone assemblages. This indicates that dynamic impact was used as a causal agent by both actors to fracture the diaphysis (Gifford-Gonzalez, 1991). The results are summarized in Table 13.

Untestable Variables

Table 17 Variables That Could not be Tested or Were Not Designed to be Tested with Supporting Reasoning

Variable	**Reason**
Fragment count	No archaeological application
Fragments with notches	Less than 5 observations in the cave roof fall sample.
Percent cortical fragments with notches	
Pseudo-notch to notch ratio	
Flake scar breadth to notch depth ratio	
Release angle(^{O})	
Notch breadth	Not tested following Capaldo & Blumenschine (1994) methodology. Used to make ratios
Maximum notch depth	
Flake scar breadth	

Nine variables could not be tested or were not tested as seen in Table 17. Five of the variables could not be tested due to it having less than five observations, which is the minimum

number of observations necessary for the Mann-Whitney U test to test for a difference. Fragment count was not tested because it is sensitive to influence by other actors, making it not applicable to archaeological sites. Three variables were purposefully not tested and not included in Table 13. These variables are notch depth, notch breadth and flake scar breadth. They were used to create the ratios of notch breadth to notch depth and flake scar breadth to notch depth. Those three variables were not tested by Mann-Whitney U test or any other test as following Capaldo & Blumenschine (1994) methodology.

4.4 Significant Variables

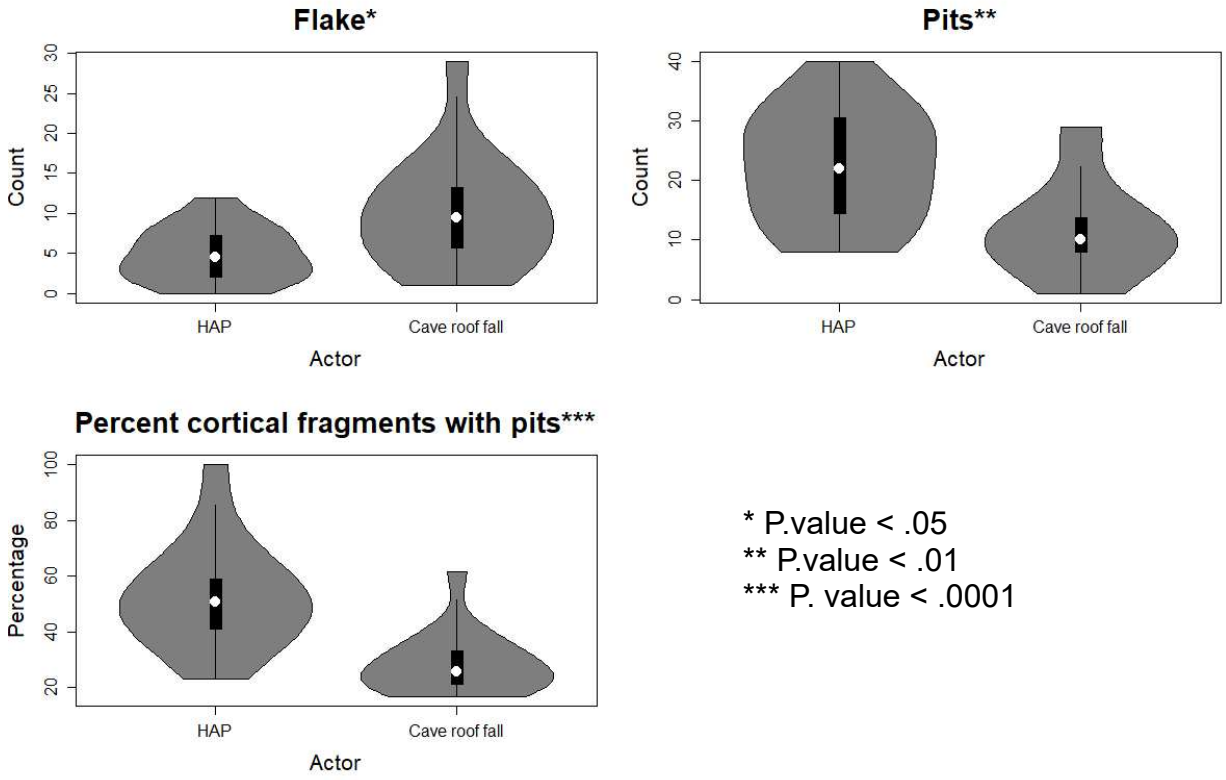

Figure 49 Violin plots of all significant variables. P-value indicators present

Figure 49 shows violin plots for all three significantly different variables. The violin plots do show that a difference exists between the two actors. This is indicated by the median (white

dot) of one actor or both actors existing outside of the interquartile range (black box). An overall difference can also be seen between the medians themselves.

Flake count

Flake count was one of the variables that was found to be significantly different between hammerstone-on-anvil percussion. The cave roof fall sample had a median of 9.5, while the hammerstone-on-anvil sample had a median of 4.5 which is half as small as seen in Table 13. This rejects the null hypothesis that there is no difference between the median of the two samples. This leaves the alternative hypothesis, that there is a difference in flake count. This difference between the medians is also seen in Figure 49. This can be reinterpreted as cave roof fall creates twice as many flakes than hammerstone-on-anvil percussion.

Pit count

Pit count was identified as a variable that was significantly different between cave roof fall and hammerstone-on-anvil percussion. This can be seen in the difference between the medians. The median of cave roof fall is 10 while the median of hammerstone-on-anvil percussion is 22 (see table 13). The hammerstone-on-anvil percussion median is almost twice as large as the cave roof fall median. This difference in medians rejects the null hypothesis. This leaves the alternative hypothesis, that the pit count in the two actors are different. This difference in medians is displayed in the violin plot in Figure 49.

Percentage of cortical fragments with pits

The percentage of cortical fragments with pits is the final variable that points towards a difference between cave roof fall and hammerstone-on-anvil percussion. The difference between the two samples can be seen in their medians and is illustrated in Figure 49. The cave roof fall median is approximated to 0.3, while the hammerstone-on-anvil percussion median is

approximated to 0.5 which is almost twice as large as illustrated in Table 13. This means that hammerstone-on-anvil percussion produces a higher percentage of fragments affected by pits and/or grooves. This difference in medians falsifies the null hypothesis. This leaves the alternative hypothesis, that there is a difference in the proportion of flakes with a pit and/or groove as the only hypothesis left.

4.5 Non-Significant Variables

The rest of the tested variables did not have a significant result for their appropriate tests, as seen in Table 14, 15 and 16. These variables can be grouped together under the following umbrella terms: fragmentation indicators, BSMs, fragment size, and ratios. The hypotheses put forward to test these variables are summarized in Table 10.

Fragmentation indicators

Fragmentation indicators encompass fragments with a cortical surface. Because the P-value provided by the Mann-Whitney test is above 0.05 as seen in Table 16, it can be inferred that there is no difference between both samples. The overlap between the medians can be seen as violin graphs in the Appendix. This falsifies the alternative hypothesis and leaves only the null hypothesis. This suggests that neither actor produces more fragments with an intact cortical surface than the other.

BSM

The BSM that were found to not be different are groove count, striation count, count of fragments with a pit or a groove, pseudo-notch count, notch, and incipient notch presence. The P-value of all these variables was above 0.05 as seen in Table 14 and 16. This implies that there is no significant difference between the medians of these variables for those tested using Mann-Whitney U test and that the binary response tested by FET is not different. This falsifies the

alternative hypotheses leaving only the null hypotheses. This can be interpreted as groove count, striation count, the count of fragments with a pit, pseudo-notch count, notch and incipient notch presence cannot be used to differentiate between the two actors, because neither actor produces more BSM than the other actor.

Fragment size

All fragment sizes proved to not be statistically significant including epiphyseal element length. All these variables had a P-value larger than 0.05 as seen in Table 15 and 16. This implies that there is no significant difference in medians for variables tested with Mann-Whitney U test and a monotonic relationship does not exists between fragment size for both actors. This falsifies the alternative hypothesis and leaves only the null hypothesis. Violin plots in the Appendix illustrate the overlap between medians for epiphyseal element length. The lack of a monotonic relationship between fragment size for each actor is seen in the scatter plots located in the Appendix. This means that fragment size variables and epiphyseal element lengths are not different or correlated between cave roof fall and hammerstone-on-anvil percussion.

Ratios

The only ratio that is part of this umbrella term is notch breadth to notch depth. The P-value, as seen in Table 16, is above 0.05 which means that there is no difference between the two sample medians. This falsifies alternative hypothesis and leaves only the null hypothesis. The overlap between the medians is visualized as a violin plot in the Appendix. The overlap between the medians means that notch breadth to notch depth is not different between the two actors because both create similarly sized notches.

4.6 Research Question Assessment

Testing indicates that out of all variables tested, three proved to be different. With this information, the null hypothesis, that the taphonomic pattern of cave roof fall is not different from hammerstone-on-anvil percussion, can be falsified because three variables were significantly different. The first alternative hypothesis that all variables collected will be different between the two assemblages can also be falsified because only three variables out of the twenty three tested variables were found to be different. This leaves the second alternative hypothesis, that only some of the variables will be different between the two assemblages, as the only viable option. In turn this informs the research question. Yes, the taphonomic signature of cave roof fall is different from hammerstone-on-anvil percussion, but only when flakes, pits, and the proportion of fragments with pits are considered.

4.7 Summary

This actualistic experiment produced three variables that are different between cave roof fall and hammerstone-on-anvil percussion. These variables are flake count, pit count, and the percentage of fragments with pits and/or pits. Cave roof fall creates a greater number of flakes than hammerstone-on anvil percussion. Hammerstone-on-anvil percussion creates more pits as cave roof fall. The percentage of fragments with pits and/or grooves likewise was larger in the hammerstone-on-anvil percussion sample than in the cave roof fall sample. These variables together inform the research question, that the taphonomic signature of cave roof fall is different from hammerstone on anvil percussion only when the significantly different variables are considered. The summary statistics for these statistically different variables are provided in Table 13 and visualized in Figure 49. The following chapter will discuss the implications of these variables and what possibly drives the difference seen in the median between both samples.

CHAPTER V: DISCUSSION

5.1 Significantly Different Variables

As presented in the Results Chapter, three variables were found to be significant different between the taphonomic pattern of cave roof fall and hammerstone-on-anvil percussion using a Mann-Whitney U test. The variables that had a significant difference in their medians are flake count, pit count, and percentage of fragments with pits. These variables are believed to be influenced by either the boulder impact force or the dual impact action of the hammerstone and anvil on the bone diaphysis. Variables that are impact force dependent seem to lean towards cave roof fall, while the variables other variables seem to be influenced by the dual impact action of the hammerstone-on-anvil percussion.

Impact Force, Dual Impact Action, and Blow Distribution

Impact force can be described as the force that an object transfers to another object at the time of impact. The impact force is usually transferred as energy into the receiving object. A higher impact force can be implied about each actor by referring to the number of blows needed to break the diaphysis as seen in Table 11 and 12. On average cave roof fall required about two blows to fracture the tibial diaphysis. This is significantly less when compared to the hammerstone-on-anvil average of 21.9. By comparing the number of blows needed to fracture the tibial diaphysis, it can be implied that cave roof fall produces a higher impact force than hammerstone-on-anvil percussion.

Blow distribution can be defined as the places along the diaphysis where the boulder or hammerstone contacted the bone surface during bone fragmentation. As seen in Table 11 and 12, cave roof fall had a small blow distribution along the diaphysis of the bone, on average delivering two blows. Hammerstone-on-anvil percussion had a much larger blow distribution, on

average requiring about twenty blows to fracture the diaphysis. While blow distribution does not influence any of the significant variables, it could influence some of the non-significant variables.

The dual impact action refers to the hammerstone and anvil impacting two separate sides of the bone diaphysis. Cave roof fall only impacts one side of the bone. This difference is based on the fracture mechanics employed by each actor. Cave roof fall impacted only the medial side of each bone. Hammerstone-on-anvil percussion required for the bone to be impacted from two sides, usually medial and lateral. While previous research has shown that blow intensity is not correlated to BSM production, it could be reasonably assumed that a two pronged assault on the diaphysis by hammerstone and anvil could produce more BSM than a unilateral assault seen in cave roof fall (Pickering & Egeland, 2006).

Bone Flakes

Bone flakes are traces created due to a stress response by the diaphysis following a loading episode (Johnson, 1985). This difference in medians seems to lean towards cave roof fall, as cave roof fall exhibits a higher median. This implies that a higher flake count is seen in the cave roof fall sample.

A possible explanation for the higher number of flakes created by cave roof fall is the higher impact force seen in cave roof fall. The falling boulder used in the cave roof fall simulations breaks the bone shaft through a massive blow concentrated on a small portion of the diaphysis. A high energy transfer is further amplified by a smaller surface area, as the energy can only dissipate at the point of impact and in the surrounding area leading to a higher energy distribution per bone surface area. This contrasts with how hammerstone-on-anvil fractures the diaphysis. Each hammerstone impact transfers less energy to the diaphysis than cave roof fall as

seen in table 11 and 12. Much like the energy transferred by the impact boulder is amplified by a small surface are, the hammerstone impact is also amplified by a small, affected surface area, but nowhere to the degree of the boulder impact. If the inference that cave roof fall does produce a higher energy transfer into the diaphysis can be made based on the impact data, then it can be assumed that more flakes will be produced by cave roof fall. This inference can be made because bone flakes are a stress relief response to energy transfer during a loading episode, so with a higher energy transfer, more flakes should be created (Johnson, 1985).

Pits and percentage of fragments with pits

Pits are created when the topographic relief of a rock's contact face imprints itself on the diaphysis of the bone (Blumenschine & Selvaggio, 1988). Mountains in this relief leave behind pits after each contact with the diaphysis. The number of pits observed in each sample and the percentage of fragments with pits have been shown to be different between cave roof fall and hammerstone-on-anvil percussion. While pits and the percentage of fragments with pits are two distinct variables, they will be discussed together because they are intimately connected. As indicated by the medians of both samples, the percussion pit count and percentage of fragments with percussion pits have much higher medians than those of impact pits and the percentage of fragments with impact pits. This suggests that hammerstone-on-anvil percussion produces more percussion pits and fragments with percussion pits than cave roof fall.

A possible driver for the difference in pit count and percentage of fragments with pits and/or grooves that is seen between the two assemblages is the way that each actor mechanically interacts with and fractures the diaphysis. Cave roof fall is a unidirectional application of force on the bone side that is pointing towards the cave roof. As a result, all BSM including pits and grooves will only occur on the impacted side of the bone. Hammerstone-on-anvil percussion in

contrast has a dual application of force from the hammerstone side and the anvil side. This means that hammerstone-on-anvil percussion has twice as many opportunities to imprint pits and grooves on the cortical surface of the bone (Blumenschine & Selvaggio, 1988). This difference in opportunities to imprint BSM on the bone surface could be a driving factor in pit expression. The percentage of fragments with pits too is likely influenced by the same driver, because pit expression and the proportion of fragments with pits are related. If more pits are created than the proportion of fragments that have a pit is likely to go up as well. While previous research has shown that there is no correlation between processing intensity (number of blows) and pit expression (Pickering & Egeland, 2006), however the dual impact of hammerstone-on-anvil versus the singular impact of roof fall could make a difference in the number of pits created. This is because hammerstone-on-anvil percussion affects both sides of the bone surface, while cave roof fall affects only one side of the bone, which in essence doubles the possible surface area that hammerstone-on-anvil percussion acts on.

5.2 Non-Significant Variables

Twenty variables were found to be not significantly different between cave roof fall and hammerstone-on-anvil percussion. The lack of significance, however, can still be informative, about the suspected drivers and blind spots in experimental design. These variables have will be discussed in broad terms and have been grouped in the same variables that were presented in the Methods section.

Visual

No magnification

Fragments that preserve cortical surface, notch count, incipient notch count, pseudo-notch count, fragments that preserve pits and grooves each proved to not be significantly

different. A common reason for the lack of significance could be attributed to the small sample size used in this experiment.

Fragments that preserve a cortical surface as a variable was not significantly different between the two actors. This suggests that one actor is not prone to stripping the cortical surface when compared to the other actor. This can be interpreted as the larger impact force associates with cave roof fall is able to remove just as much cortical bone as the dual attack of hammerstone-on-anvil percussion or vice versa.

Notches did not appear at a different rate in either assemblage. This is interesting because notches were predicted to appear more in the hammerstone-on-anvil sample, than the cave roof fall sample. This was predicted based on the dual impact action of the hammerstone and anvil affecting two sides of the bone increasing the chances that a notch will form. Animal size could be a different possible explanation, as suggested by Capaldo & Blumenschine (1994), where they found less notches on size 3 animals than size 1 and 2. The bison bones used in this experiment are size 4, which could dampen notch production regardless of impact force, or the dual impact action of hammerstone-on-anvil percussion. incipient notches did not appear at a different rate in the two assemblages.

Incipient notches appeared at the same rate in both assemblages. Cave roof fall was predicted to create more incipient notches because of more energy transfer and dissipation from the impact site. This was thought to create more incipient notches away from impact site, as the fracture front fails to penetrate the thickness of the bone. A possible explanation for this is either that cave roof fall does not dissipate enough energy to promote incipient notches, or that hammerstone-on-anvil percussion dissipates a similar amount of energy over the whole surface area of the bone.

Neither actor seems to have produced an overabundance of pseudo-notches compared to the other. This suggests that while pseudo-notches are seen as an incomplete stress relief trace, neither the energy generated impact force nor the dual impact action of the hammerstone and anvil seem to influence pseudo-notch count.

Finally, fragments that preserve pits and grooves were not shown to be different between the two actors. This is an interesting result when compared to pit count and the percentage of fragments with pits. This might suggest that both actors create fragments with pits at a similar rate, but differ in imprinting pits, and the proportion of fragments with pits. It should be noted that the p-value associated with fragments with pits (0.073) is close to the 0.05 threshold to be significantly different between the two actors. With a larger sample size this variables might prove to be different between the two actors.

Magnification

Striation count and grooves count both proved to not be different between the actors. This is interesting because both were suspected to be higher in the cave roof fall sample. The controlled and methodological breakage technique seen in hammerstone-on-anvil percussion was suspected to dampen the expression of grooves and striations. Cave roof fall was projected to create more striations and grooves due to the random interaction between the diaphysis and the boulder coming to rest on the ground after the impact. This extra movement and contact with an abrasive surface were thought to produce more striations and pits. As indicated by the results this was not the case. It could be possible that while hammerstone-on-anvil percussion is done in a more methodological manner, anvil slippage and other unaccounted variables do enable the expression of grooves and striations. Likewise, it could be possible that the extra contact that the boulder has with the bone is not enough to promote the overexpression of grooves and striations.

Alternatively, a small sample size might have had a role to play in the lack of a significant difference observed in striation count and groove count. With a larger sample size, these two variables might be significantly different.

Presence/Absence

Ribs and hackle marks were present in at least one fragment in each bone assemblage. This does indicate that both actors fracture bone using dynamic loading as a causal agent, however, this does not help in differentiating between the two. If both actors fracture bones through dynamic loading, this means that a sample of bones fractured by cave roof fall cannot be distinguished from a sample of bones fractured through hammerstone-on-anvil percussion, based solely on the presence or absence of ribs and hackle marks, maintaining the equifinality between the two actors.

Measured

Fragment Size

All the fragment size categories proved to not have a monotonic relationship between actors. One possible explanation for the lack of a relationship between fragment size categories for each actor is sample size. The lack of sample size can be seen in the discrepancy between sample size and rho coefficient. This is not a statistical interpretation, rather its an illustration of the idea that adding more data to a correlation test makes the correlation coefficient stronger (Mangiafico, 2018). In Table 15 fragments under 2 cm and over 10 cm have the most data, smallest p-value (0.099 and 0.13) and the highest correlation coefficient (0.43 and 0.4). In contrast, fragments between 8-8.99 cm and 9-9.99 cm have the least data, highest p-values (0.874 and 0.879) and smallest correlation coefficient (0.043 and -0.04). This means that there is not enough data to identify a correlation, especially in the variables with the lowest correlation

coefficient (Mangiafico, 2018). With a larger data set some of the correlations between opposing actor fragment sizes could come to light.

Epiphyseal elements lengths

Epiphyseal element lengths were found not to be different. This is interesting, because both variables, proximal element length, and distal element length, were suspected to be statistically different due to the random nature of boulder strikes. A possible explanation is that enough energy was transferred into the diaphysis by impact force during the cave roof fall experiments to fully fracture the diaphysis outside of the impact area and mimic the epiphyseal element lengths produced by hammerstone-on-anvil percussion. Another possibility might be that the overlap between epiphyseal lengths produced by cave roof fall and hammerstone-on-anvil percussion are an artifact of the small sample size. With a larger sample size, these two variables might prove to be different.

Ratios

The only tested ratio, notch breadth to notch depth, proved not to be significant different between cave roof fall and hammerstone-on-anvil percussion. This ratio describes the overall shape of the notch. It is likely that loading type and animal size category contributed to the lack of a significant difference. As indicated in Capaldo & Blumenschine (1994) with size 3 animals notch breadth to notch depth can no longer distinguish between carnivore created notches and hammerstone-on-anvil percussion created notches. Since buffalos are considered size 4 it can be inferred that differences in notch shape between cave roof fall and hammerstone-on-anvil percussion would be minimized (Blumenschine, 1986). Another possibility might be that the same loading mechanism, in this case, dynamic loading, creates similar or indistinguishable notches (Johnson, 1985). A third possibility might be that an overlap in notch shape is an artifact

of the small sample size. With a larger sample size, notch shape might be a statistically different variable.

5.3 Archaeological Implications

Flake count, pit count and proportion of fragments with pits and/or grooves were the variables that were different between actors. From those variables it can be inferred that the taphonomic signature of cave roof fall is one with more flakes (higher median) and less pits and proportions of fragments with a pit and/or groove (smaller median), when compared to hammerstone-on-anvil percussion. The data gathered from these two single actor assemblages is not applicable to a multi-actor assemblage. This would be an assemblage where both hominins and cave roof fall modified the bones present. The lack of applicability is because while counts and proportions were calculated on the segregated assemblages a pit for example could not be attributed to one actor or the other without prior knowledge of where the pit came from. There were no reliable qualifying or quantifying criteria to accurately differentiate an impact pit from a percussion pit or an impact flake from a percussion flake without prior knowledge of its provenience. This means that these variables are not viable to be applied to a multi-actor archaeological assemblage, which are the most common type of assemblage (Gifford-Gonzalez, 1991).

The lack of criteria to reliably link BSM and the responsible actor is not the only problem with using those variables. Other processes can modify the expression of these variables within an archaeological setting. For example, pits can be abraded away by rough surfaces like sand (Fisher, 1995). This might cause a hammerstone-on-anvil made assemblage to look like a cave roof fall modified assemblage by decreasing the number of observable pits. Flakes are subject to the same attritional forces that can alter other types of assemblages (Gifford-Gonzalez, 2018c). A

cave roof fall created assemblage can resemble a hominin modified assemblage if flakes are deleted through trampling, weathering, or transport. The high potential for additional taphonomic forces to interact with assemblages makes even the significant variables found during this actualistic experiment less conducive determining roof fall as an actor.

This experiment has shown that cave roof fall and hammerstone-on-anvil percussion operate through the same causal agent (dynamic loading) and effector (a rock impact to the bone diaphysis). Furthermore, both actors produce the same traces as seen in the bone flakes, pits, grooves, striations, notches, incipient notches, and pseudo-notches collected from both assemblages. These traces do occur in different counts and frequencies as illustrated by this experiment, but the traces themselves are indistinguishable from a qualitative descriptive approach. This implies that within a hominin modified cave assemblage, cave roof fall would simply amplify the hominin signature adding more of the same BSMs to the assemblage.

Identification of cave roof fall as the definitive actor can only be achieved if the assaulting debris is found on top of the afflicted bone as seen at Shanidar cave (Solecki, 1957; Trinkaus, 1983). However, there are cases as seen in this experiment where boulder 1 broke on impact. A similar situation can be applied to cave sites, where a bedrock fragment breaks on impact with a bone, fractures it imprinting BSMs on the bone surface and vanishing from the archaeological record through erosion. This scenario can influence the way that assemblages believed to be hominin modified are evaluated. For example, a small hominin modified assemblage can be exaggerated if bones are covertly added by cave roof fall, distorting the interpreted size and function of a site. A more extreme example is if cave roof fall modifies hominin bones that were defleshed as part of a mortuary practice and left on the cave floor. The regulated climate of the cave would increase the time that defleshed bone would remain fresh.

The extended period of freshness increases the chance that green, defleshed bones are impacted by falling debris. In this instance, hominin modified bones with cutmarks would further be modified by traces associated with dynamic loading by a falling bedrock boulder. This could happen multiple times on different bones, in different time periods. The interpretation of this assemblage would likely be that the hominin bones were processed for their nutritional value. The error of this interpretation is evident in a laboratory experiment but much more difficult to interpret in a practical capacity. These types of interpretation has been made at sites like Krapina Cave that have a suspected cave roof fall component (Mann & Monge, 2006; Trinkaus, 1985; Ullrich, 2005)

To summarize the variables that proved to be significantly different in this experiment are not applicable to the archaeological record. The lack of archaeological application is because while counts and frequencies were created around each trace, the traces themselves did not have any reliable distinguishing properties. This is problematic in a multi-actor assemblage, because of traces themselves cannot be distinguished between percussion and cave roof fall derived, then all the distinguishing criteria at higher levels, that were investigated in this experiment are fraught with errors. The lack of distinction can also be applied to archaeological sites with a suspected roof fall component. The lack of a proper trace actor connection can greatly distort the interpretation of an assemblage. A large sample size might yield better indicators, such as quantifiable notch dimensions proposed by Capaldo & Blumenschine (1994). A different approach would be to quantify BSM dimensions using a profilometer as proposed by Pante et al. (2017).

5.4 Limitations of the study

This study was the first step in characterizing the taphonomic pattern of cave roof fall. However, there are certain limitation which should be considered. The pulley system that was used to simulate cave roof fall had some inherent flaws. The sample size and animal size category used for this study do have some flaws. Finally, the untested variables are a reminder that this study does have some limitations in its interpretations.

Pulley Design

Cave roof fall was simulated by looping a rope around two different tree branches to achieve the intended heights. This simple design was used to avoid the rental of machinery which would overcomplicate the experiment through higher expenses, scheduling, and proper certifications. This pulley design however had its draw backs. The first one was human error, as there were many times when the rock was slowed down either by mistakenly stepping on the rope, or through other human errors. The other draw back was friction. This was evident in the second part of the experiments where the rope would enter grooves or notches in the tree bark and slow down descent of the rock to a crawl. These incidents were recorded, but nothing could be done to rectify them.

Sample Size

Sample size was a severe limitation in this study. This limitation was in part due to the supply of tibiae available as High Point Bison (the supplier) only slaughters a set number of bison during the spring and fall, this means that a limited number of tibiae were available. While sixteen bones are a good starting number, it should be a priority to expand this number in future.

Animal Size Class

Bison as a size 4 animal might also have been a limitation (Blumenschine, 1986). As indicated in Capaldo & Blumenschine (1994) notch frequency and diagnostic notch properties diminish when going from a size 2 animal bone to a size 3 animal bone. With this trend it is entirely possible that a size 4 animal bone might not harbor as many diagnostic variables, as say a size 2 animal bone might harbor.

Untested Variables

Most of the variables related to notches were untestable due to fewer than 5 observations in the cave roof fall sample. These notch-related variables were fragments that exhibit a notch, percentage of fragments with a notch, pseudo-notch to notch ratio, flake scar breadth to notch depth and release angle. With a higher sample size these variables might be able to be tested to ascertain their significance potential. Of the untested notch variables, it is likely that overall flake dimension would not be different due to the use of a size 4 animal and the similarity is used causal agent (Capaldo & Blumenschine, 1994).

5.5 Summary

Impact force, dual impact action by the hammerstone and anvil and blow distribution are suspected to be the drivers behind the statistically different variables flake count, pit count and percentage of fragments with pits. Impact force seems to be the driver for cave roof fall influenced variables, while the dual impact action by the hammerstone and anvil, and blow distribution seems to be the driver for hammerstone-on-anvil influenced variables. All the other tested variables are either inherently not different or are not significantly different due to a small sample size. These variables are not useful in an archaeological setting because the traces themselves are not identifiable. Future attempts should focus on a quantifiable approach to

describe and differentiate the traces produced by both actors. The study has some limitation in boulder drop mechanism, sample size, animal size category and untested variables due to a small sample size. These limitations should be considered for any future studies.

CHAPTER VI: CONCLUSION

6.1 The Experiment

The purpose of this experiment was to characterize the taphonomic signature of cave roof fall and compare it to the taphonomic signature of hammerstone-on-anvil percussion. This was done to solve the current equifinality that exists between the two actors (Oliver, 1989). This equifinality exists because both actors leave the same basic traces, fracture the diaphysis through the same causal agent and have the same effector. Before a comparison between the two actors could be made, actualistic experiments were carried out to create a sample for each actor following the suggestion of Binford (1981b). The hammerstone-on-anvil sample was created by placing a bone on an anvil and hitting the diaphysis longitudinally with a hammerstone. The cave roof fall sample was generated by simulating a cave roof fall from various heights and with various weights over bones. To explore the current equifinality, the traces of both actors were described, quantified and compared.

Thirty-four variables were created to categorize the data gathered from the traces. These variables were organized by the method with which they were gathered. Visually gathered variables were identified by an unaided visual inspection, aided visual inspection using a 3x magnifying glass and a 10x hand lens, or most simplistically by their presence or absence. Measured variables were measured using digital calipers or a tape measure. Composite variables were ratios that were constructed using either visual data or measured data. The same variables were gathered from both the hammerstone-on-anvil and the simulated roof fall assemblages. Notch and incipient notch presence was tested using FET. Fragment size categories were tested for a monotonic correlation using Spearman's rank order test. All other testable variables were tested using a Mann-Whitney U test to test for a difference. Presence/absence variables were

counted and recoded as a percentage. Nine variables were not tested. Eight of these variables could not be tested, as seen with the notch measurements (Capaldo & Blumenschine, 1994), or had less than five observations in the cave roof fall sample, as illustrated by most of the data pertaining to notches. Fragment count was not tested because it can easily be influenced by other actors and is not taphonomically informative.

Three variables were shown to be significant different between cave roof fall and hammerstone-on-anvil percussion. The three significant variables were flake count, pits count, and percentage of cortical fragments with pits. Twenty variables proved not be significantly different between cave roof fall and hammerstone-on-anvil percussion. These results suggest that there is a difference between the taphonomic signature of cave roof fall and hammerstone-on-anvil percussion.

The variables that proved to be significant are most likely influenced by impact force and the dual impact of the hammerstone and anvil. A higher number of flakes seem to be driven by the higher impact force generated by cave roof fall. Higher pit count, percentage of fragments with pits are likely influenced by the dual impact of the hammerstone and anvil acting on both sides of the bone. Other variables might prove significant if the sample size is increased and more observations are recorded. The archaeological potential of the significantly different variables is called into question however, because the lack of differentiation at the trace level makes the identification of traces in a complex multi-actor assemblage unattainable.

6.2 Future Directions

This experiment characterized the taphonomic signature of cave roof fall by analyzing the trace patterns leftover from an actualistic simulation of cave roof fall. This data was compared to data collected from an actualistically derived hammerstone-on-anvil sample, which yielded some

significantly different variables. However, the sample size was small, with only sixteen bones in each sample. Some variables were not able to be tested because not enough observations were recorded. Future research needs to expand the cave roof fall sample size. Furthermore, the different variables need to be verified after the sample size has been expanded to validate that the variables are still different and not an artifact of the small sample size. Finally, with an expanded sample size, the variables that could not be tested need to be reanalyzed to find their significance potential. A future study is recommended to investigate the two assemblages through quantitative means to effectively identify and characterize the two assemblages at a trace level.

The findings of this experiment are the first steps toward investigating and defining the taphonomic pattern of cave roof fall. If the statistically different variables do survive the verification process, then the taphonomic signature seen in this experiment can be connected to cave roof fall only within an actualistic setting. However, the significant variables cannot be applied to the archaeological record because the traces that the variables are built upon are not descriptively unique and cannot be differentiated between actors. Future research should describe the traces created by both actors through quantifiable means. A qualitative approach to explore the equifinality between the two actors failed to do so, however a future quantitative approach might provide the means to refine the hominin taphonomic signature by potentially eliminating any interference caused by cave roof fall.

APPENDIX

Appendix 1: Materials

Table 18 Materials used in Cave Roof Fall and Percussion Actualistic Studies

Material	Type	Quantity	Use	Notes
Bison bone[d]	Tibia	16	To be broken	Defleshed
Bison bone[a]	Tibia	16	Percussion sample	Bones were broken in a different experiment
Sandstone boulder[b]	6.8 kilograms	2	To be dropped on bones	Duplicates bought in case one breaks
	13.6 kilograms	2		
Rope	30.5 meters	1	To hoist boulder up	
Heights	4.6 meters	1	For boulder to be hoisted up to	Achieved using tree branches
	7.6 meters	1		
Tarp	Generic	1	Prevent the loss of fragments	
Hand scale	Generic	1	Weight potential rocks	Up to 22.7 kg recommended
Cloth bag	Generic	1	To weigh potential rocks in	
Ladder	3 meters	1	Used to reach tree branches	
Metamorphic Hammerstone	River cobble	1	Bone percussion	
Metamorphic Anvil	N/A	1	Bone percussion platform	
Cooler	Generic	1	Store and keep the bones at a stable temperature	
Garbage bags	White	32	Keep bones and fragments separate before boiling	
Permanent marker	Black	1	Mark garbage bags with bone ID	
Canning pot	21.5 qt/20.3 L	2	Boil broken bones in	
Enzyme detergent	Ecos Plus Liquid Laundry Detergent	.25 L/bone	Used as degreaser agent	
Borax	20 Mule Team	.25 L/bone	Degreaser booster	
Tongs	Silicone tipped	1	Remove bones from the boiling pot	Silicone tips were necessary to prevent any bone modifications
Dishwashing rubber gloves	Generic	4	Handle bones before and after boiling	Bristles on the palm were used to remove residual tissue after boiling
Paper bags	Generic	16	Used to keep and dry fragments separate after boiling	Stored outside
Plastic bin	Generic	1	Used to protect bones from animals	Holes drilled in walls to allow airflow
Hydrogen Peroxide	Liquid form	~4 Gallon bottles	Bleaching and antibiotic agent	40V or 12 %
Underbed storage bin	Generic	1	Receptacle to wash bones in	
Nail polish	Generic	1	Accessioning	

Permanent marker	Black	2	Accessioning	Fine point
Plastic bags	Generic	32	Fragments storage	Zip top
Magnifying glass & Hand lens	3x & 10x	1	Identify BSM	
Lamp	Incandescent	1	Provide light for BSM identification	
Putty	Impressive Putty	9 oz	To create a mold of notches	Reusable putty was used to bring down the cost
Goniometer	Generic	1	To measure release angle	
Digital Calibers	Generic	1	To measure notch molds and fragments	
R studio	Program	N/A	Statistical software	Vioplot package used
[a]- Bison tibiae were procured from High Point Bison Ranch, Wyoming [b]-Sandstone boulder was donated by Rock Garden, Fort Collins, and Pioneer Landscaping, Fort Collins				

Appendix 2: Cave Roof Fall Raw Data Tables

Table 19 7.6 m Boulder Drops

Bone Number	Bone Side	Impact Plane	Rock (boulder)	Number of contacts before breakage occurred	Number of trials before breakage occurred
1	Left	Medial	2 (13.6 kg)	1	1
2	Right	Medial	2 (13.6 kg)	1	1
3	Right	Medial	2 (13.6 kg)	2	2
4	Left	Medial	2 (13.6 kg)	1	1
5	Left	Lateral^	1*/3 (6.8 kg)	2	3
6	Right	Medial	3 (6.8 kg)	1	1
7	Left	Medial	3 (6.8 kg)	1	1
8	Right	Medial	3 (6.8 kg)	1	3

^Lateral side used due to the presence of cut marks from the butcher on the medial side
*Rock(boulder) #1 only used for one drop because it broke upon impact. Rock #3 used for remainder of experiment

Table 20 4.6 m Boulder Drops

Bone Number	Bone Side	Impact Plane	Rock (boulder)	Number of contacts before breakage occurred	Number of trials before breakage occurred
9	Right	Medial	3 (6.8 kg)	1	1
10	Left	Medial	3 (6.8 kg)	3	4
11	Right	Medial	3 (6.8 kg)	1	1
12	Right	Medial	3 (6.8 kg)	2	2
13	Right	Medial	2 (13.6 kg)	3	3
14	Left	Medial	2 (13.6 kg)	1	1
15	Left	Medial	2 (13.6 kg)	4	4
16	Right	Medial	2 (13.6 kg)	3	3

Table 21 Raw Data from the Roof Fall Simulation Experiment Trials

Bone	Trial	Trail Results	Drop Height	Rock Number	Rock Weight
ASH-T-01	1	Contact with bone. Breakage occurred.	7.6 Meters	Boulder 2	13.6 KG
ASH-T-02	1	Contact with bone. Breakage occurred.			
ASH-T-03	1	Contact with bone. No breakage.			
ASH-T-03	2	Contact with bone. Breakage occurred.			
ASH-T-04	1	Contact with bone. Breakage occurred.			
ASH-T-05	1	Contact with bone. No bone breakage. Rock breakage occurred.		Boulder 1	6.8 KG
ASH-T-05	2	No contact		Boulder 3	
ASH-T-05	3	Contact with bone. Breakage occurred.			
ASH-T-06	1	Contact with bone. Breakage occurred.			
ASH-T-07	1	Contact with bone. Breakage occurred.			
ASH-T-08	1	No contact.			
ASH-T-08	2	No contact.			
ASH-T-08	3	Contact with bone. Breakage occurred.			
ASH-T-09	1	Contact with bone. Breakage occurred.	4.6 Meters	Boulder 3	6.8 KG
ASH-T-10	1	Contact with bone. Breakage did not occur.			
ASH-T-10	2	Contact with bone. Breakage did not occur.			
ASH-T-10	3	No contact with bone.			
ASH-T-10	4	Contact with bone. Breakage occurred.			
ASH-T-11	1	Contact with bone. Breakage occurred.			
ASH-T-12	1	Contact with bone. Breakage did not occur.			
ASH-T-12	2	Contact with bone. Breakage occurred.			
ASH-T-13	1	Contact with bone. Breakage did not occur.		Boulder 2	13.6 KG
ASH-T-13	2	Contact with bone. Breakage did not occur.			
ASH-T-13	3	Contact with bone. Breakage occurred.			
ASH-T-14	1	Contact with bone. Breakage occurred.			
ASH-T-15	1	Contact with bone. Breakage did not occur.			
ASH-T-15	2	Contact with bone. Breakage did not occur.			
ASH-T-15	3	Contact with bone. Breakage did not occur.			
ASH-T-15	4	Contact with bone. Breakage occurred.			
ASH-T-16	1	Contact with bone. Breakage did not occur.			
ASH-T-16	2	Contact with bone. Breakage did not occur.			
ASH-T-16	3	Contact with bone. Breakage occurred.			

Table 22 Raw Cave Roof Fall and Hammerstone-on-Anvil Percussion Collected from All Fractured Bison Bones

Bone ID	Actor	Fragment count	Incipient notch count	Flake number count	Notch count	Pit count	Groove count	Striation count	Fragments <2 cm	Fragment 2-2.99 cm	Fragment 3-3.99 cm	Fragment 4-4.99 cm	Fragment 5-5.99 cm	Fragment 6-6.99 cm	Fragment 7-7.99 cm	Fragment 8-8.99 cm	Fragment 9-9.99 cm	Fragment > 10 cm
ASH-T-1	Roof fall	14	0	10	0	18	3	8	5	1	2	2	1	0	1	0	0	2
ASH-T-2	Roof fall	21	0	11	0	28	1	8	11	5	1	1	0	1	0	0	0	2
ASH-T-3	Roof fall	28	0	17	0	29	6	10	12	10	0	0	1	1	1	0	0	3
ASH-T-4	Roof fall	34	0	13	0	13	1	12	16	5	2	2	2	0	3	0	1	3
ASH-T-5	Roof fall	7	0	3	0	4	0	9	3	0	0	1	1	0	0	0	0	2
ASH-T-6	Roof fall	8	0	2	0	11	3	16	5	0	0	0	0	0	0	0	0	3
ASH-T-7	Roof fall	31	0	12	0	9	1	8	13	5	2	4	1	0	0	2	0	4
ASH-T-8	Roof fall	19	0	6	0	8	1	9	13	2	0	0	0	0	2	0	0	2
ASH-T-9	Roof fall	12	1	9	0	8	0	4	4	1	1	1	1	0	1	0	1	2
ASH-T-10	Roof fall	5	0	1	0	2	1	7	1	0	1	0	0	0	0	0	1	2
ASH-T-11	Roof fall	8	0	0	0	1	0	2	2	1	0	0	1	0	1	0	0	3
ASH-T-12	Roof fall	31	0	14	0	16	1	11	13	4	2	0	3	2	1	0	0	4
ASH-T-13	Roof fall	8	0	4	0	12	1	5	3	1	1	0	0	0	1	1	0	1
ASH-T-14	Roof fall	19	1	13	2	9	2	14	10	4	1	1	0	0	0	0	0	3
ASH-T-15	Roof fall	54	0	29	1	13	0	8	29	7	4	1	3	2	1	2	0	5
ASH-T-16	Roof fall	16	0	6	0	8	3	16	8	1	2	2	0	1	0	0	0	2
RSK-001	Hammerstone-on-anvil	4	0	0	0	11	1	4	0	0	0	0	0	1	0	0	1	2
RSK-002	Hammerstone-on-anvil	14	0	2	1	32	2	20	0	1	0	4	2	2	2	0	1	2
RSK-003	Hammerstone-on-anvil	11	1	3	1	15	3	1	0	0	2	2	2	1	0	1	0	3
RSK-004	Hammerstone-on-anvil	37	0	12	5	18	4	2	22	2	2	2	2	3	1	0	0	3
RSK-005	Hammerstone-on-anvil	10	0	3	0	30	3	5	0	5	0	1	1	0	0	0	1	2
RSK-006	Hammerstone-on-anvil	10	1	2	0	28	3	17	0	0	2	3	0	0	1	1	0	3
RSK-007	Hammerstone-on-anvil	18	0	2	0	32	3	7	0	7	1	3	0	1	1	0	0	5
RSK-008	Hammerstone-on-anvil	11	0	3	0	21	0	4	1	0	3	2	0	2	0	0	0	3
RSK-009	Hammerstone-on-anvil	17	0	7	0	20	2	14	2	1	2	3	1	1	0	1	1	5
RSK-010	Hammerstone-on-anvil	3	0	1	0	10	1	2	0	1	0	0	0	0	0	0	0	2
RSK-011	Hammerstone-on-anvil	7	1	3	0	26	1	7	1	0	0	0	3	0	1	0	0	2
RSK-012	Hammerstone-on-anvil	20	0	7	1	40	2	9	4	3	3	3	0	1	1	0	0	5
RSK-014	Hammerstone-on-anvil	19	1	4	1	13	0	5	2	5	5	1	1	0	2	0	1	2
RSK-015	Hammerstone-on-anvil	19	0	9	0	8	2	7	6	4	1	2	0	0	1	1	0	4
RSK-016	Hammerstone-on-anvil	33	2	8	0	23	1	5	10	11	4	3	0	1	0	1	1	2
RSK-017	Hammerstone-on-anvil	10	0	8	2	32	1	10	5	5	0	2	1	0	0	0	0	3

Bone ID	Actor	Distal fragment in cm	Proximal fragment in cm	Fragments with cortical surface count	Fragments with pits and grooves count	Fragments with notches count	Fragments with pits and grooves to total cortical	Fragments with notches to total cortical	Psudonotch count	Psudonotch to notch ratio	Ribs	Hackle marks	Comments
ASH-T-1	Roof fall	19.4	15.5	13	8	0	0.615384615	0	2	0	Yes	Yes	
ASH-T-2	Roof fall	23.3	12.7	18	7	0	0.388888889	0	1	0	Yes	Yes	One Fragment created before 11/20
ASH-T-3	Roof fall	5.6	15.8	26	6	0	0.230769231	0	2	0	Yes	Yes	
ASH-T-4	Roof fall	18	15.4	27	6	0	0.222222222	0	2	0	Yes	Yes	one ratic fragment generated 3/1/1Two fragments created before 11/19
ASH-T-5	Roof fall	24.4	16.1	6	2	0	0.333333333	0	3	0	Yes	Yes	
ASH-T-6	Roof fall	16.8	16	7	2	0	0.285714286	0	5	0	Yes	Yes	
ASH-T-7	Roof fall	8.1	12.1	27	6	0	0.222222222	0	4	0	Yes	Yes	1 Fragment created on 6/4
ASH-T-8	Roof fall	11.5	24.7	14	3	0	0.214285714	0	2	0	Yes	Yes	1 fragment created 3/1/1One fragment created before 11/18
ASH-T-9	Roof fall	19.9	13.5	10	2	0	0.2	0	0	0	Yes	Yes	Question pit
ASH-T-10	Roof fall	8.43	24.5	5	1	0	0.2	0	2	0	Yes	Yes	
ASH-T-11	Roof fall	24.7	10	6	1	0	0.166666667	0	5	0	Yes	Yes	2 fragments created later 2/27
ASH-T-12	Roof fall	14.2	12.5	27	9	0	0.333333333	0	1	0	Yes	Yes	Multiple fragments created on an unknown date/One fragment created on 6/8/2021/One fragment created before 2/18/2022
ASH-T-13	Roof fall	8.2	24.6	7	2	0	0.285714286	0	3	0	Yes	Yes	lateral side drop due to cutmark
ASH-T-14	Roof fall	17.7	15.8	14	4	1	0.285714286	0.071428571	3	1.5	Yes	Yes	1 Fragment created before 11/18/21
ASH-T-15	Roof fall	11.72	11.76	44	9	1	0.204545455	0.022727273	5	5	Yes	Yes	Frag 23 weirdness ask paige/2 fragments created on 3/31 due to molding process
ASH-T-16	Roof fall	14.67	17.9	13	5	0	0.384615385	0	2	0	Yes	Yes	
RSK-001	Hammerstone-on-anvil	18.4	14.2	4	4	0	1	0	2	0	Yes	Yes	
RSK-002	Hammerstone-on-anvil	16.1	12.24	14	9	1	0.642857143	0.071428571	2	0.5	Yes	Yes	One Frag created at some point before 2/23/2022
RSK-003	Hammerstone-on-anvil	10.25	15.3	11	6	2	0.545454545	0.181818182	5	1.666666667	Yes	Yes	
RSK-004	Hammerstone-on-anvil	11.17	18.5	26	6	2	0.230769231	0.076923077	3	0.6	Yes	Yes	One fragment generated on 5/11
RSK-005	Hammerstone-on-anvil	8.37	20.6	9	6	0	0.666666667	0	2	0	Yes	Yes	
RSK-006	Hammerstone-on-anvil	13.93	19.7	9	7	0	0.777777778	0	1	0	Yes	Yes	
RSK-007	Hammerstone-on-anvil	11.7	19.6	17	7	1	0.411764706	0	4	0	Yes	Yes	
RSK-008	Hammerstone-on-anvil	16.8	22.8	10	5	0	0.5	0	4	0	Yes	Yes	One frage created before 3/1/2022 counted
RSK-009	Hammerstone-on-anvil	10.29	11.78	17	8	1	0.470588235	0	3	0	Yes	Yes	One frag created before 12/7
RSK-010	Hammerstone-on-anvil	17.5	19	9	1	0	0.333333333	0	1	0	Yes	Yes	
RSK-011	Hammerstone-on-anvil	15.4	21.3	7	4	0	0.571428571	0	5	0	Yes	Yes	Two frag created on 2/23/2022, not counted
RSK-012	Hammerstone-on-anvil	14.23	10.3	18	10	2	0.555555556	0.111111111	5	5	Yes	Yes	1 Frag created before 12/8/21 not counted because it could be fitted back
RSK-014	Hammerstone-on-anvil	6.93	19	17	6	1	0.352941176	0.166666667	2	2	Yes	Yes	3 Frags created before 3/3/2022/Frags counted
RSK-015	Hammerstone-on-anvil	11.37	16.1	17	7	0	0.411764706	0	4	0	Yes	Yes	1 frag created before 12/9/2021 Frag counted
RSK-016	Hammerstone-on-anvil	12.81	21	27	14	0	0.518518519	0	4	0	Yes	Yes	2 fragments created on 12/4/2021/4 additional fragments created before 2/28/2022/ All frags counted/One frag created on 3/1/2022 not counted
RSK-017	Hammerstone-on-anvil	22.9	10.88	14	6	1	0.428571429	0.071428571	4	2	Yes	Yes	

Table 23 Notch and Incipient Notch Dimensions, Ratios and Release Angle

Notch ID	Actor	Notch Breadth	Notch Depth	Flake scar breadth	Notch Breadth: Notch Depth	Flake scar breadth: Notch depth	Release Angle
ASH-T-14-I	rf	1.56	0.25	1.53	6.24	6.12	36
ASH-T-14-II	rf	0.8	0.14	0.93	5.714285714	6.642857143	33
ASH-T-15-I	rf	1.35	0.26	3.25	5.192307692	12.5	35
ASH-T-9-N1	rf	2.72	0.66	NA	4.121212121	NA	NA
ASH-T-14-N1	rf	1.94	0.36	NA	5.388888889	NA	NA
RSK-002-I	hap	0.64	0.17	1.17	3.764705882	6.882352941	32
RSK-003-I	hap	0.98	0.32	1.53	3.0625	4.78125	39
RSK-003-II	hap	1.92	0.35	2.53	5.485714286	7.228571429	38
RSK-003-III	hap	1.4	0.18	0.248	7.777777778	1.377777778	33
RSK-004-I	hap	1.01	0.31	1.52	3.258064516	4.903225806	34
RSK-004-II	hap	1.62	0.47	1.86	3.446808511	3.957446809	42
RSK-004-III	hap	1.01	0.22	2.05	4.590909091	9.318181818	34
RSK-004-IV	hap	1.56	0.27	1.84	5.777777778	6.814814815	35
RSK-004-V	hap	1.45	0.53	2.16	2.735849057	4.075471698	36
RSK-012-I	hap	0.84	0.43	1.93	1.953488372	4.488372093	50
RSK-014-I	hap	2.02	0.31	2.75	6.516129032	8.870967742	36
RSK-017-I	hap	2.21	0.5	4.33	4.42	8.66	38
RSK-017-II	hap	0.84	0.18	1.33	4.666666667	7.388888889	35
RSK-011-N1	hap	1.36	0.42	NA	3.238095238	NA	NA
RSK-006-N1	hap	1.17	0.35	NA	3.342857143	NA	NA
RSK-014-N1	hap	2.15	0.77	NA	2.792207792	NA	NA
RSK-016-N2	hap	3.78	0.57	NA	6.631578947	NA	NA
RSK-016-N1	hap	3.68	0.74	NA	4.972972973	NA	NA
RSK-003-N1	hap	3.43	0.41	NA	8.365853659	NA	NA

Table 24 Total Fragment Size Categories per Assemblage and Percentage of Fragment Size Categories to Total Fragment Count

Fragment size category	Actor Fragment Size Total		Actor fragment total		Fragment category/Fragment total		Percentage	
	RF	HAP	RF	HAP	RF	HAP	RF	HAP
Fragments <2 cm	150	53	315	249	0.48	0.21	47.62	21.29
Fragment 2-2.99 cm	47	45	315	249	0.15	0.18	14.92	18.07
Fragment 3-3.99 cm	19	25	315	249	0.06	0.10	6.03	10.04
Fragment 4-4.99 cm	15	31	315	249	0.05	0.12	4.76	12.45
Fragment 5-5.99 cm	14	13	315	249	0.04	0.05	4.44	5.22
Fragment 6-6.99 cm	7	13	315	249	0.02	0.05	2.22	5.22
Fragment 7-7.99 cm	12	10	315	249	0.04	0.04	3.81	4.02
Fragment 8-8.99 cm	5	5	315	249	0.02	0.02	1.59	2.01
Fragment 9-9.99 cm	3	6	315	249	0.01	0.02	0.95	2.41
Fragment > 10 cm	43	48	315	249	0.14	0.19	13.65	19.28

Appendix 3: Results Histograms

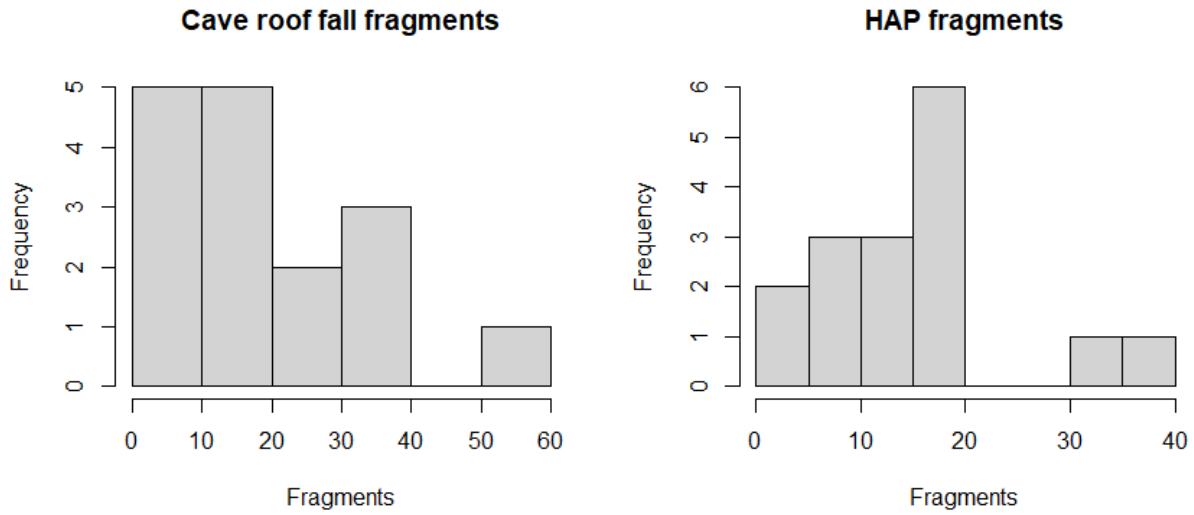

Figure 50 Fragment count

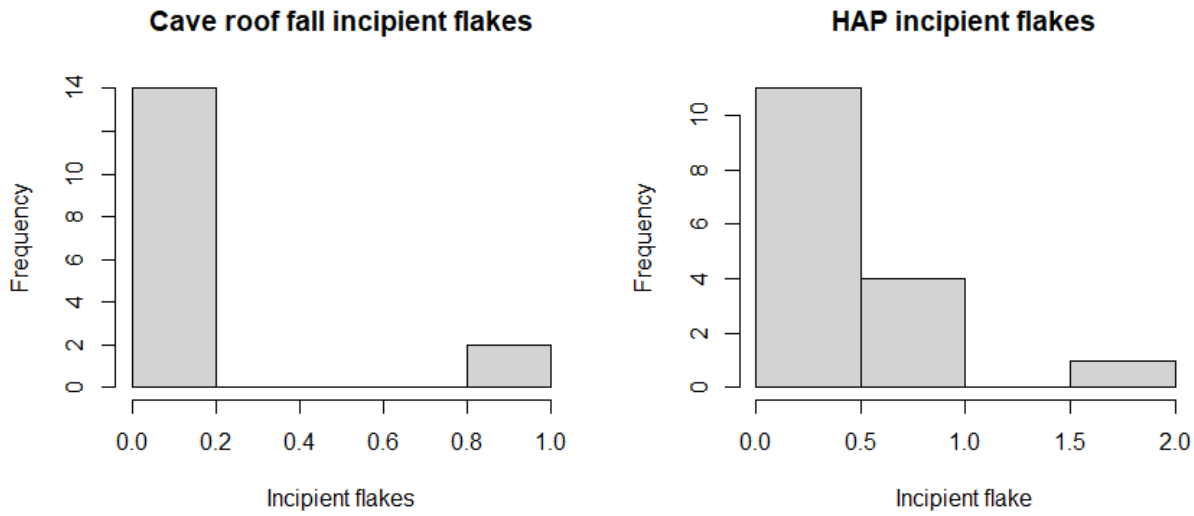

Figure 51 Incipient flake count

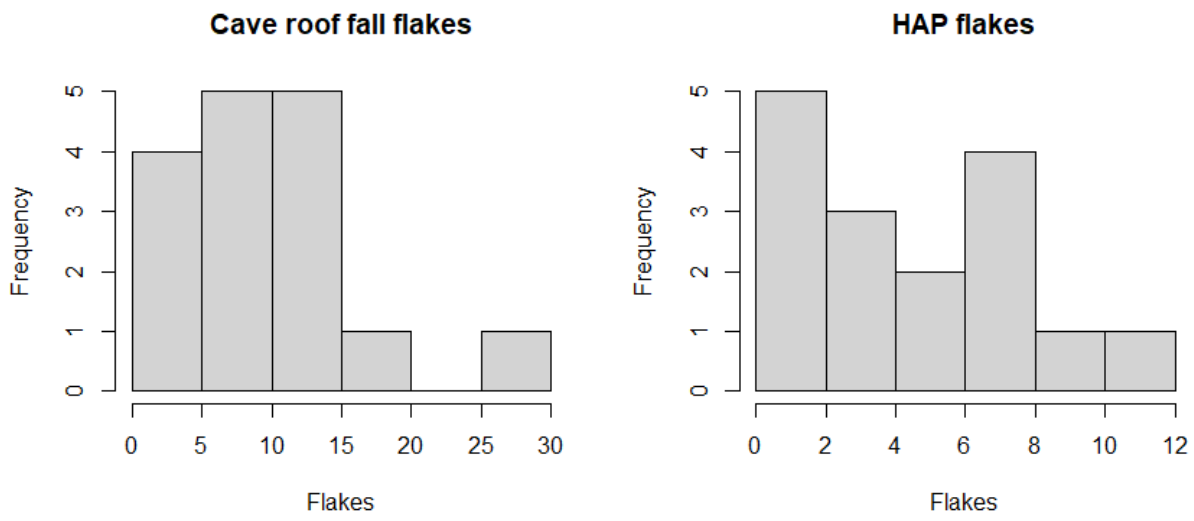

Figure 52 Flake count

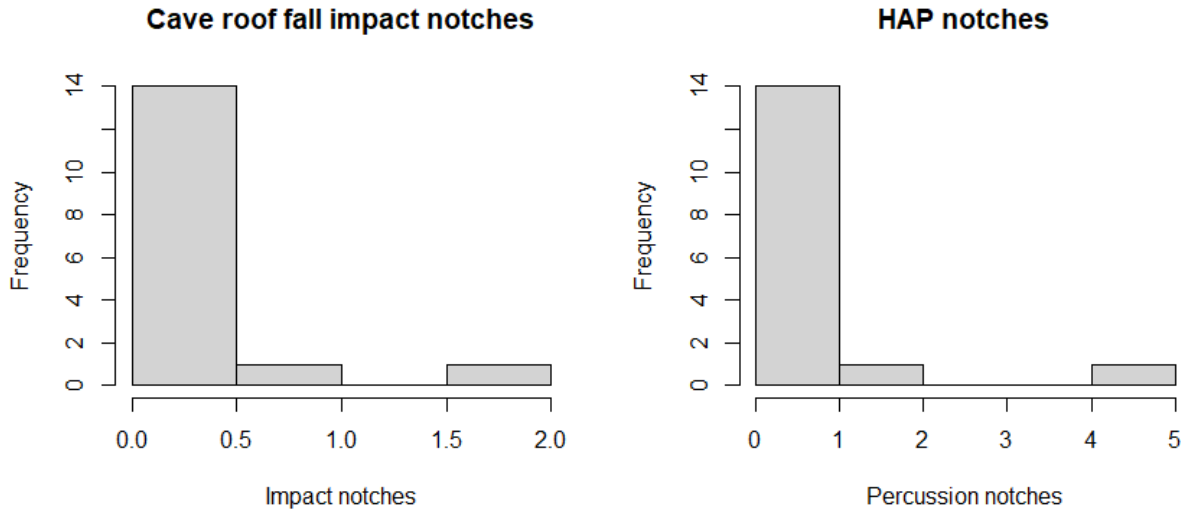

Figure 53 Notch count

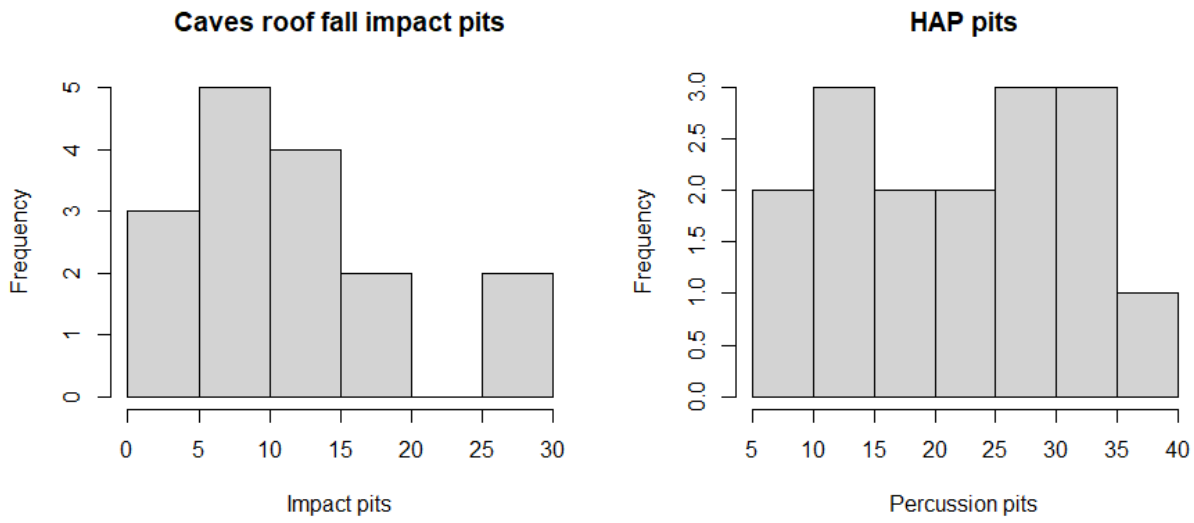

Figure 54 Pit count

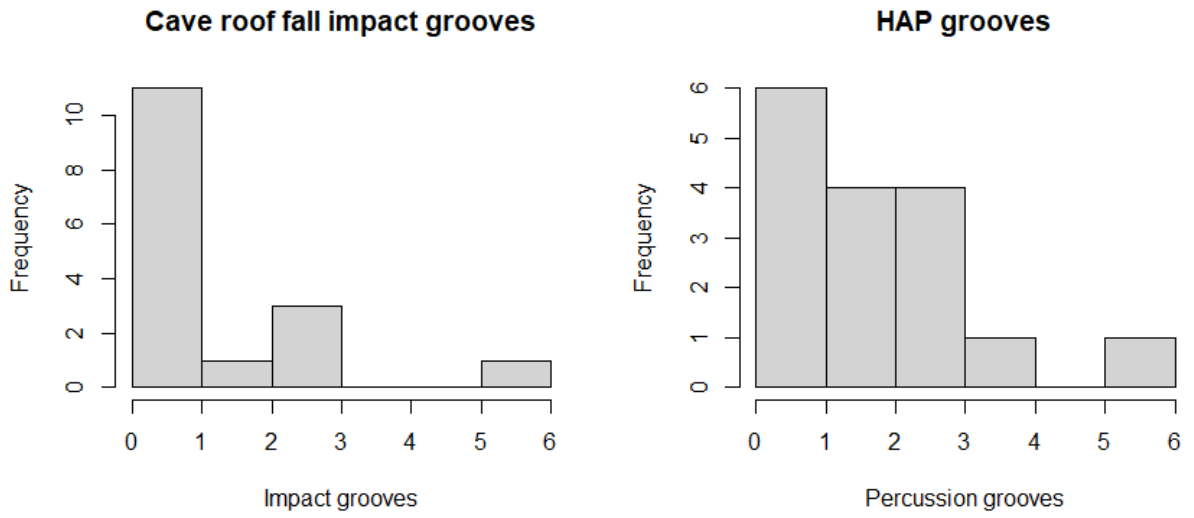

Figure 55 Groove count

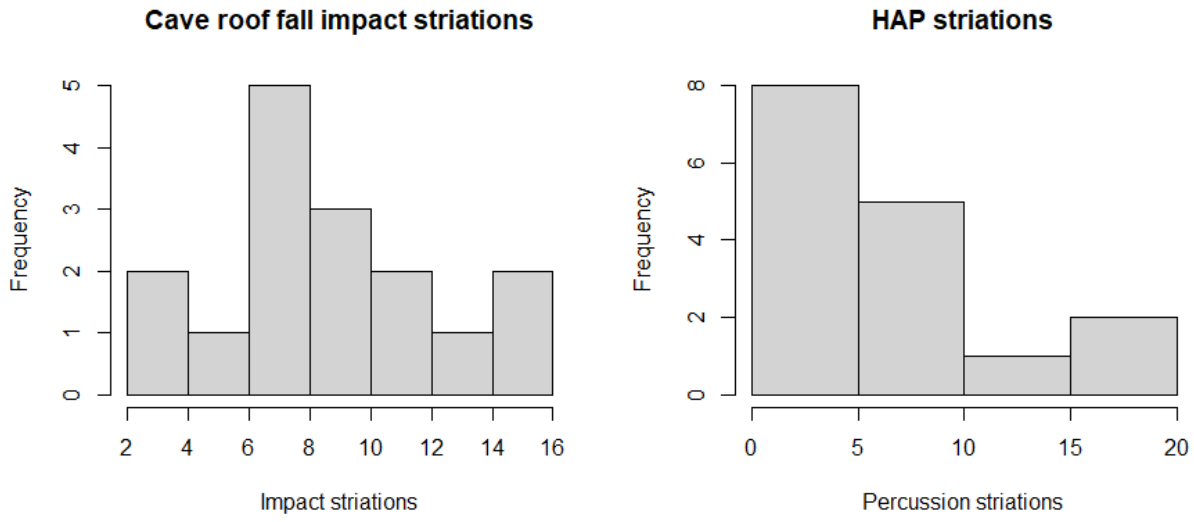

Figure 56 Striation count

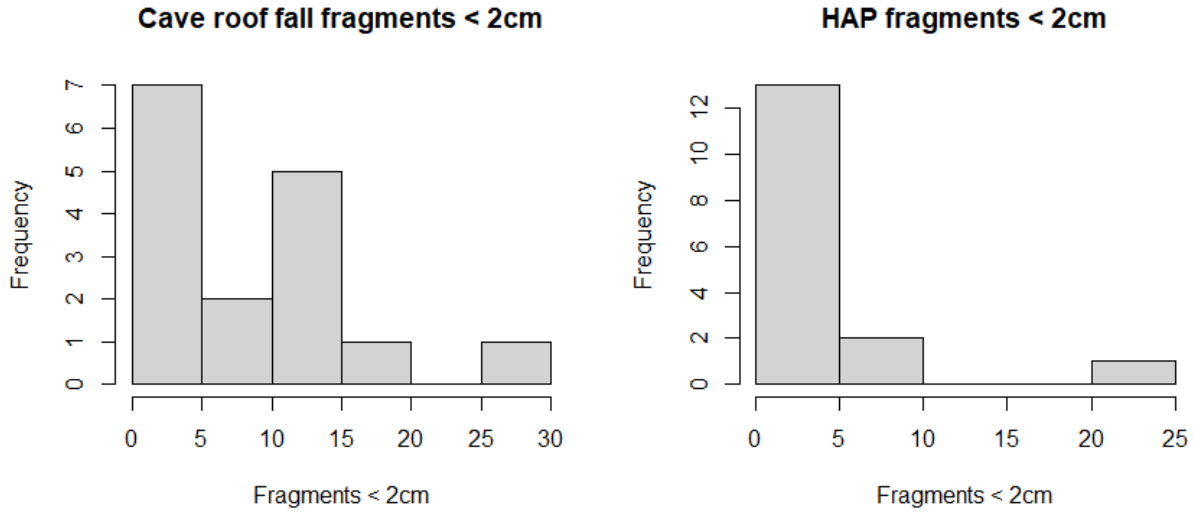

Figure 57 Fragments less than 2 cm count

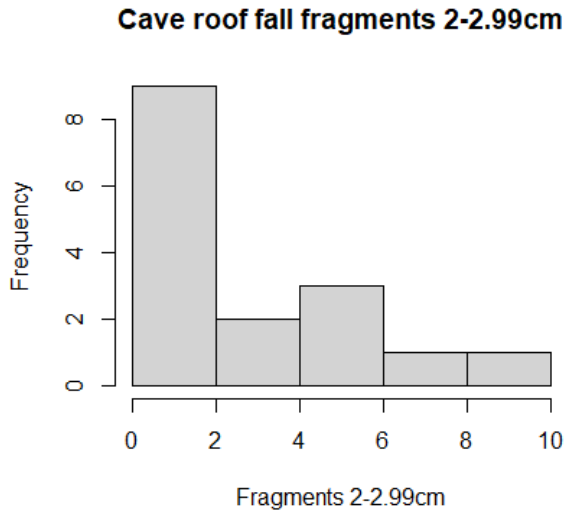

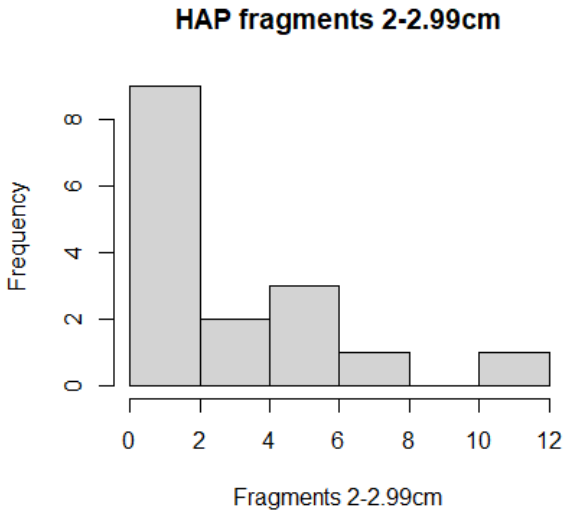

Figure 58 Fragments 2-2.99 cm count

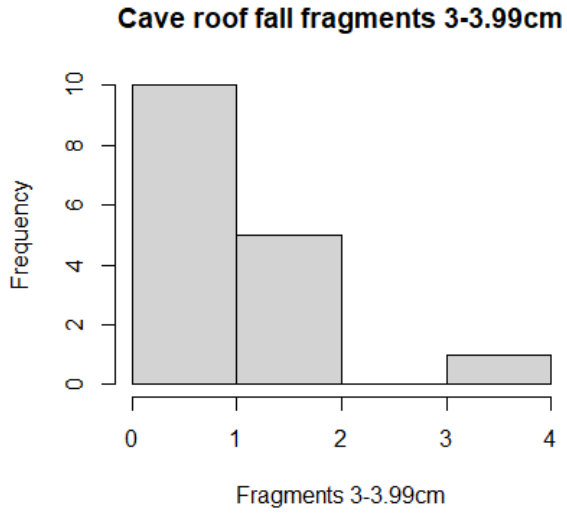

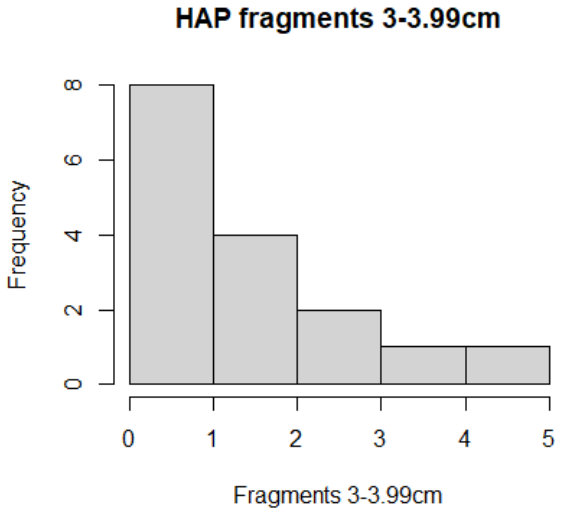

Figure 59 Fragments 3-3.99 cm count

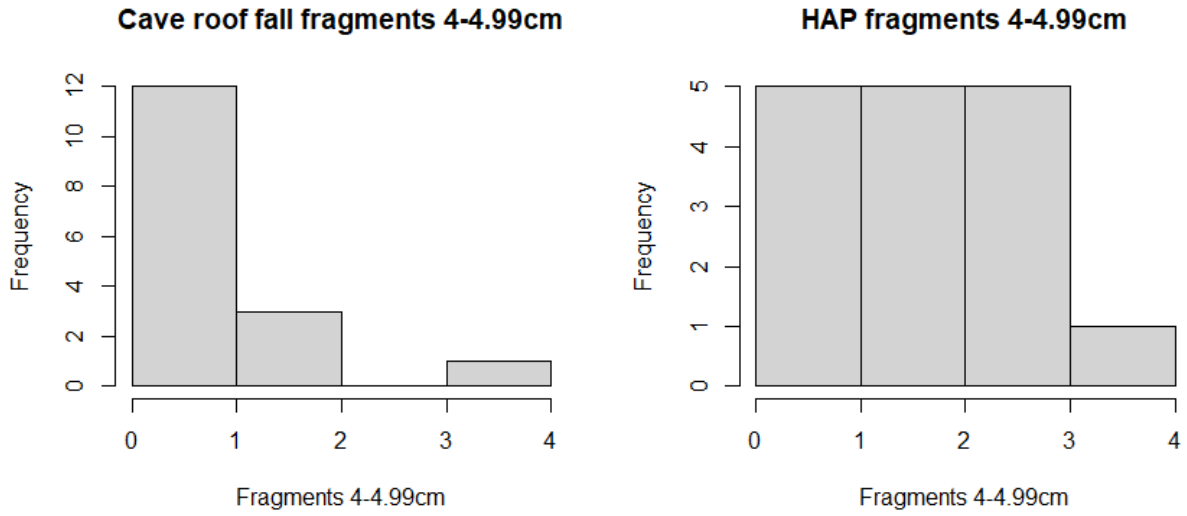

Figure 60 Fragments 4-4.99 cm count

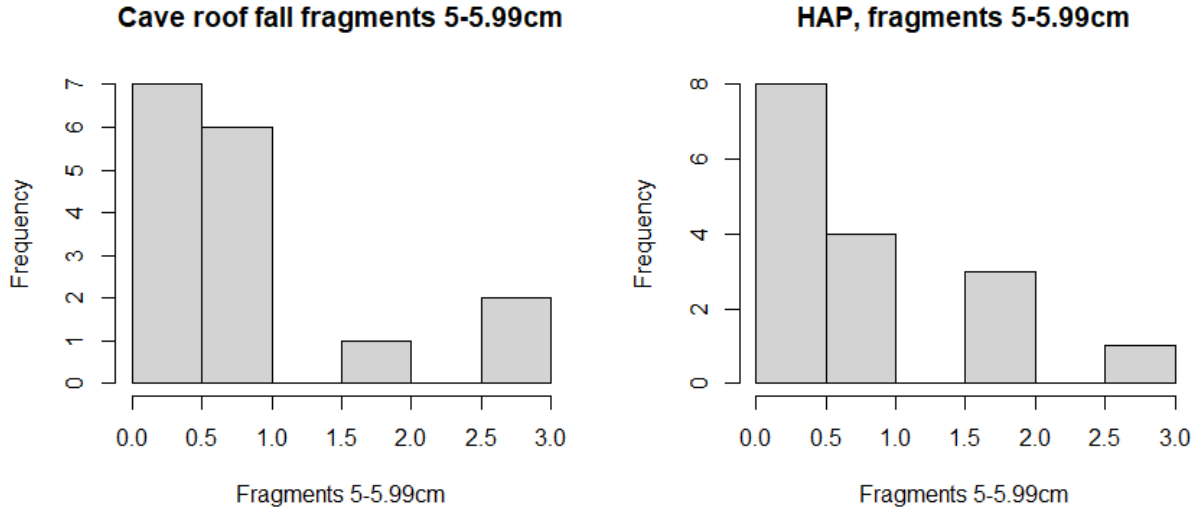

Figure 61 Fragments 5-5.99 cm count

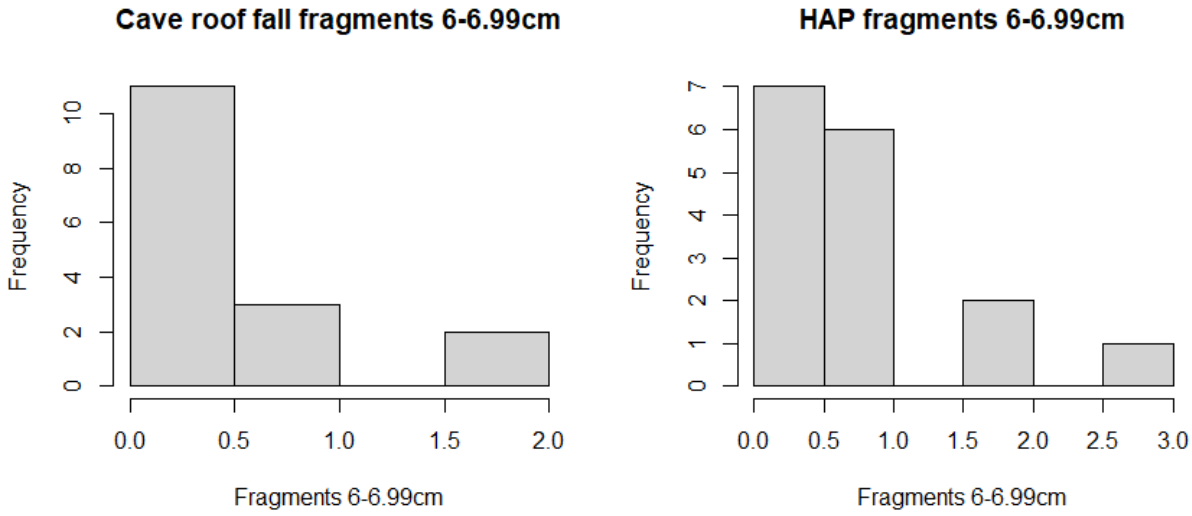

Figure 62 Fragments 6-6.99 cm count

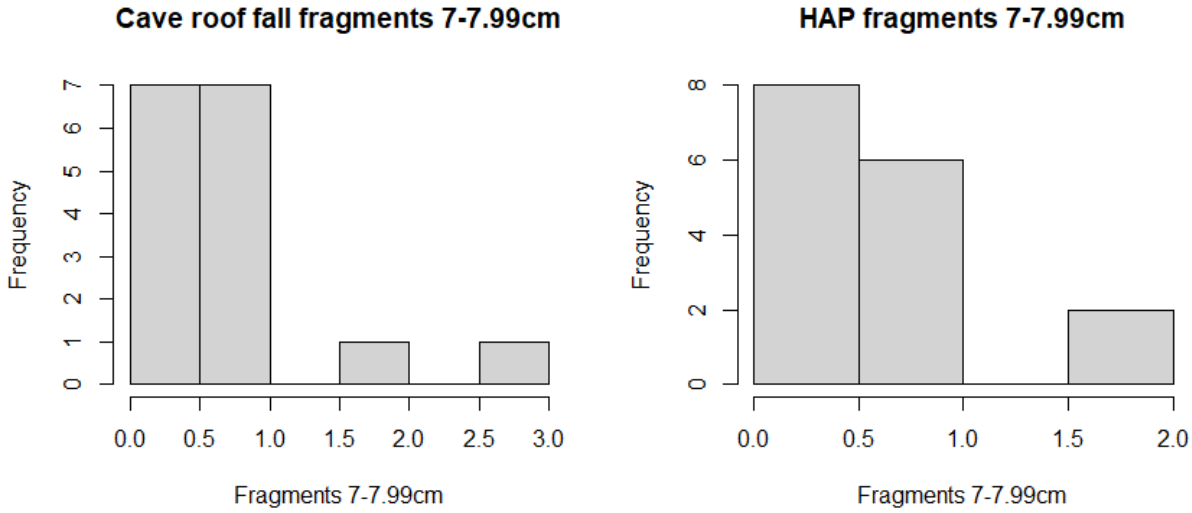

Figure 63 Fragments 7-7.99 cm count

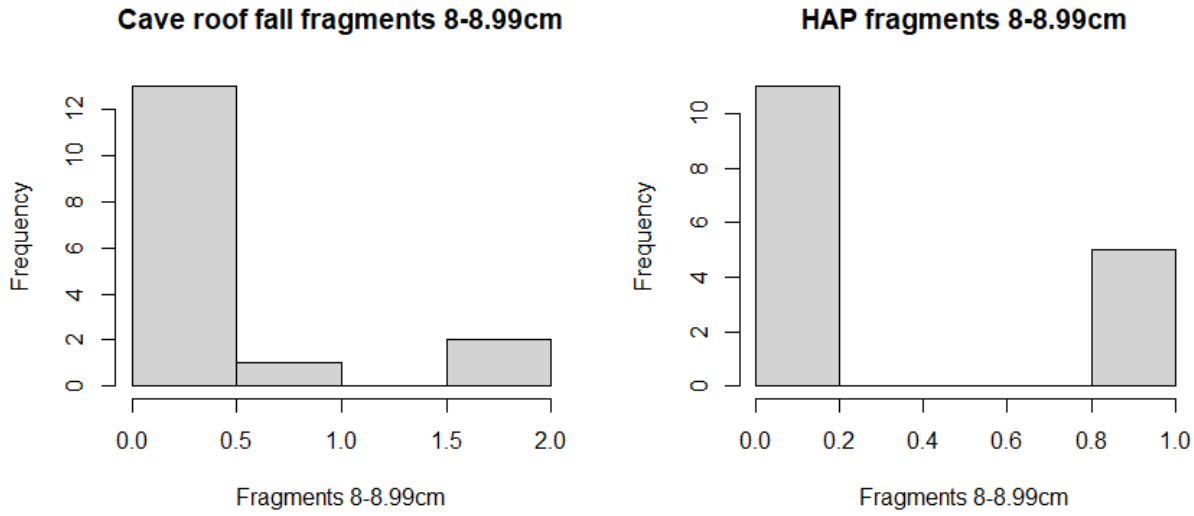

Figure 64 Fragments 8-8.99 cm count

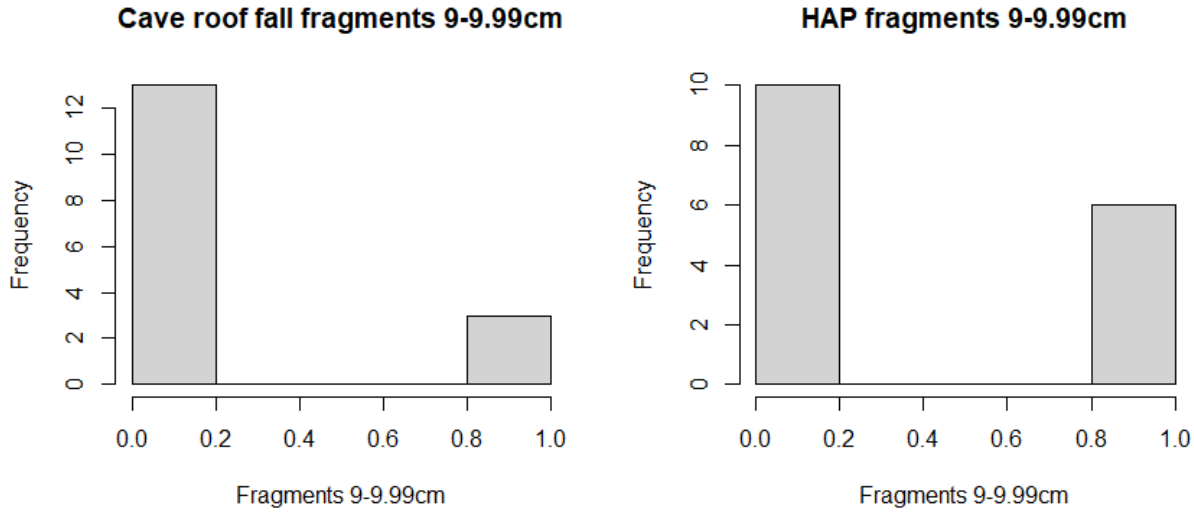

Figure 65 Fragments 9-9.99 cm count

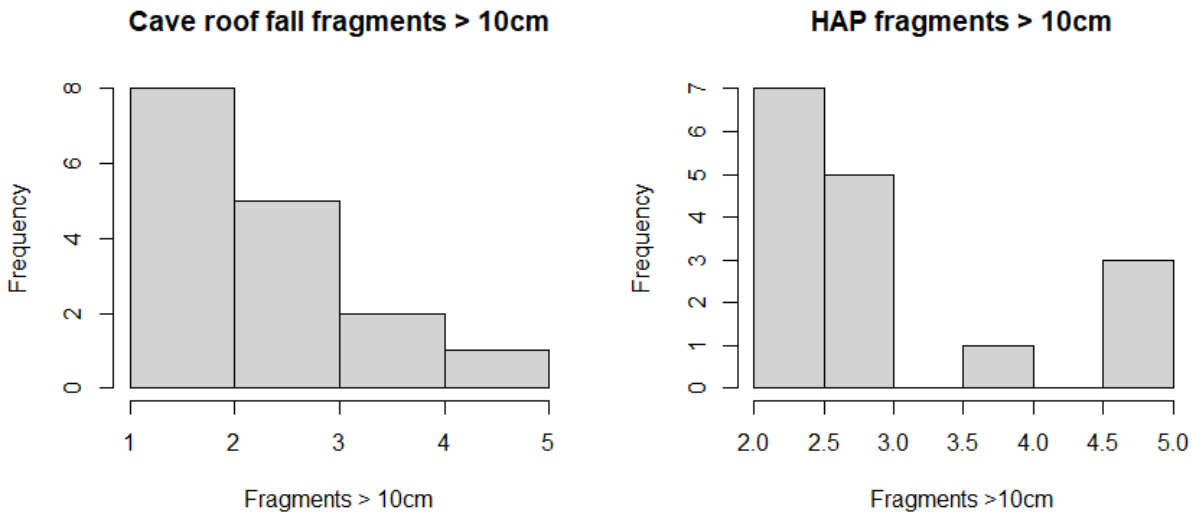

Figure 66 Fragments more than 10 cm count

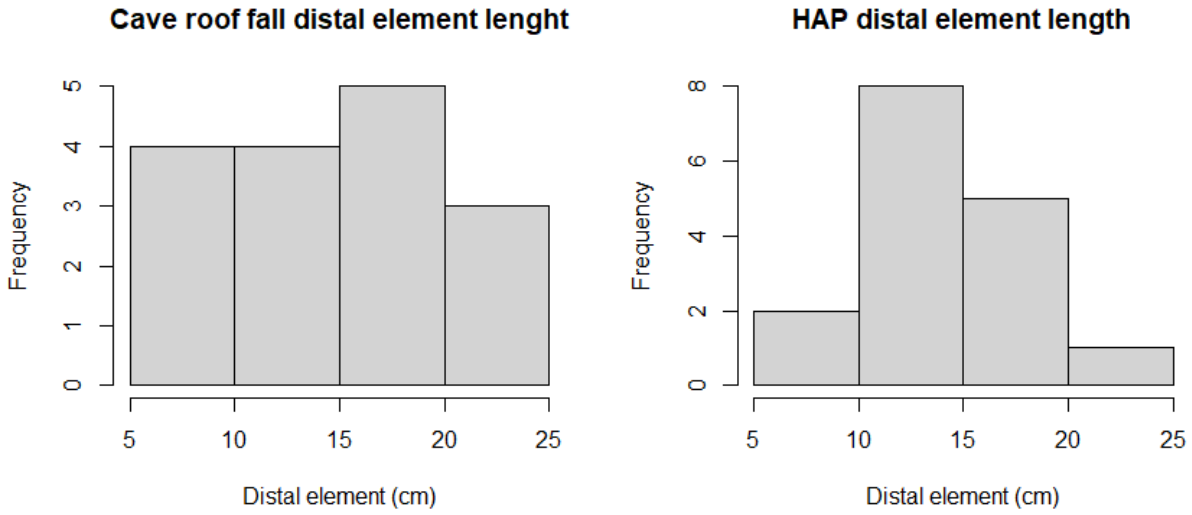

Figure 67 Distal element length in centimeters

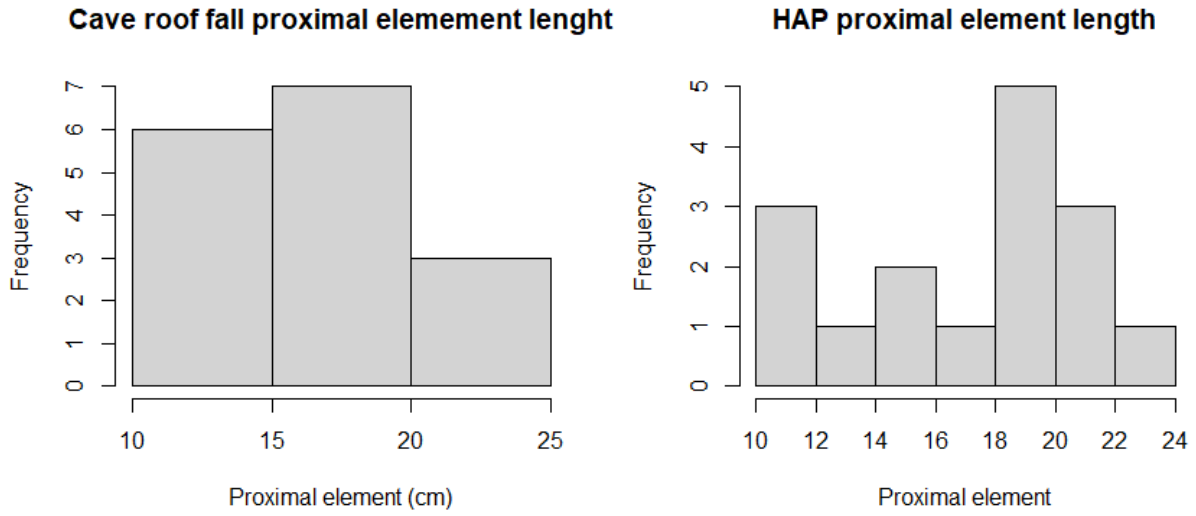

Figure 68 Proximal element length in centimeters

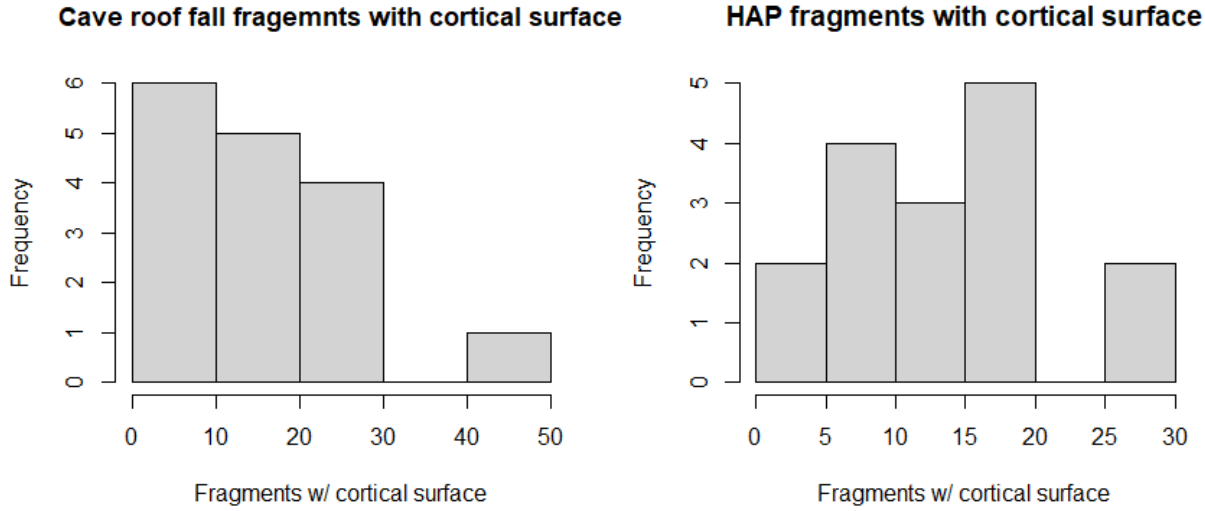

Figure 69 Fragments that preserve cortical surface count

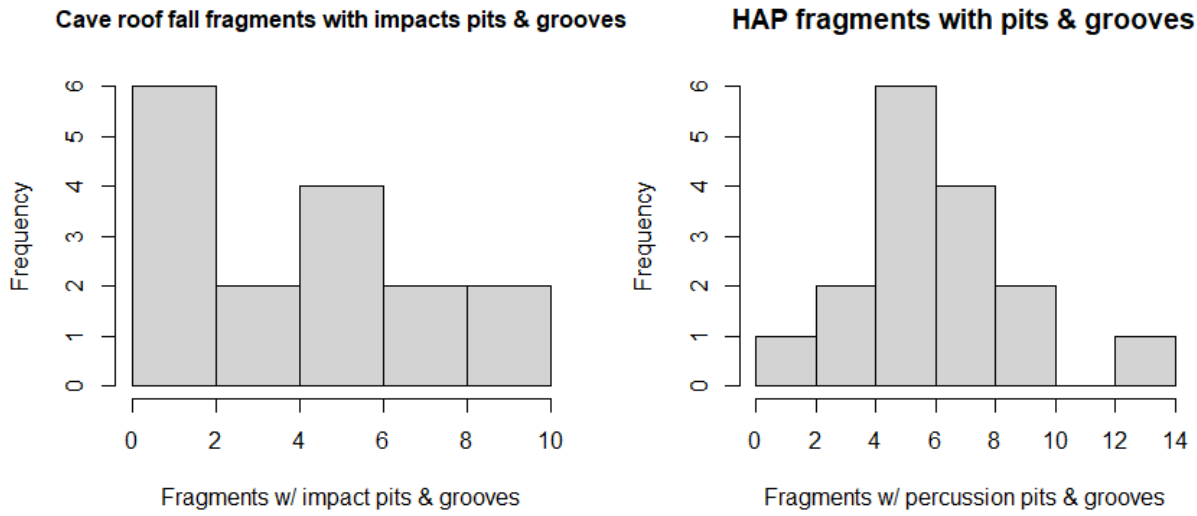

Figure 70 Fragments that exhibit at least one pit and/or groove count

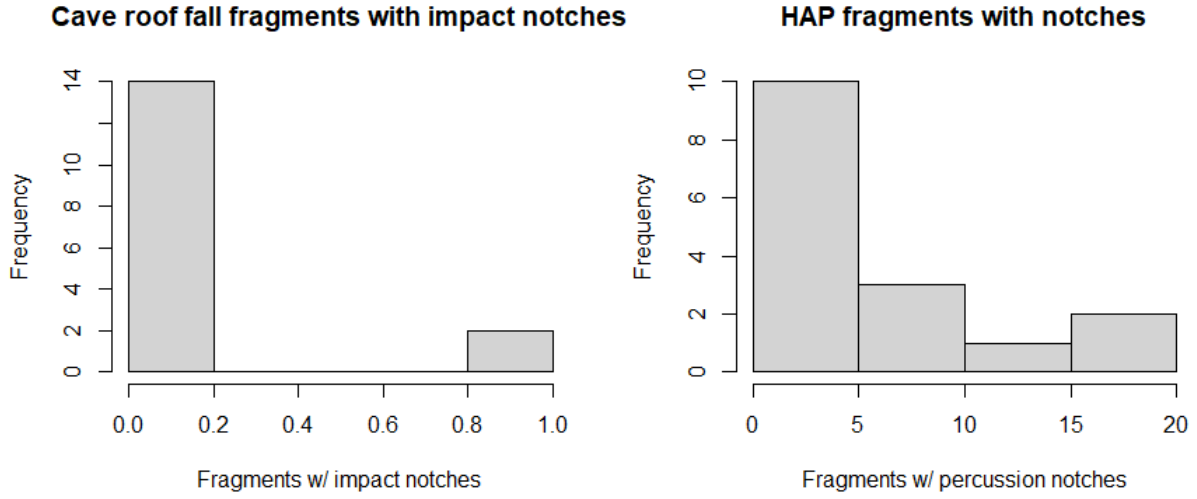

Figure 71 Fragments that exhibit at least one notch

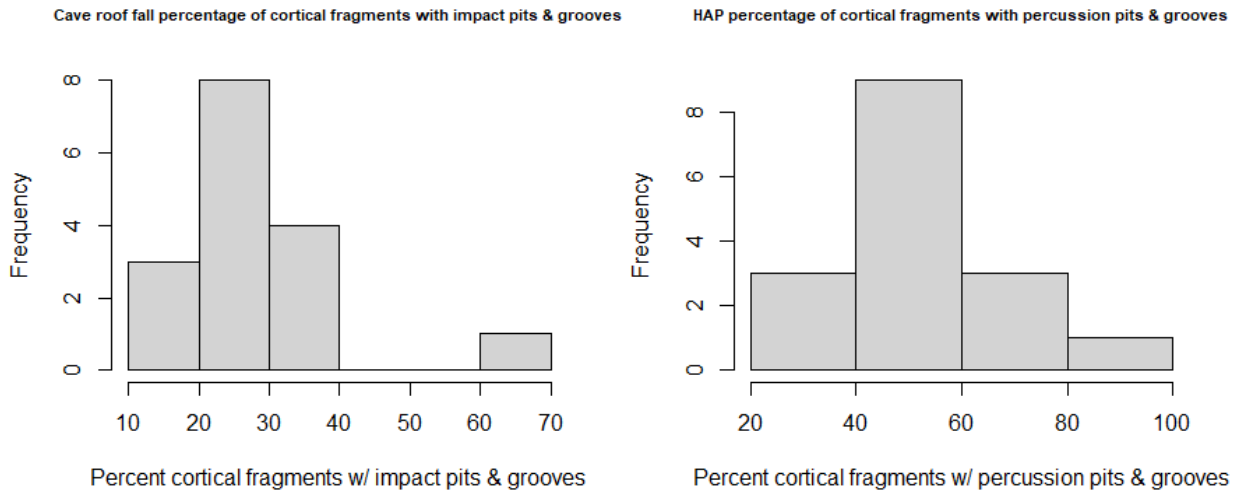

Figure 72 Percentage of cortical fragments with pits and grooves

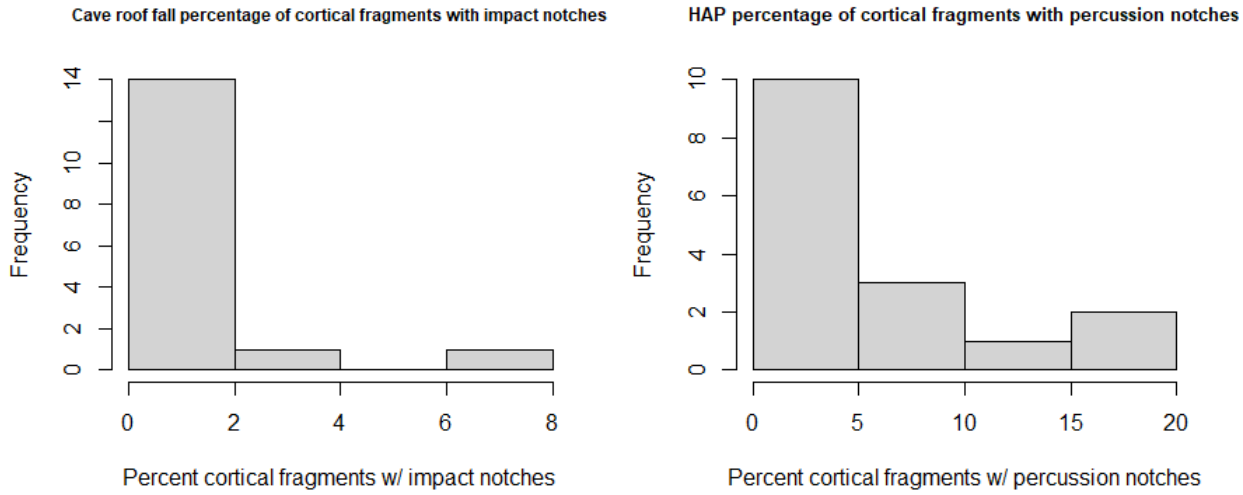

Figure 73 Percentage of cortical fragments with notches

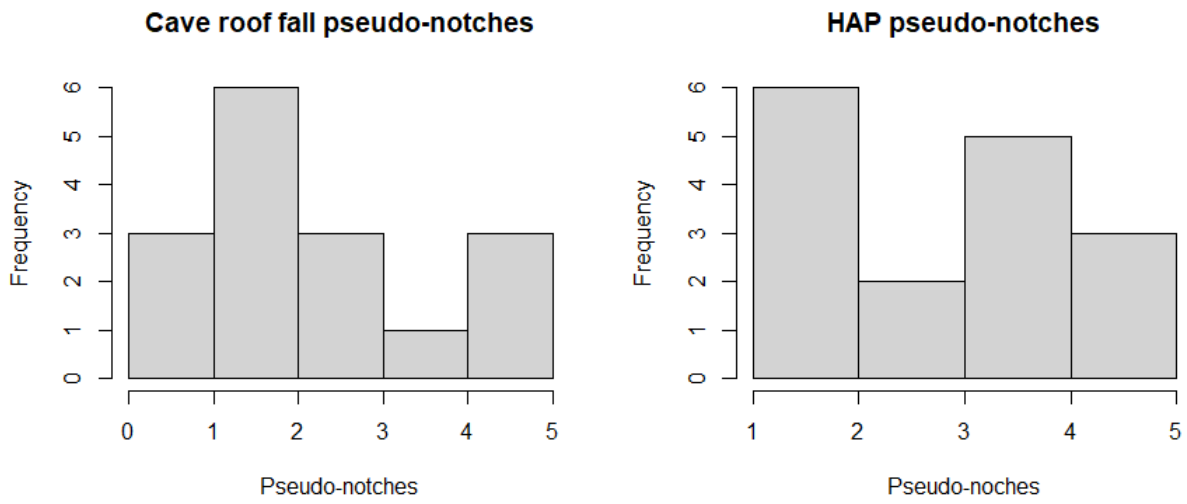

Figure 74 Pseudo-notch count

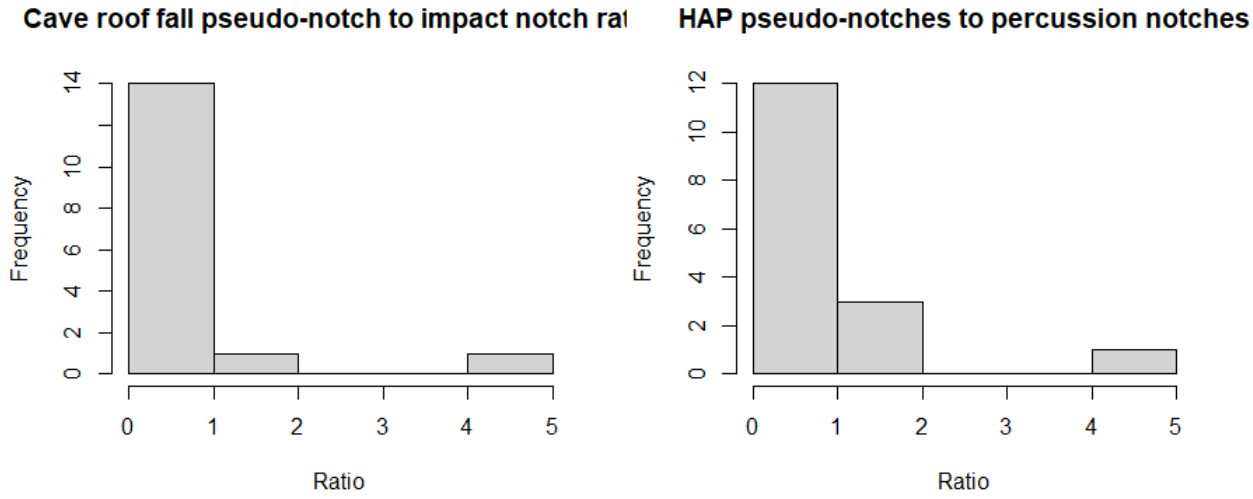

Figure 75 Ratio of pseudo-notches to notches

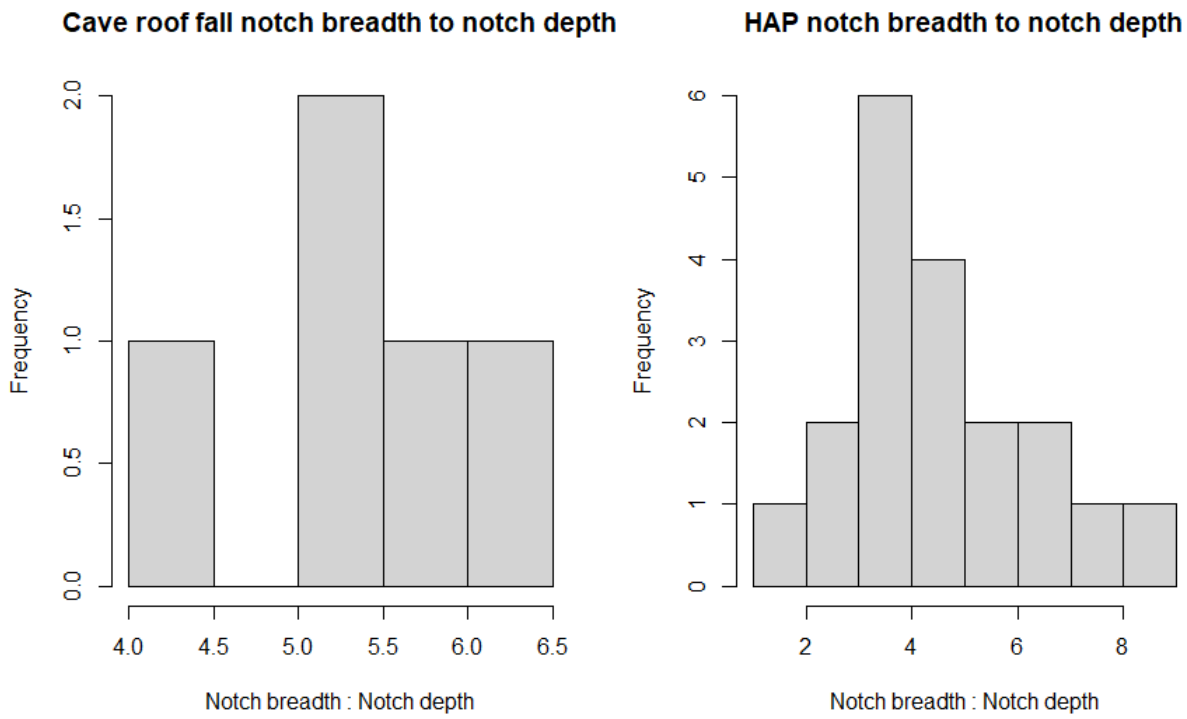

Figure 76 Ratio of notch breadth to notch depth

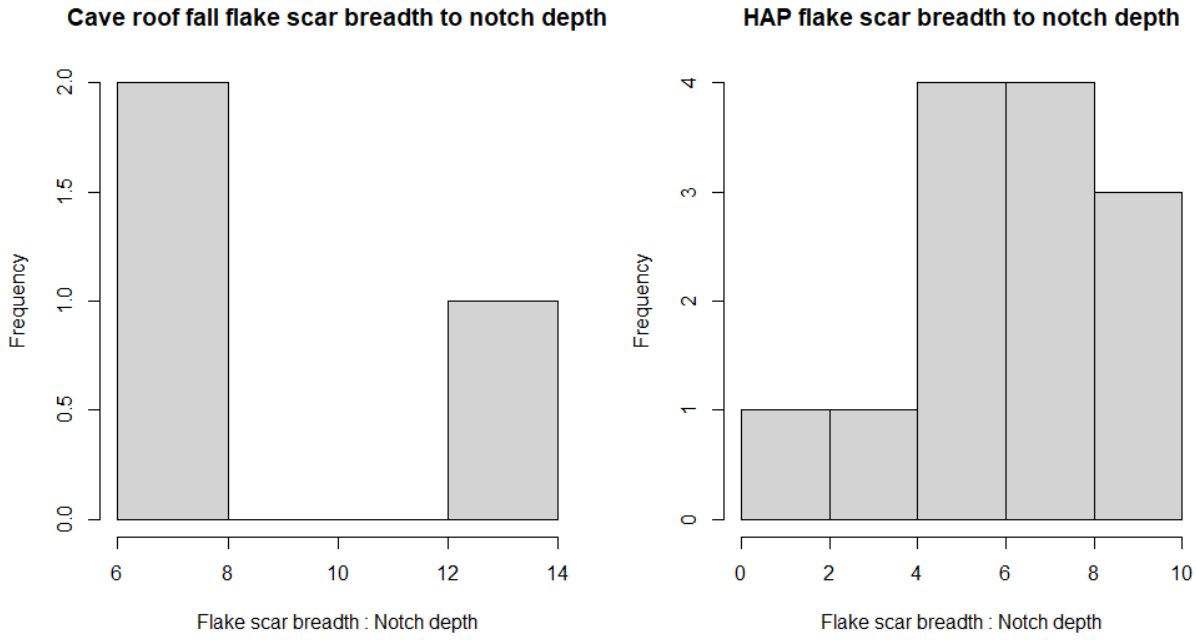

Figure 77 Ratio of notch breadth to notch depth

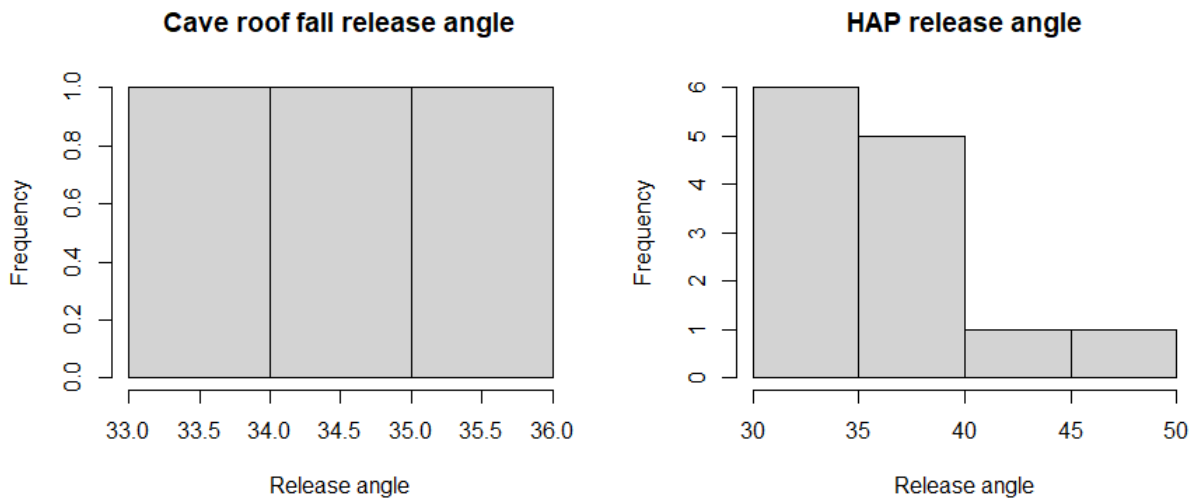

Figure 78 Notch release angle

Appendix 4: Results Violin Plots

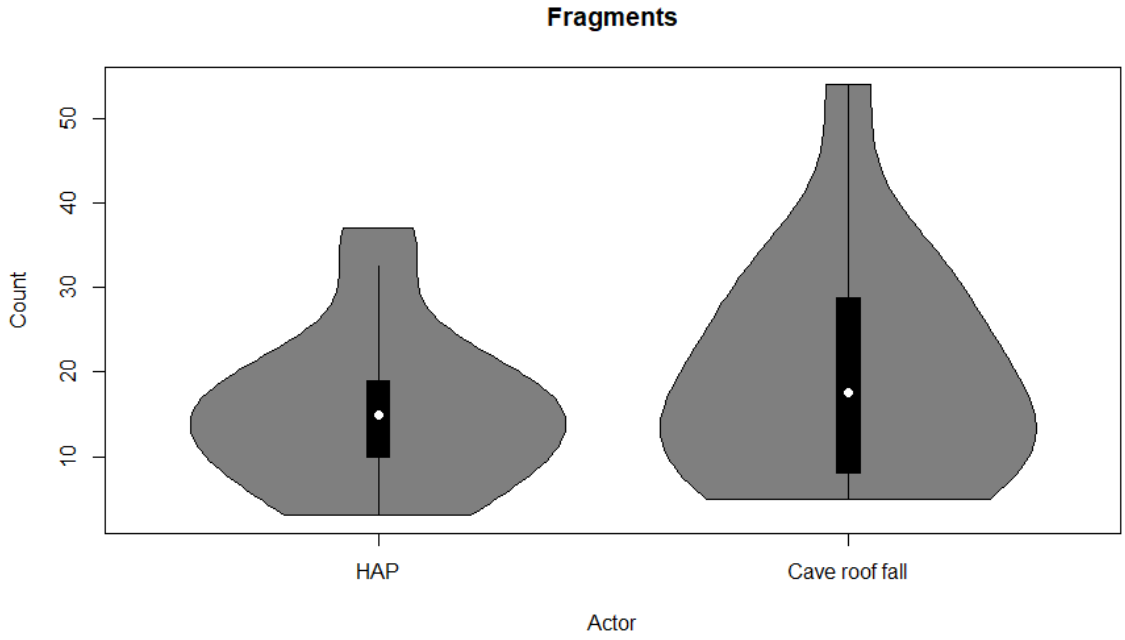

Figure 79 Fragment count

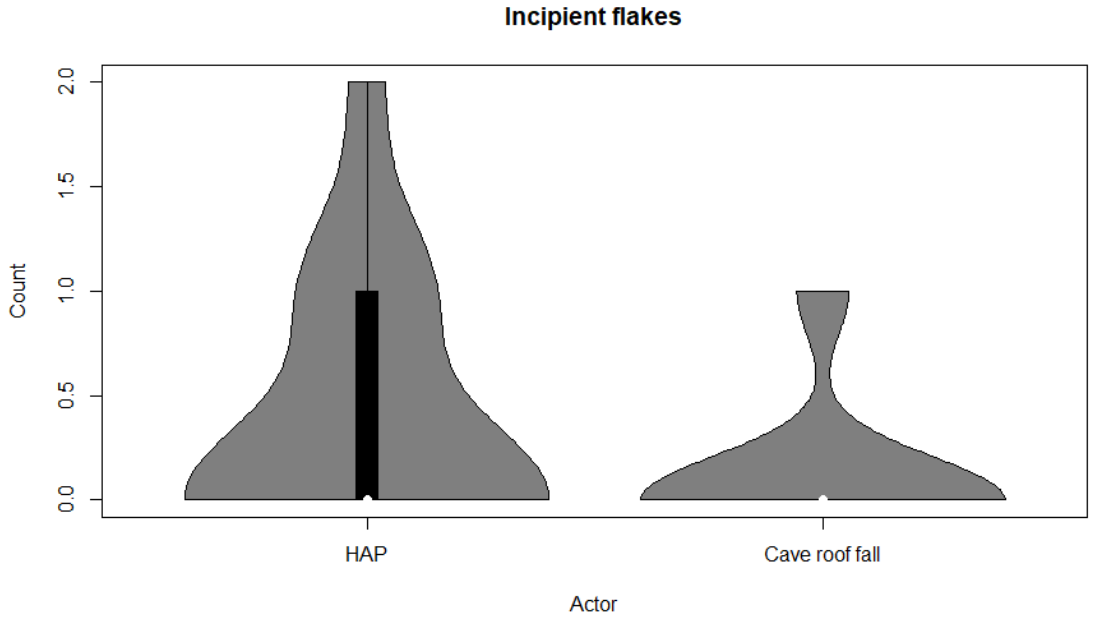

Figure 80 Incipient flake count

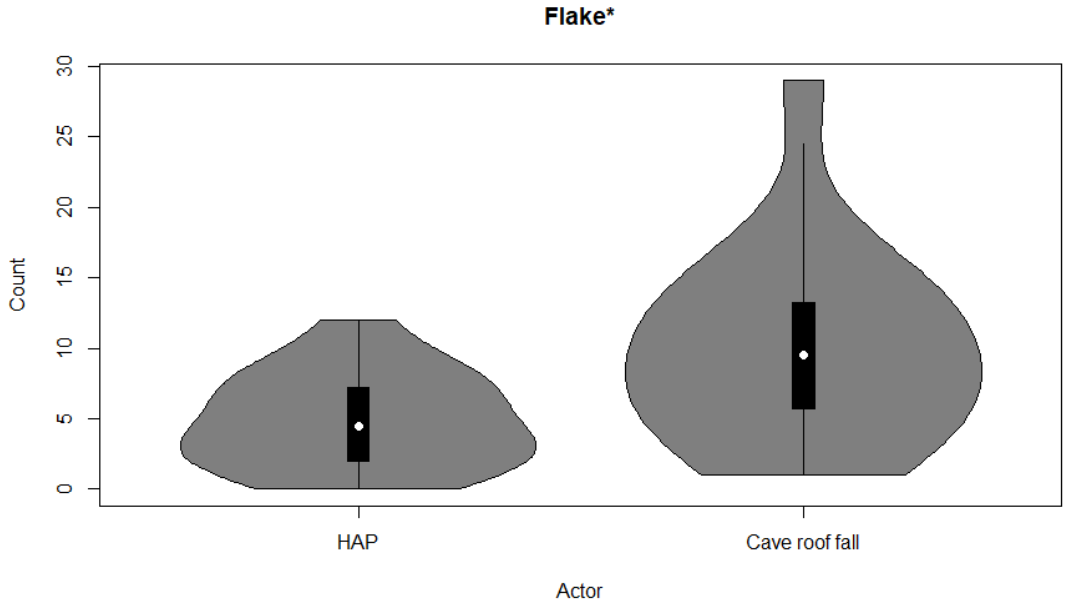

Figure 81 Flake count

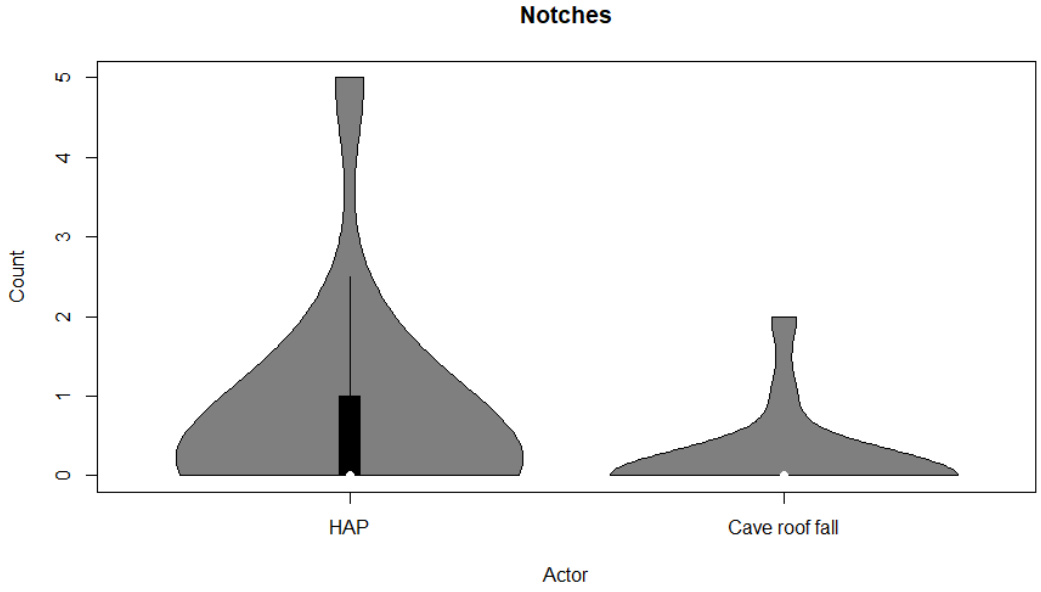

Figure 82 Notch count

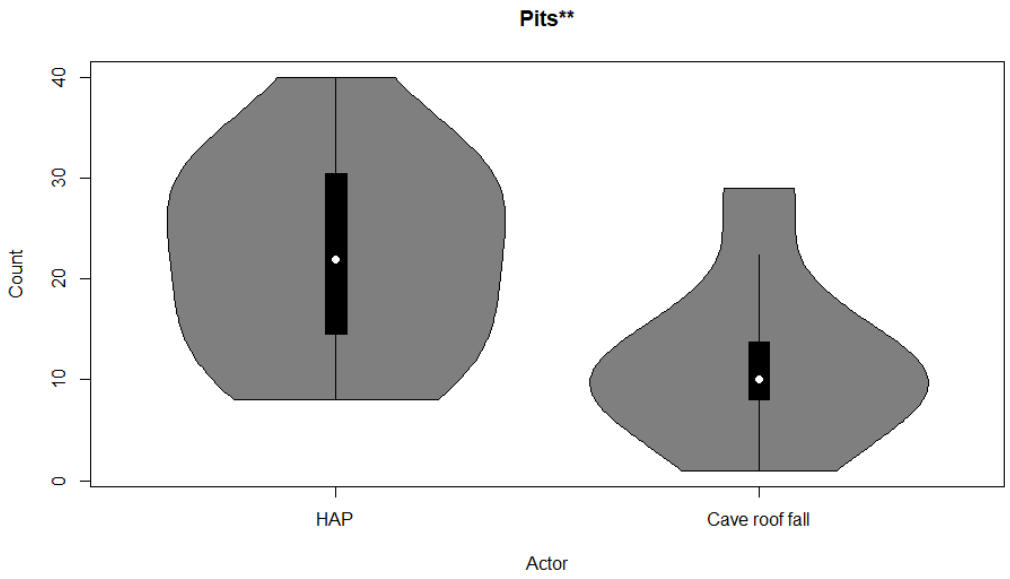

Figure 83 Pit count

Figure 84 Groove count

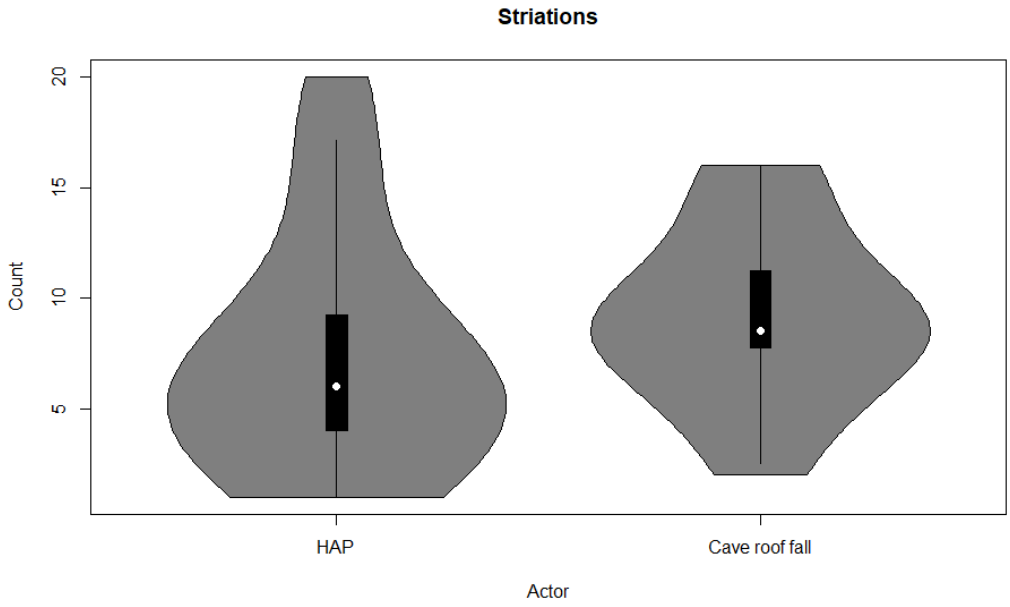

Figure 85 Striation count

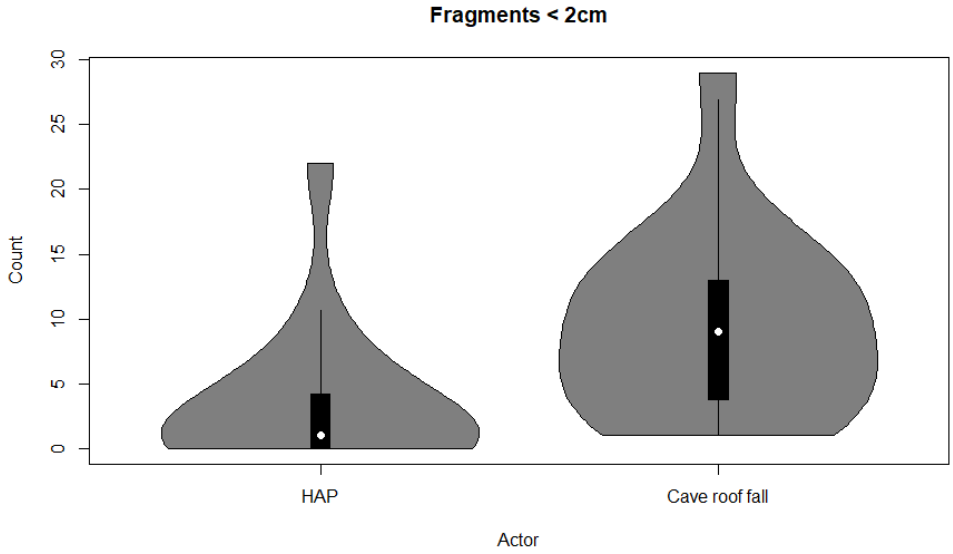

Figure 86 Fragments less than 2 cm count

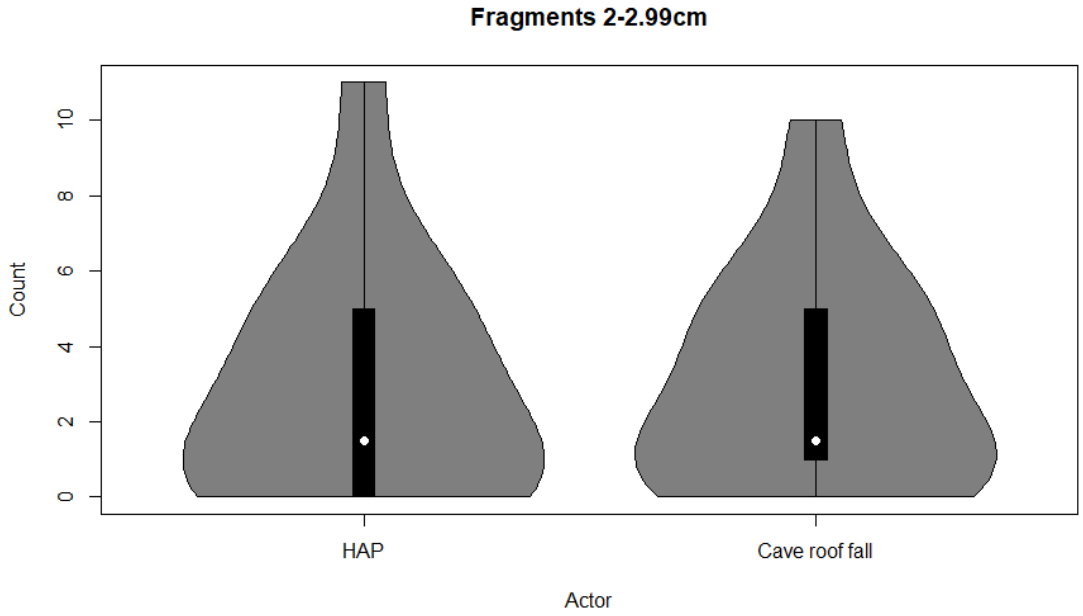

Figure 87 Fragments 2-2.99 cm count

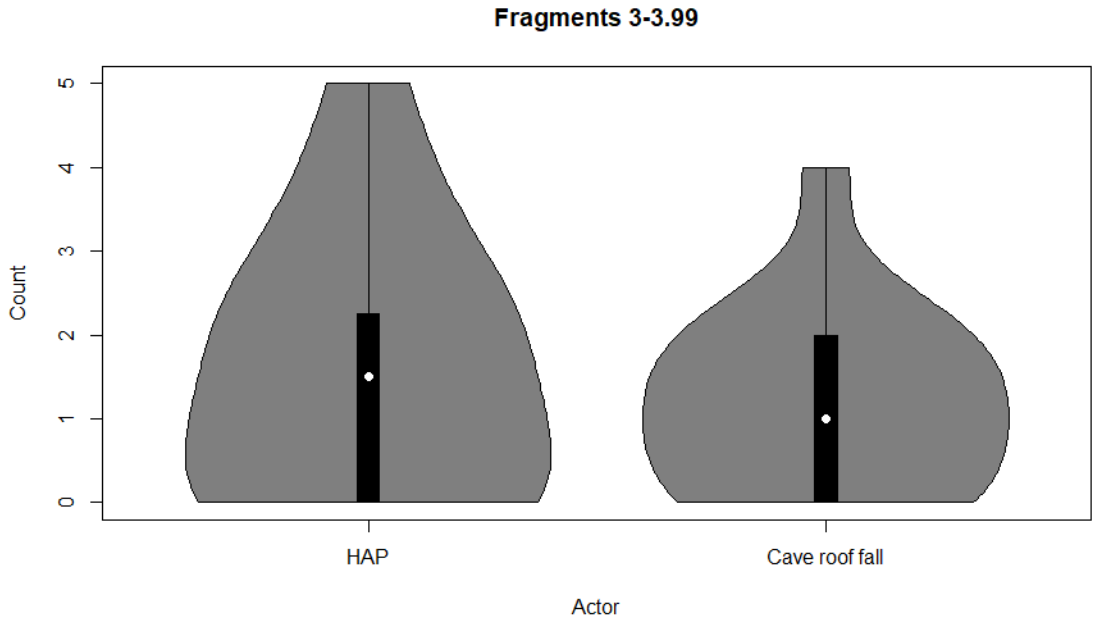

Figure 88 Fragments 3-3.99 cm count

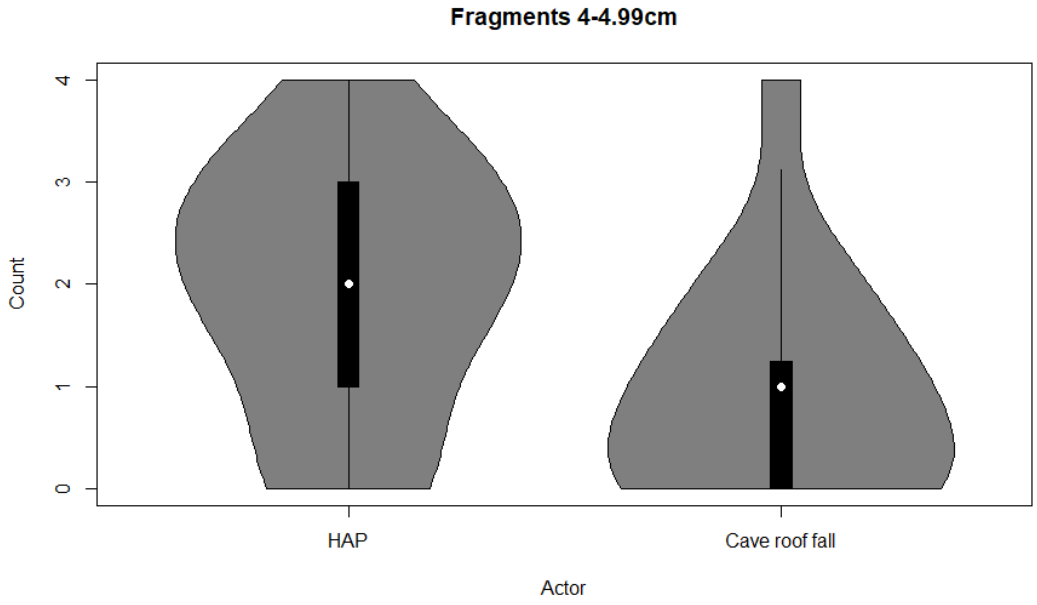

Figure 89 Fragments 4-4.99 cm count

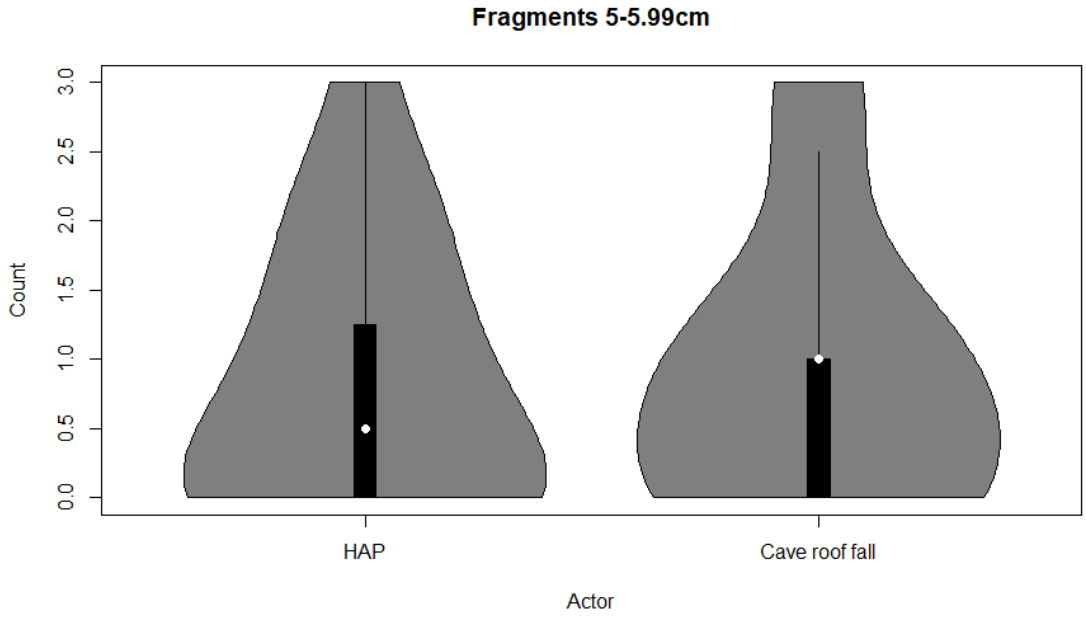

Figure 90 Fragments 5-5.99 cm count

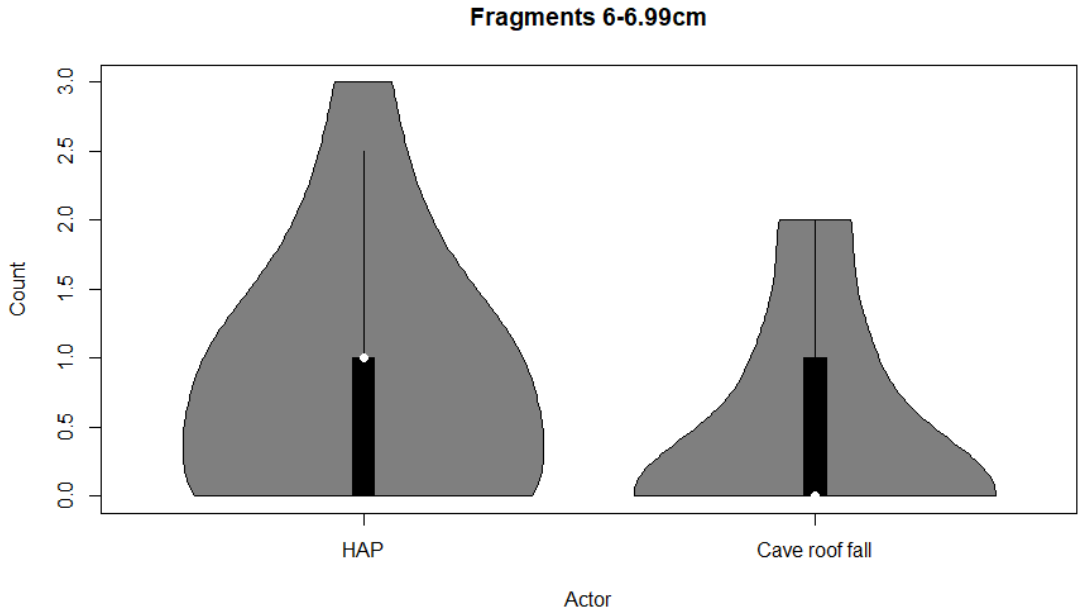

Figure 91 Fragments 6-6.99 cm count

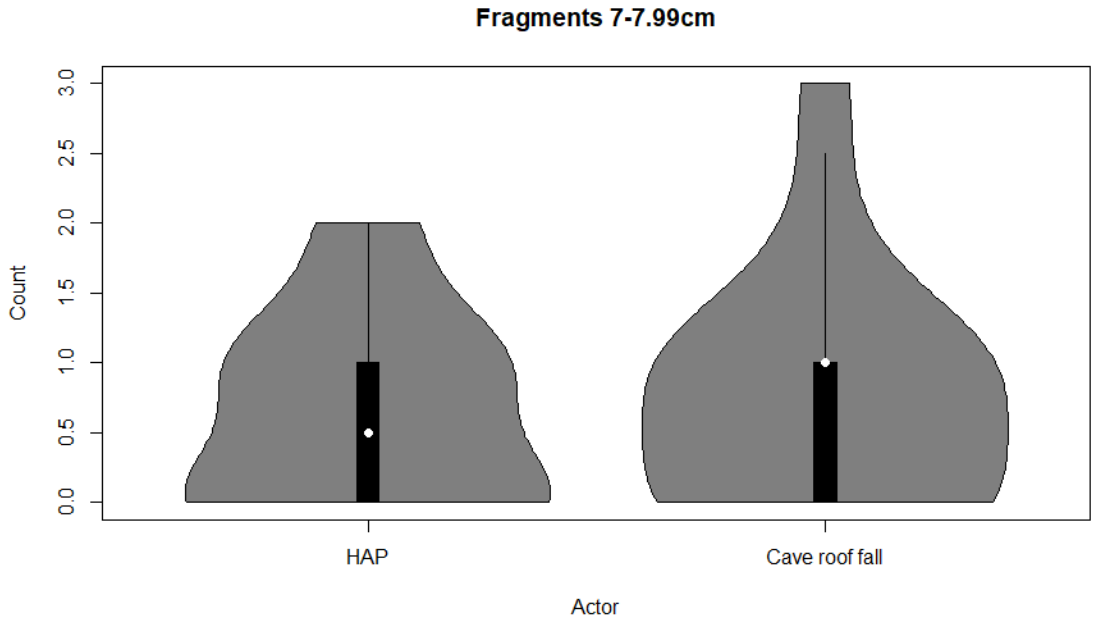

Figure 92 Fragments 7-7.99 cm count

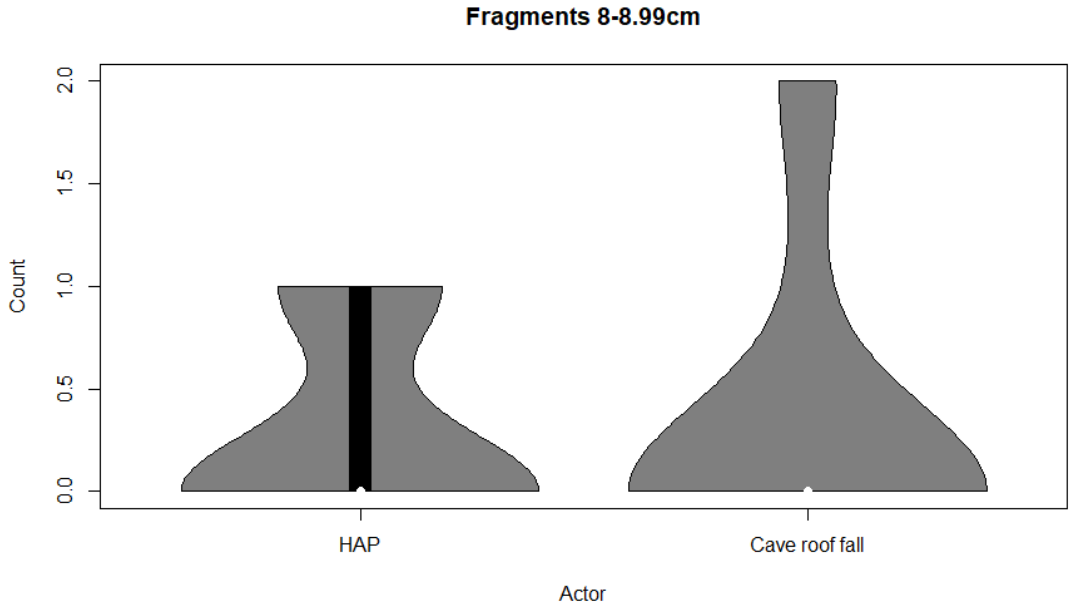

Figure 93 Fragments 8-8.99 cm count

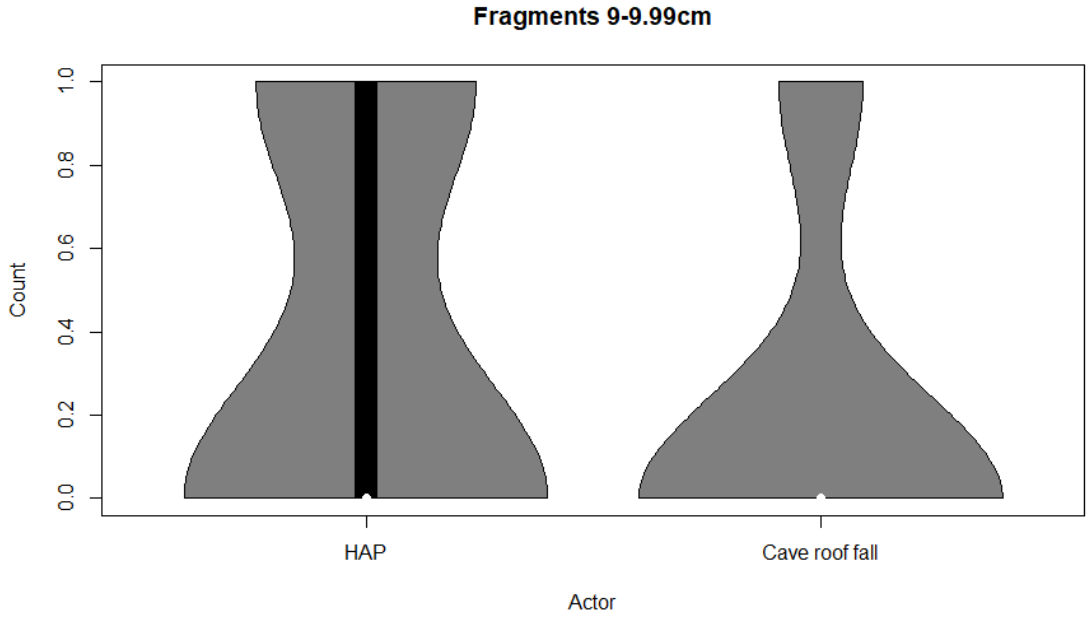

Figure 94 Fragments 9-9.99 cm count

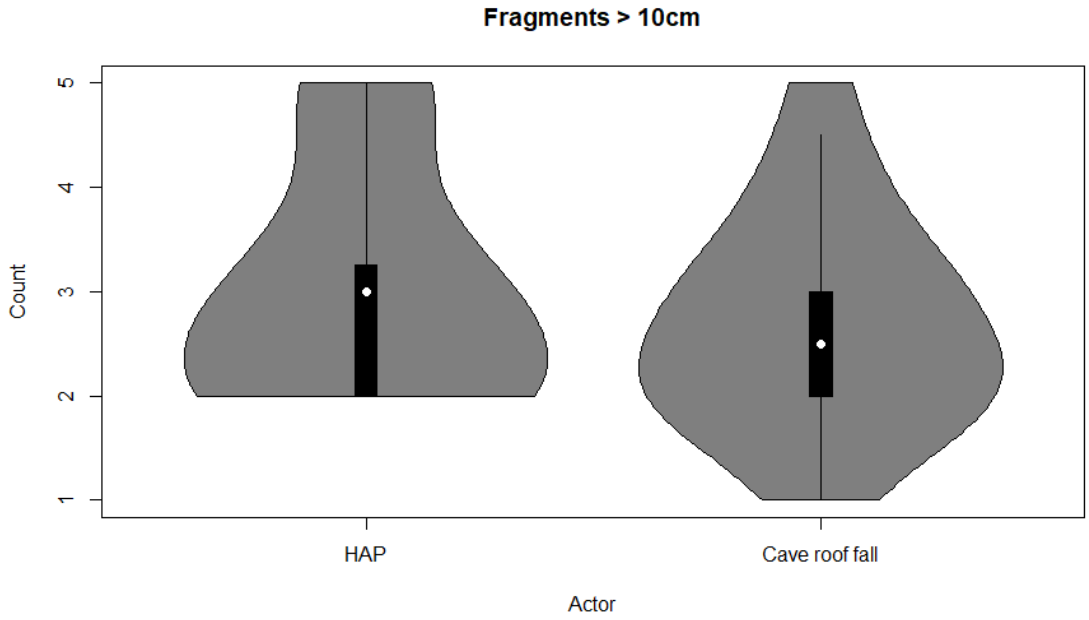

Figure 95 Fragments larger than 10 cm count

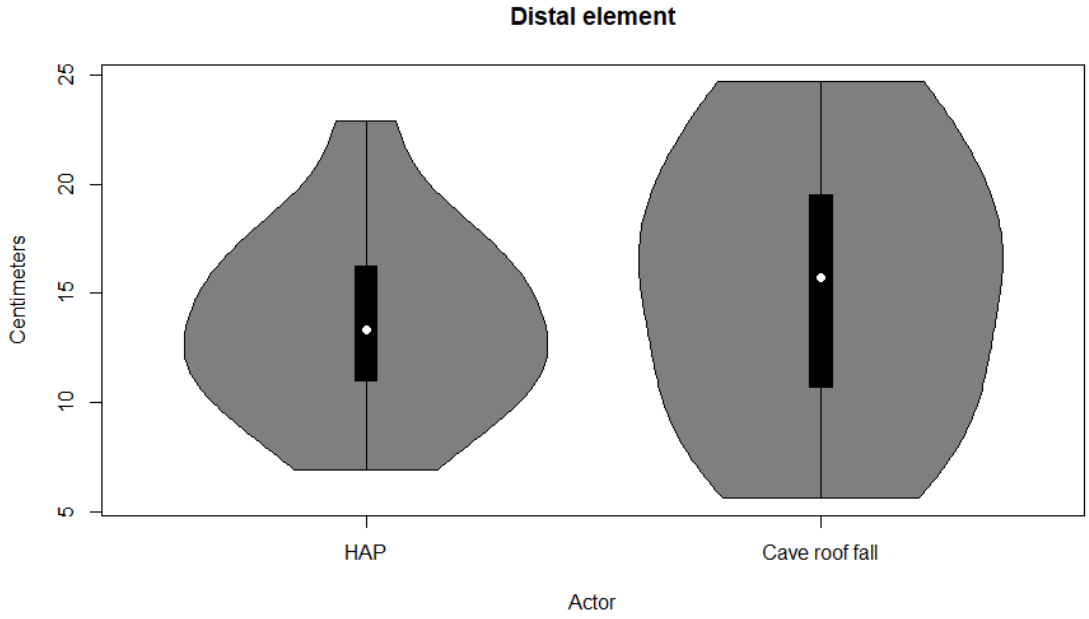

Figure 96 Distal element length in cm

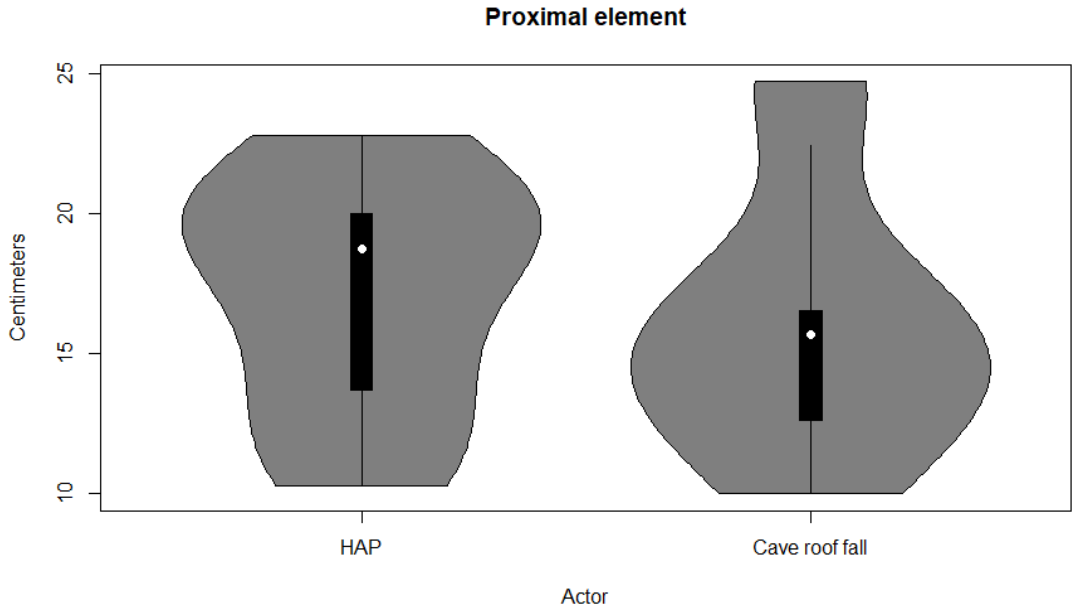

Figure 97 Proximal element length in cm

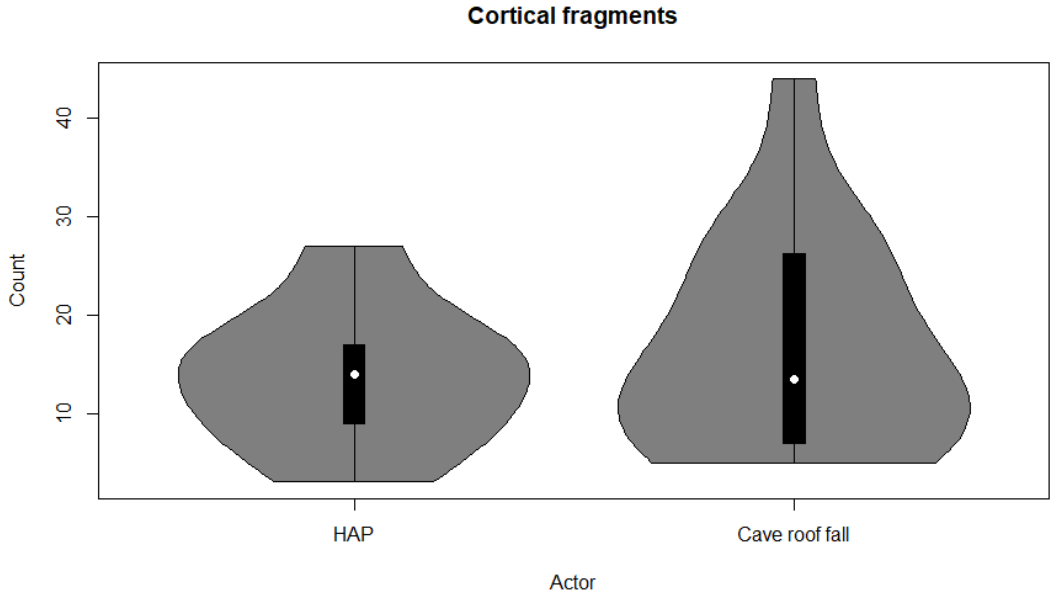

Figure 98 Cortical fragment count

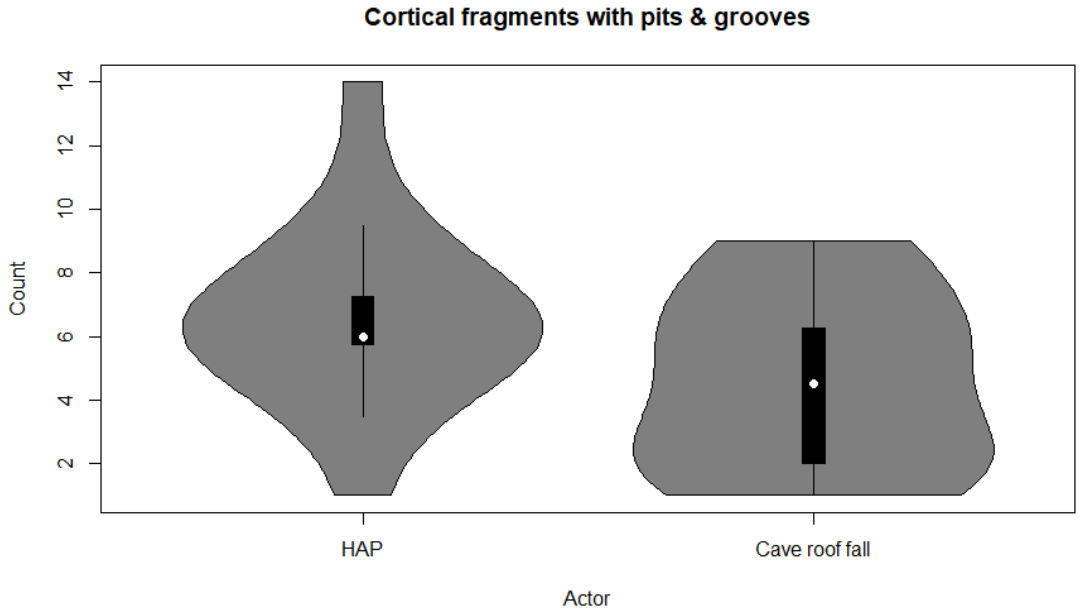

Figure 99 Cortical fragments with a pit and/or groove count

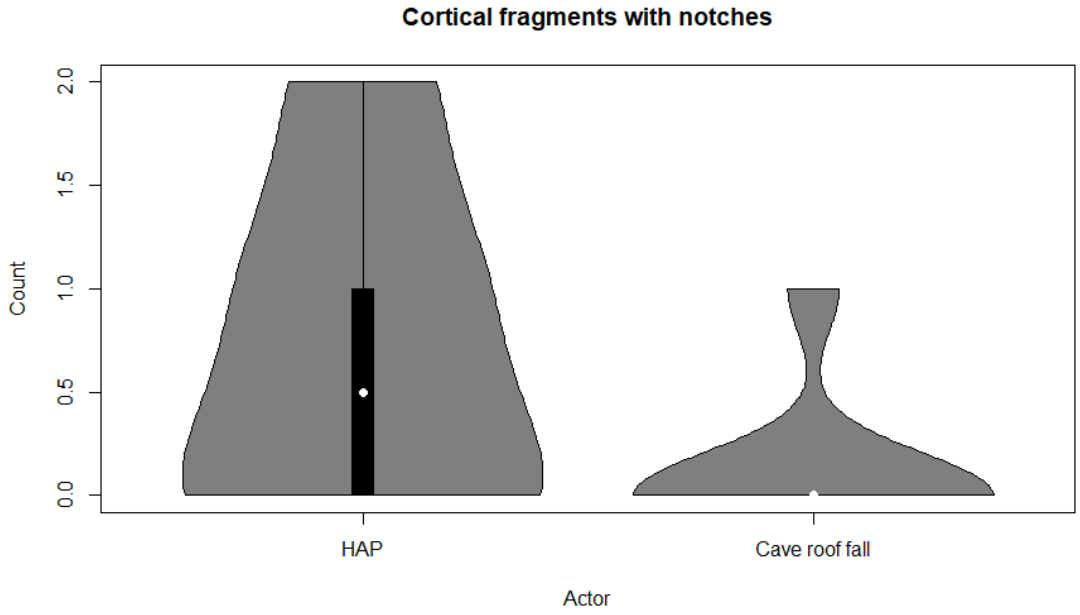

Figure 100 Cortical fragments with at least one notch

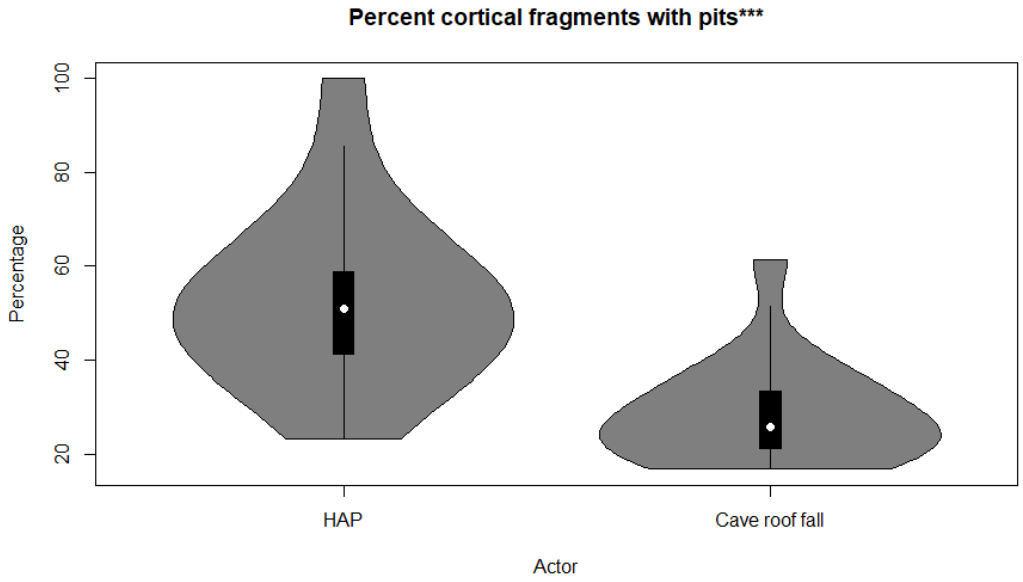

Figure 101 Percentage of fragments with pits and/or grooves

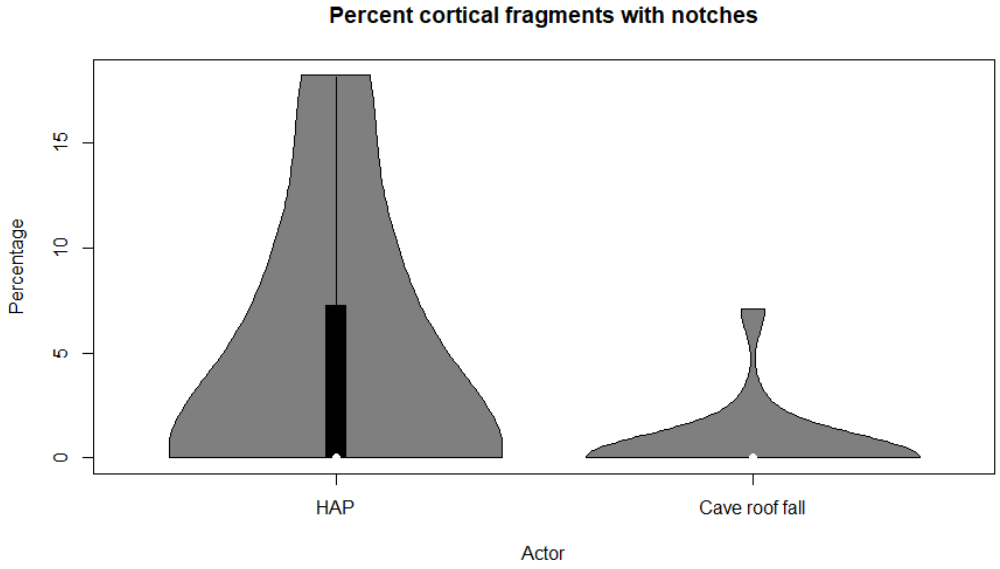

Figure 102 Percentage of fragments with at least one notch

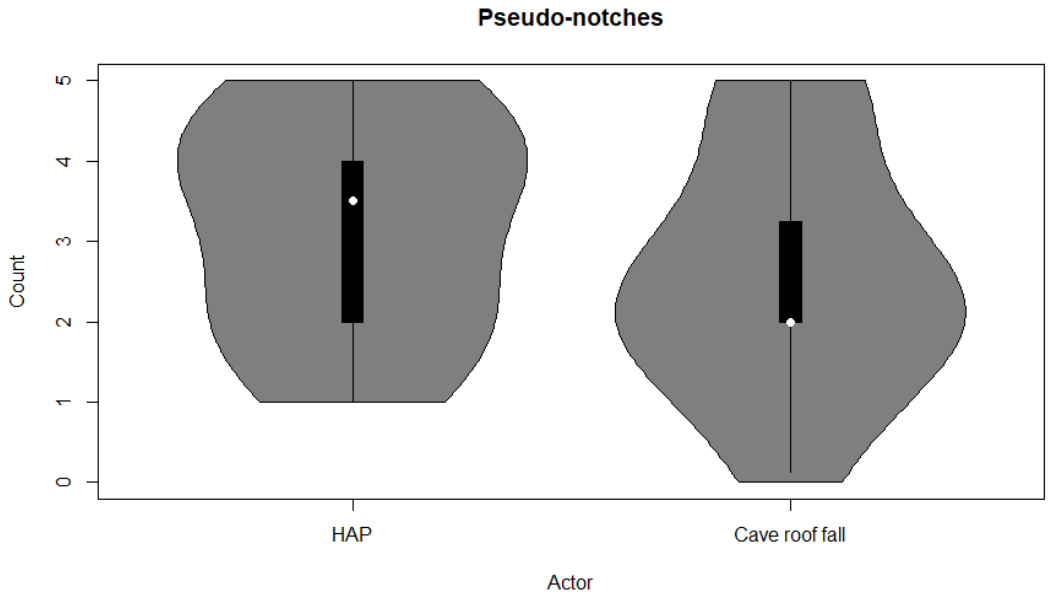

Figure 103 Pseudo-notch count

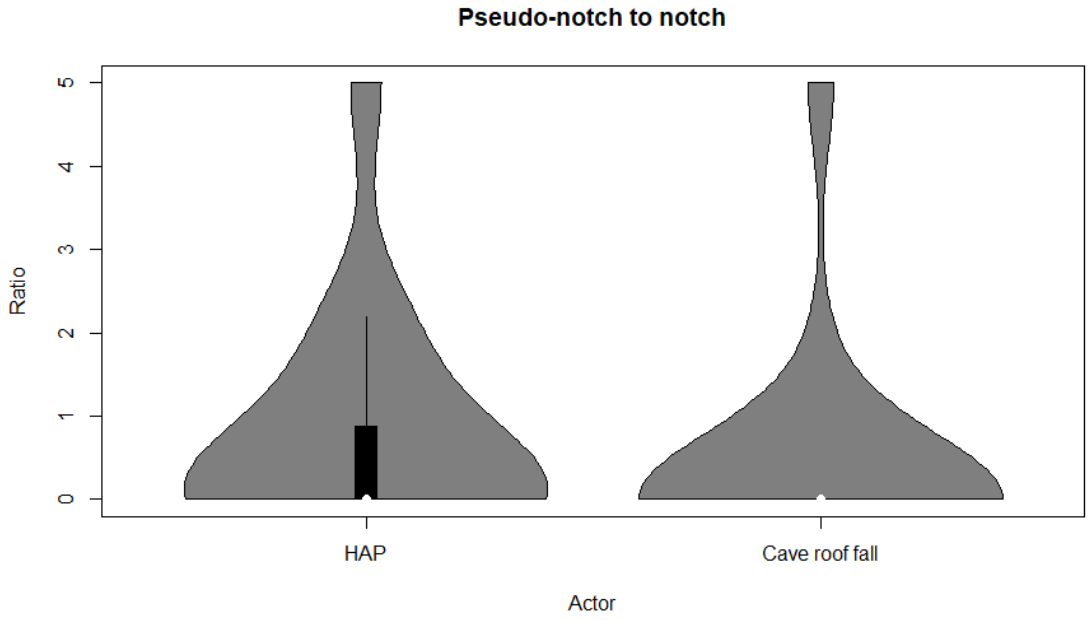

Figure 104 Ratio of pseudo-notches to notches

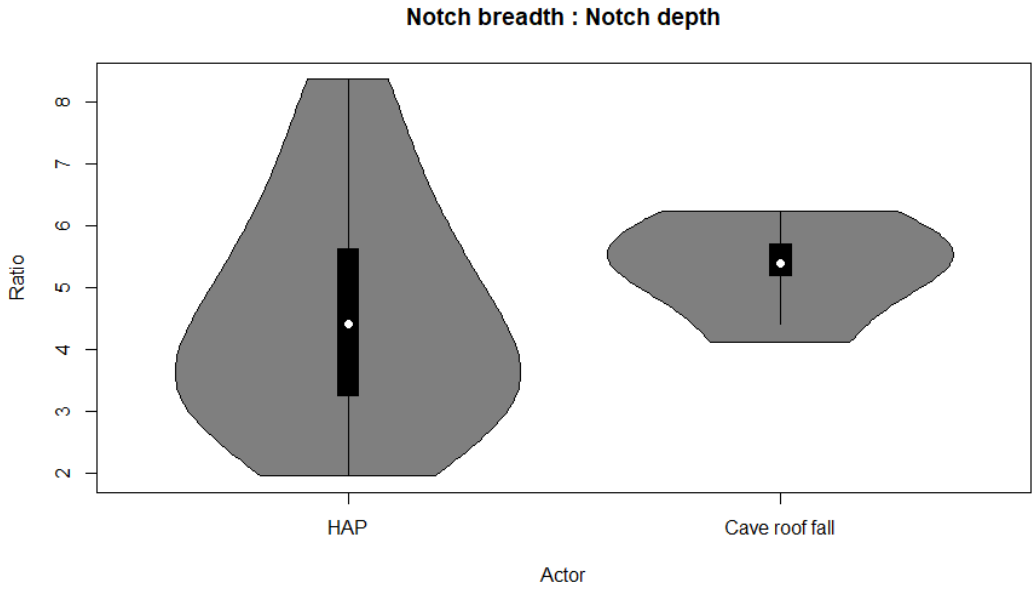

Figure 105 Ratio of notch breadth to notch depth

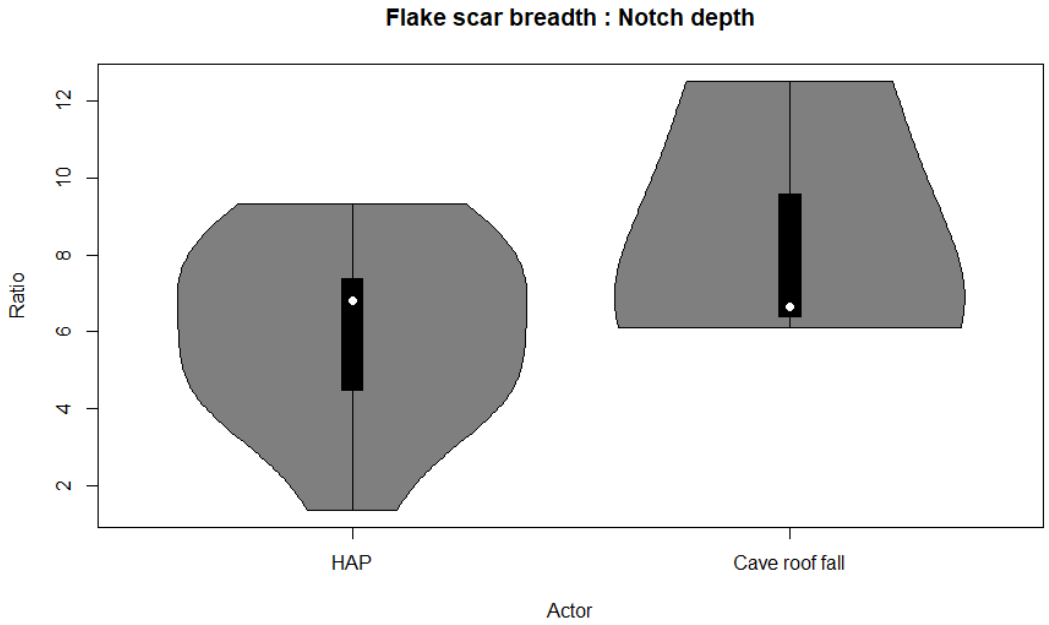

Figure 106 Ratio of flake scar breadth to notch depth

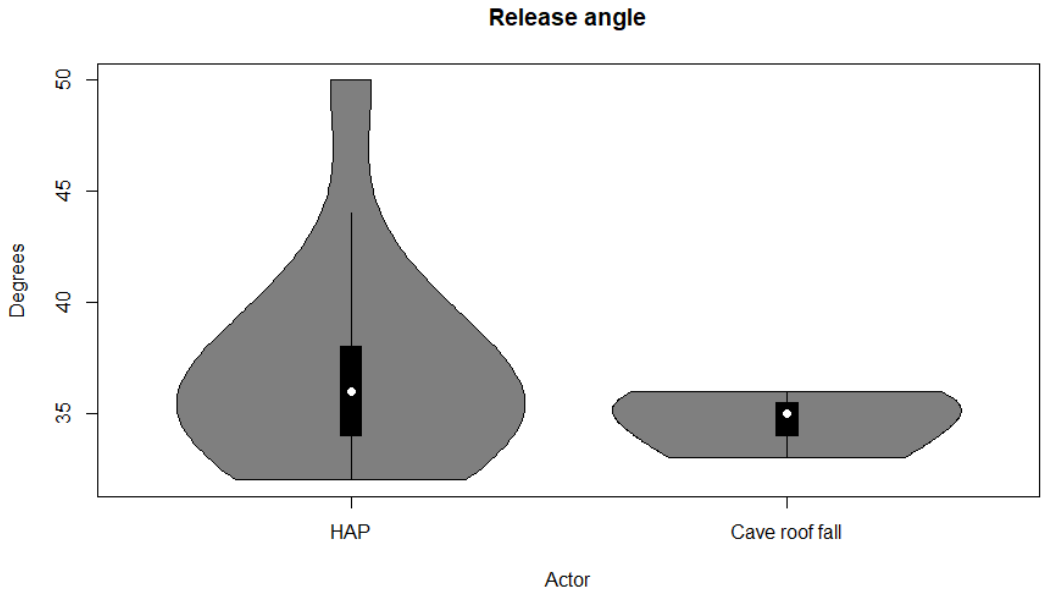

Figure 107 Release angle in degrees

Appendix 5: Scatter plots

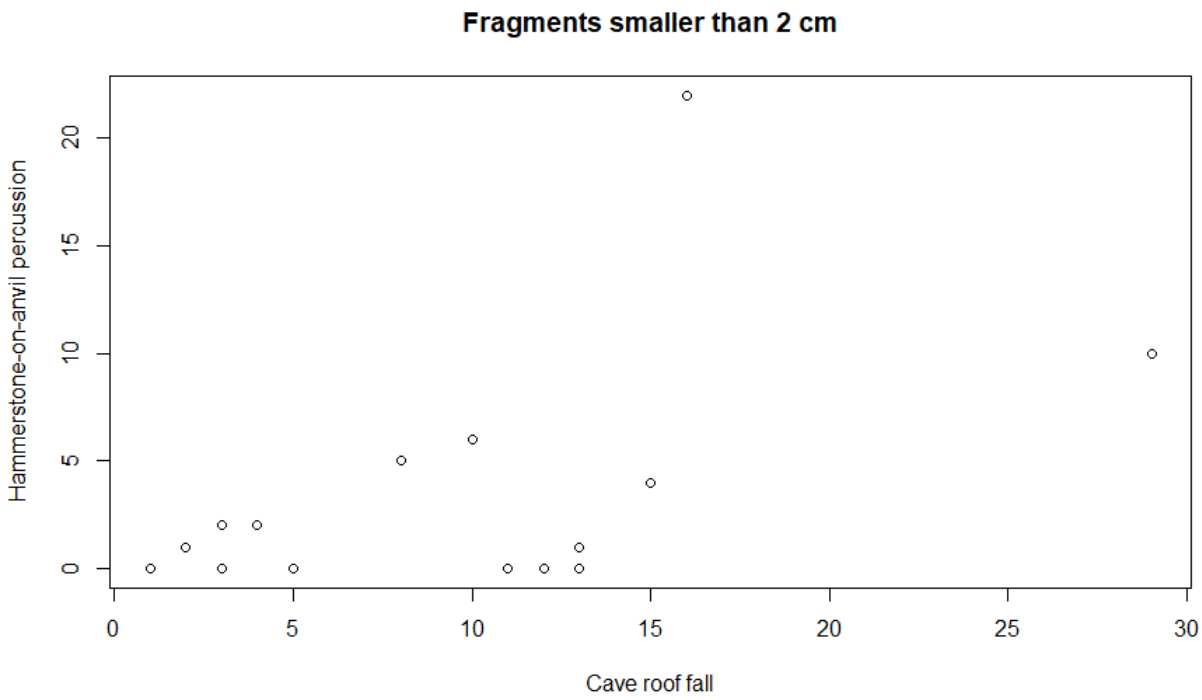

Figure 108 Scatter plot of fragments smaller than 2 cm from both actors

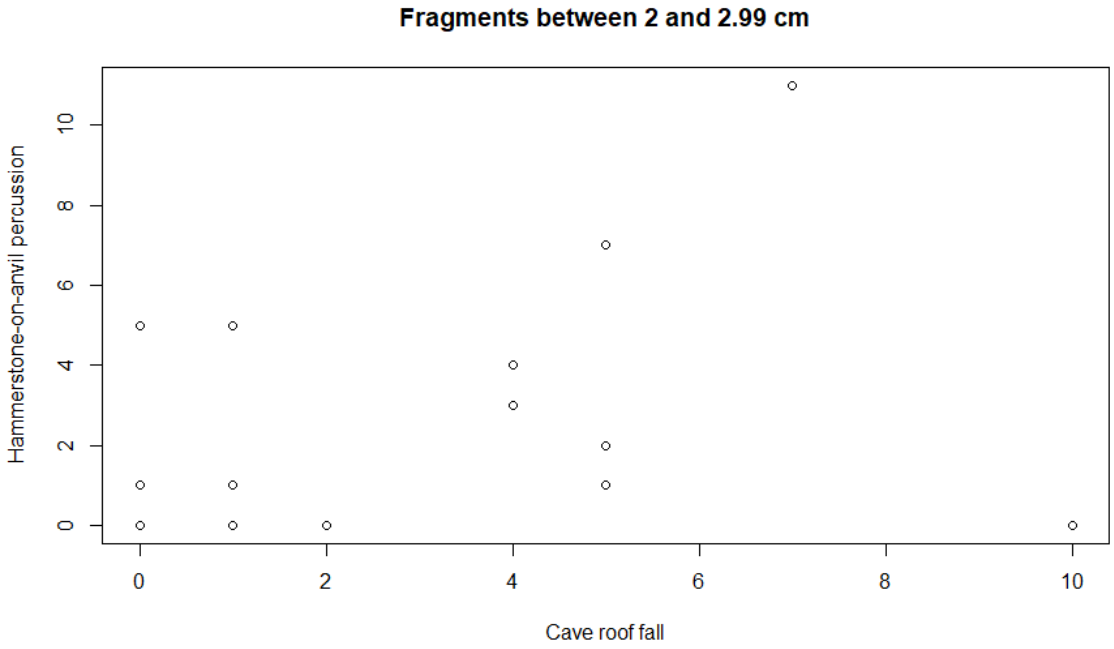

Figure 109 Scatter plot of fragments between 2 and 2.99 cm from both actors

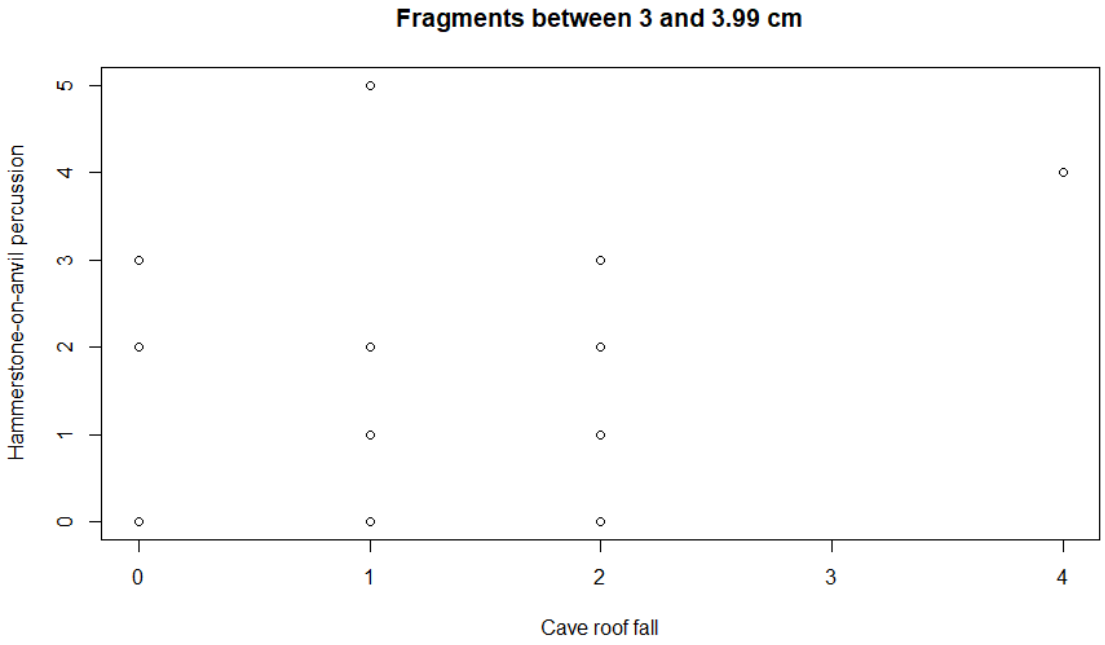

Figure 110 Scatter plot of fragments between 3 and 3.99 cm from both actors

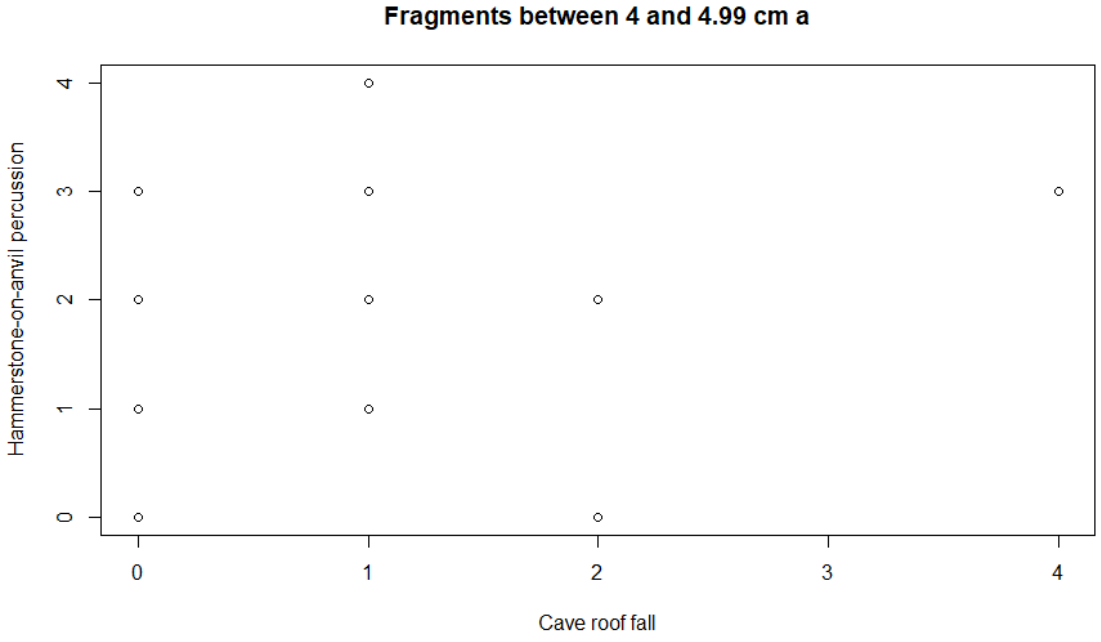

Figure 111 Scatter plot of fragments between 4 and 4.99 cm from both actors

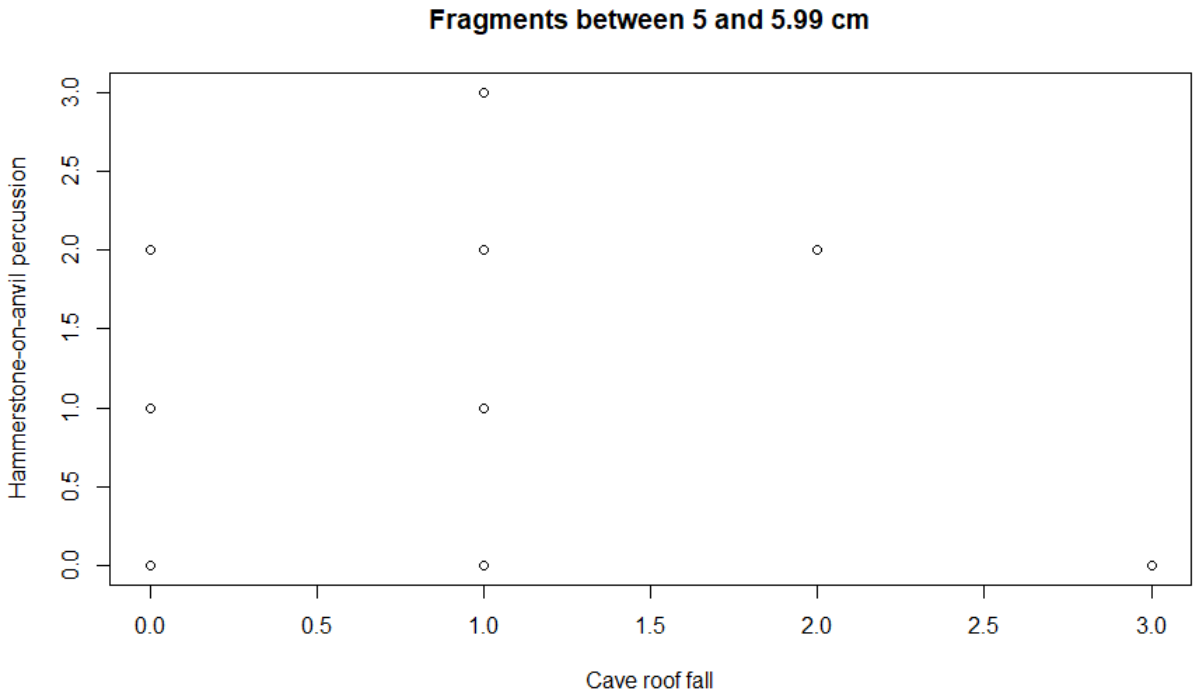

Figure 112 Scatter plot of fragments between 5 and 5.99 cm from both actors

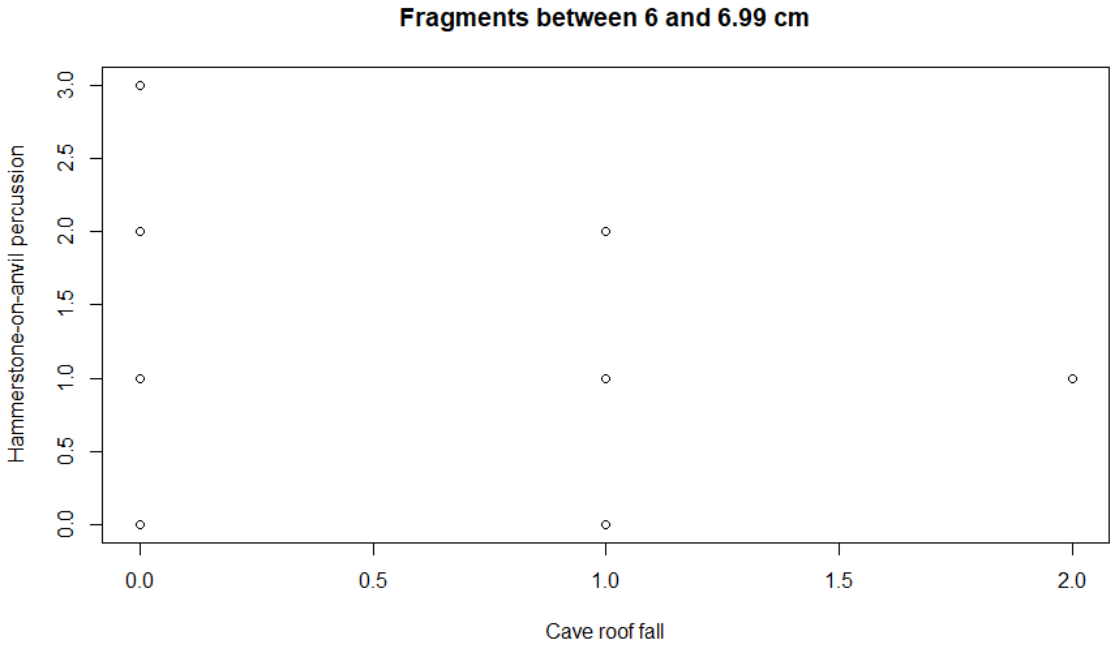

Figure 113 Scatter plot of fragments between 6 and 6.99 cm from both actors

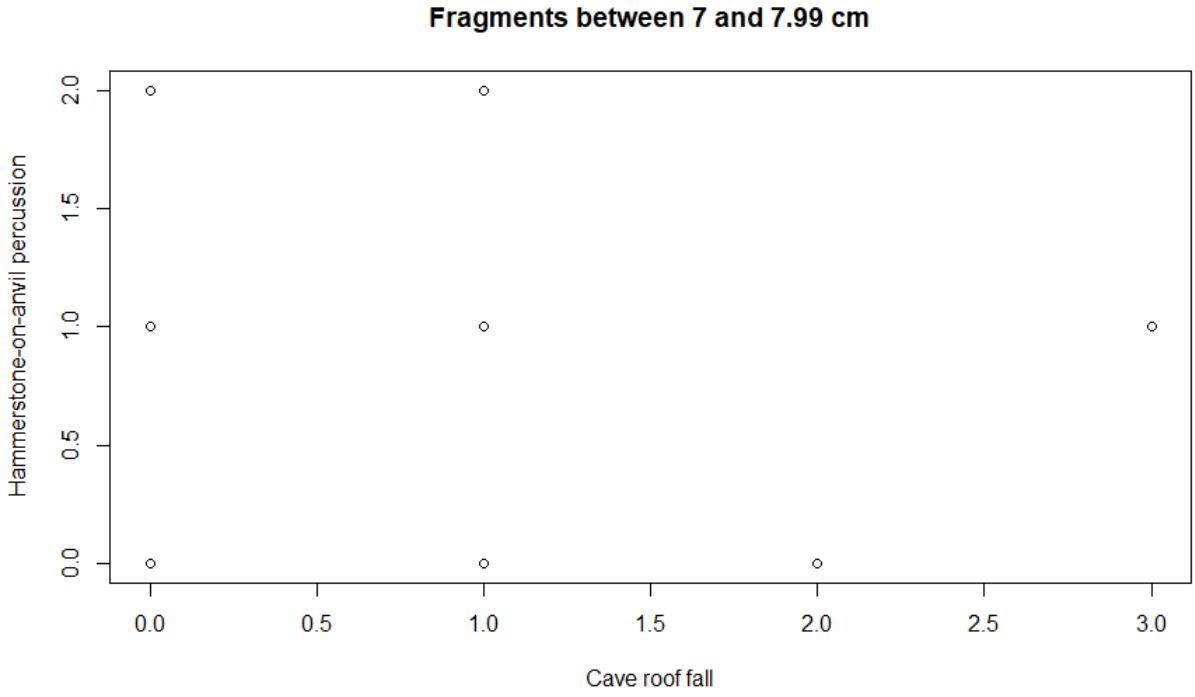

Figure 114 Scatter plot of fragments between 7 and 7.99 cm from both actors

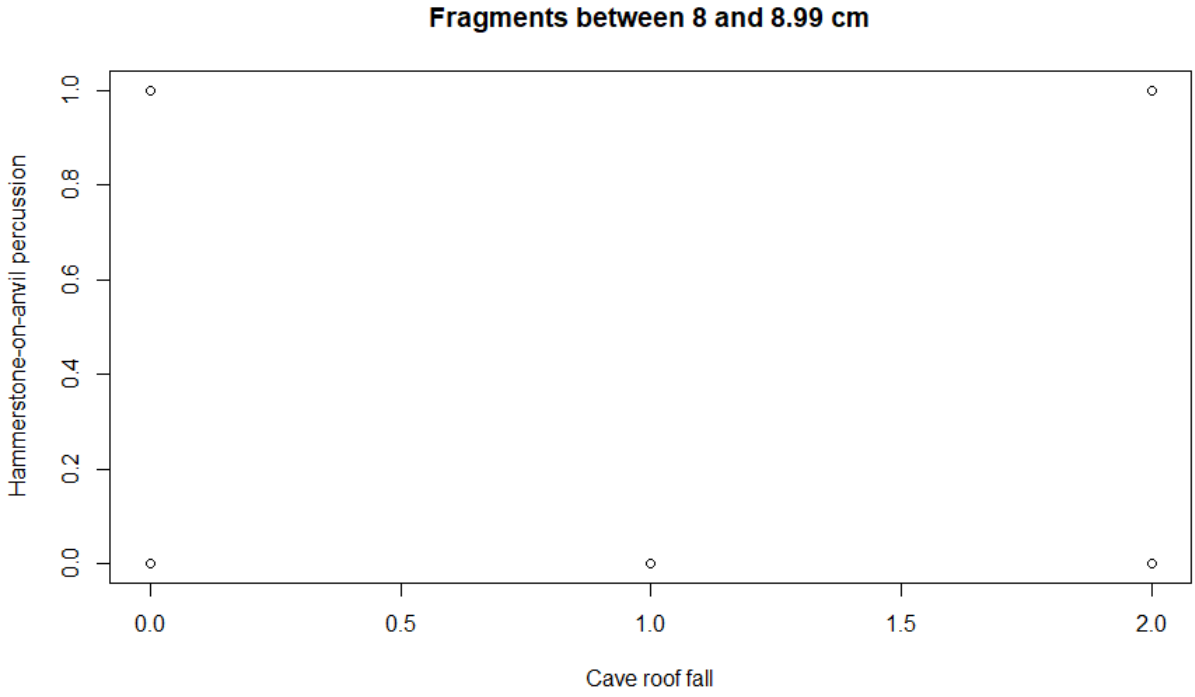

Figure 115 Scatter plot of fragments between 8 and 8.99 cm from both actors

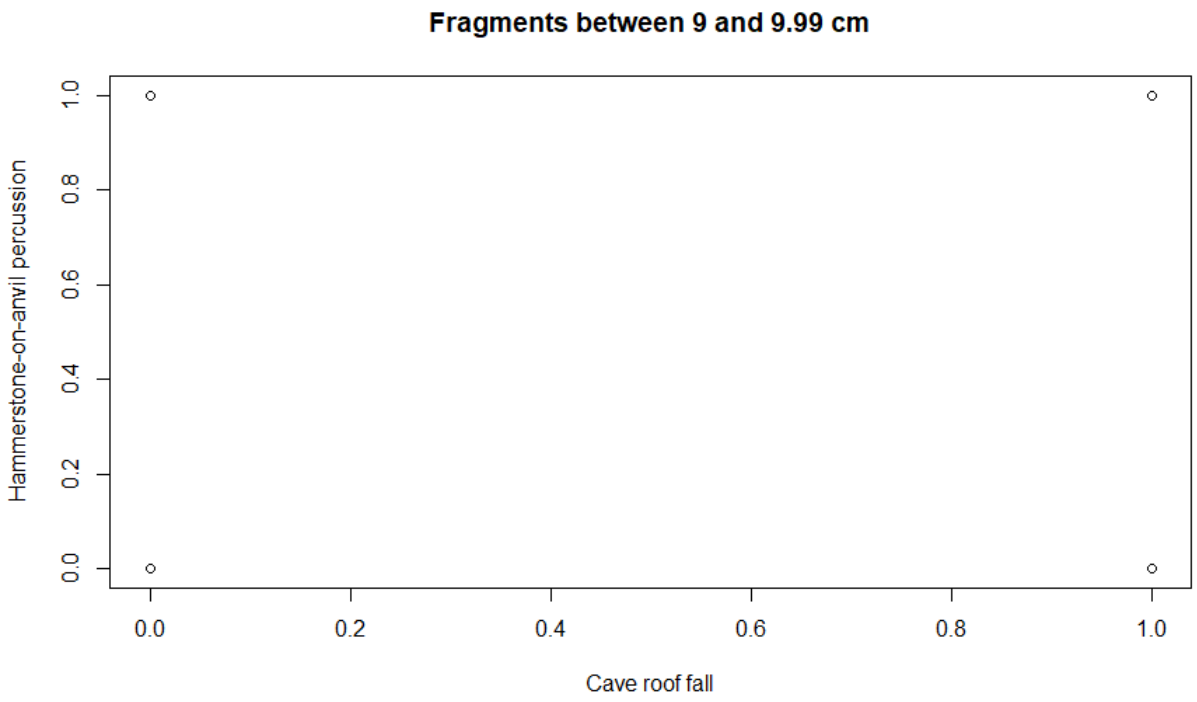

Figure 116 Scatter plot of fragments between 9 and 9.99 cm from both actors

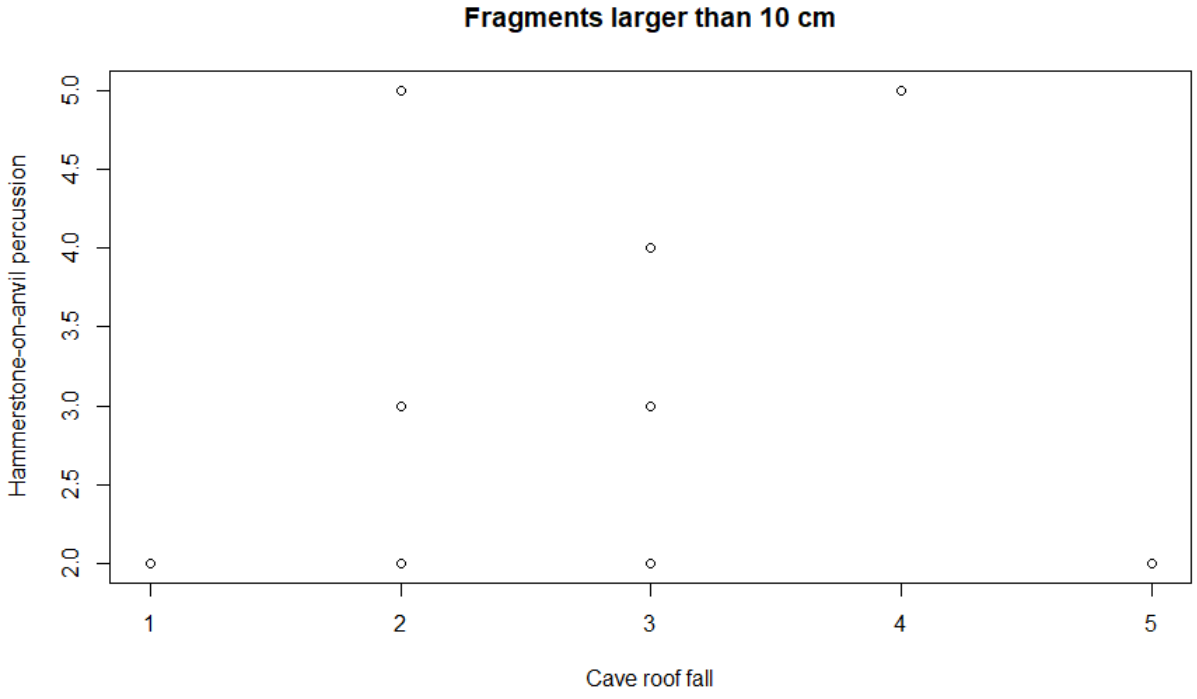

Figure 117 Scatter plot of fragments larger than 10 cm

Reference Page

Aldeias, V., Goldberg, P., Sandgathe, D., Berna, F., Dibble, H. L., McPherron, S. P., Turq, A., & Rezek, Z. (2012). Evidence for Neandertal use of fire at Roc de Marsal (France). *Journal of Archaeological Science*, *39*(7), 2414–2423. https://doi.org/10.1016/j.jas.2012.01.039

Anderson, D. D. (1997). Cave archaeology in southeast Asia. *Geoarchaeology: An International Journal*, *12*(6), 607–638.

Andrews, P., & Whybrow, P. (2005). Taphonomic Observations on a Camel Skeleton in a Desert Environment in Abu Dhabi. *Palaeontologia Electronica*, *8*.

Aranburu, A., Arsuaga, J. L., & Sala, N. (2017). The Stratigraphy of the Sima De Los Huesos (Atapuerca, Spain) and Implications for the Origin of the Fossil Hominin Accumulation. *Quaternary International*, *433*, 5–21. https://doi.org/10.1016/j.quaint.2015.02.044

Bar-Yosef, O., Vandermeersch, B., Arensburg, B., Belfer-Cohen, A., Goldberg, P., Laville, H., Meignen, L., Rak, Y., Speth, J. D., & Tchernov, E. (1992). The excavations in Kebara Cave, Mt. Carmel [and comments and replies]. *Current Anthropology*, *33*(5), 497–550.

Baryshnikov, G., Hoffecker, J., & Burgess, R. (1996). Palaeontology and Zooarchaeology of Mezmaiskaya Cave, north-western Caucasus. *J. Archaeol. Sci*, *23*(313), e335.

Behrensmeyer, A. K. (1978). Taphonomic and Ecologic Information from Bone Weathering. *Paleobiology*, *4*(2), 150–162. https://doi.org/10.1017/S0094837300005820

Behrensmeyer, A. K. (1987). Taphonomy and Hunting. In M. H. Nitecki & D. V. Nitecki (Eds.), *The Evolution of Human Hunting* (pp. 423–450). Springer US. https://doi.org/10.1007/978-1-4684-8833-3_10

Binford, L. R. (1981a). Chapter 1 - Relics to Artifacts and Monuments to Assemblages: Changing Conceptual Frameworks. In L. R. Binford (Ed.), *Bones* (pp. 3–20). Academic Press. https://doi.org/10.1016/B978-0-12-100036-3.50011-0

Binford, L. R. (1981b). Chapter 2—Middle-Range Research and the Role of Actualistic Studies. In L. R. Binford (Ed.), *Bones* (pp. 21–30). Academic Press. https://doi.org/10.1016/B978-0-12-100036-3.50012-2

Binford, L. R. (1981c). Chapter 3—Patterns of Bone Modifications Produced by Nonhuman Agents. In L. R. Binford (Ed.), *Bones* (pp. 35–86). Academic Press. https://doi.org/10.1016/B978-0-12-100036-3.50014-6

Binford, L. R. (1981d). Chapter 5 - Assemblage Composition: Patterns of Association Stemming from the Behavior of Man Versus That of Beast. In L. R. Binford (Ed.), *Bones* (pp. 183–242). Academic Press. https://doi.org/10.1016/B978-0-12-100036-3.50016-X

Blasco, R., Rosell, J., Arsuaga, J. L., Bermúdez de Castro, J. M., & Carbonell, E. (2010). The hunted hunter: The capture of a lion (Panthera leo fossilis) at the Gran Dolina site, Sierra de Atapuerca, Spain. *Journal of Archaeological Science*, *37*(8), 2051–2060. https://doi.org/10.1016/j.jas.2010.03.010

Blasco, R., Rosell, J., Fernández Peris, J., Cáceres, I., & Vergès, J. M. (2008). A New Element of Trampling: An Experimental Application on the Level Xii Faunal Record of Bolomor Cave (valencia, Spain). *Journal of Archaeological Science*, *35*(6), 1605–1618. https://doi.org/10.1016/j.jas.2007.11.007

Blumenschine, R. J. (1986). *Early Hominid Scavenging Opportunities: Implications of Carcass Availability in the Serengeti and Ngorongoro Ecosystems*. B.A.R.

Blumenschine, R. J. (1988). An experimental model of the timing of hominid and carnivore influence on archaeological bone assemblages. *Journal of Archaeological Science*, *15*(5), 483–502. https://doi.org/10.1016/0305-4403(88)90078-7

Blumenschine, R. J. (1995). Percussion Marks, Tooth Marks, and Experimental Determinations of the Timing of Hominid and Carnivore Access to Long Bones at Flk Zinjanthropus, Olduvai Gorge, Tanzania. *Journal of Human Evolution*, *29*(1), 21–51. https://doi.org/10.1006/jhev.1995.1046

Blumenschine, R. J., Cavallo, J. A., & Capaldo, S. D. (1994). Competition for Carcasses and Early Hominid Behavioral Ecology: A Case Study and Conceptual Framework. *Journal of Human Evolution*, *27*(1–3), 197–213.

Blumenschine, R. J., Marean, C. W., & Capaldo, S. D. (1996). Blind Tests of Inter-Analyst Correspondence and Accuracy in the Identification of Cut Marks, Percussion Marks, and Carnivore Tooth Marks on Bone Surfaces. *Journal of Archaeological Science*, *23*(4), 493–507.

Blumenschine, R. J., & Selvaggio, M. M. (1988). Percussion Marks on Bone Surfaces as a New Diagnostic of Hominid Behaviour. *Nature*, *333*(6175), 763–765. https://doi.org/10.1038/333763a0

Borrero, L. A. (1990). Taphonomy of Guanaco Bones in Tierra Del Fuego. *Quaternary Research*, *34*(3), 361–371. https://doi.org/10.1016/0033-5894(90)90047-O

Borrero, L., Barberena, R., Martin, F., & Borrazzo, K. (2007). Collapsed Rockshelters in Patagonia. In *On Shelter's Ledge. Histories, Theories and Methods of Rockshelter Research* (pp. 135–139).

Boyer Ontl, K., & Pruetz, J. D. (2020). Mothers Frequent Caves: Lactation Affects Chimpanzee (Pan troglodytes verus) Cave Use in Southeastern Senegal. *International Journal of Primatology*, *41*(6), 916–935. https://doi.org/10.1007/s10764-020-00165-4

Brain, C. K. (1983). *The Hunters or the Hunted?: An Introduction to African Cave Taphonomy*. University of Chicago Press.

Bunn, H. T., Kroll, E. M., Ambrose, S. H., Behrensmeyer, A. K., Binford, L. R., Blumenschine, R. J., Klein, R. G., McHenry, H. M., O'brien, C. J., & Wymer, J. (1986). Systematic Butchery by Plio/Pleistocene Hominids at Olduvai Gorge, Tanzania [and Comments and Reply]. *Current Anthropology*, *27*(5), 431–452.

Capaldo, S. D., & Blumenschine, R. J. (1994). A Quantitative Diagnosis of Notches Made by Hammerstone Percussion and Carnivore Gnawing on Bovid Long Bones. *American Antiquity*, *59*(4), 724–748. JSTOR. https://doi.org/10.2307/282345

Chase, P. G. (1987). The cult of the Cave Bear. *Expedition*, *29*(2), 4.

Coil, R., Tappen, M., & Yezzi-Woodley, K. (2017). New Analytical Methods for Comparing Bone Fracture Angles: A Controlled Study of Hammerstone and Hyena (crocuta Crocuta) Long Bone Breakage. *Archaeometry*, *59*(5), 900–917. https://doi.org/10.1111/arcm.12285

Dart, R. (1957). The Osteodontokeratic Culture of Australopithecus Promethius: The Total Contents of the Breccia Hitherto. *Transvaal Museum Memoirs*, *10*(1), 21–35.

de Ruiter, D. J., & Berger, L. R. (2000). Leopards as Taphonomic Agents in Dolomitic Caves—Implications for Bone Accumulations in the Hominid-bearing Deposits of South Africa. *Journal of Archaeological Science*, *27*(8), 665–684. https://doi.org/10.1006/jasc.1999.0470

Denys, C. (2002). Taphonomy and Experimentation. *Archaeometry*, *44*(3), 469–484. https://doi.org/10.1111/1475-4754.00079

Derricourt, R. (2009). The Enigma of Raymond Dart. *The International Journal of African Historical Studies*, *42*(2), 257–282.

Dibble, H. L., Aldeias, V., Alvarez-Fernandez, E., Blackwell, B. A., Hallett-Desguez, E., Jacobs, Z., Goldberg, P., Lin, S. C., Morala, A., & Meyer, M. C. (2012). New excavations at the site of Contrebandiers Cave, Morocco. *PaleoAnthropology*, *2012*, 145–201.

Diez, J. C., Ferna´ndez-Jalvo, Y., Rosell, J., & Ca´ceres, I. (1999). Zooarchaeology and Taphonomy of Aurora Stratum (gran Dolina, Sierra De Atapuerca, Spain). *Journal of Human Evolution*, *37*(3), 623–652. https://doi.org/10.1006/jhev.1999.0346

Dixon, E. J. (1984). Context and Environment in Taphonomic Analysis: Examples from Alaska's Porcupine River Caves 1. *Quaternary Research*, *22*(2), 201–215.

Efremov, I. (1940). Taphonomy: New Branch of Paleontology. *Pan-American Geologist*, *74*, 81–93.

Fernández-Jalvo, Y., & Andrews, P. (2019). Spy Cave (belgium) Neanderthals (36,000y Bp). Taphonomy and Peri-Mortem Traumas of Spy I and Spy Ii: Murder or Accident. *Quaternary Science Reviews*, *217*, 119–129. https://doi.org/10.1016/j.quascirev.2019.03.028

Fisher, J. (1995). Bone Surface Modifications in Zooarchaeology. *Journal of Archaeological Method and Theory*, *2*(1), 7–68. https://doi.org/10.1007/BF02228434

Fraser, R. A., & Wells, R. T. (2006). Palaeontological excavation and taphonomic investigation of the late Pleistocene fossil deposit in Grant Hall, Victoria Fossil Cave, Naracoorte, South Australia. *Alcheringa: An Australasian Journal of Palaeontology*, *30*(S1), 147–161.

Gargett, R. H. (1999). Middle Palaeolithic Burial Is Not a Dead Issue: The View from Qafzeh, Saint-Césaire, Kebara, Amud, and Dederiyeh. *Journal of Human Evolution*, *37*(1), 27–90. https://doi.org/10.1006/jhev.1999.0301

Gargett, R. H., Bricker, H. M., Clark, G., Lindly, J., Farizy, C., Masset, C., Frayer, D. W., Montet-White, A., Gamble, C., Gilman, A., Leroi-Gourhan, A., Ossa, P., Trinkaus, E., & Weber, A. W. (1989). Grave Shortcomings: The Evidence for Neandertal Burial [and Comments and Reply]. *Current Anthropology*, *30*(2), 157–190. https://doi.org/10.1086/203725

Gifford, D. P. (1981). Taphonomy and Paleoecology: A Critical Review of Archaeology's Sister Disciplines. In M. B. Schiffer (Ed.), *Advances in Archaeological Method and Theory* (pp. 365–438). Academic Press. https://doi.org/10.1016/B978-0-12-003104-7.50013-2

Gifford-Gonzalez, D. (1991). Bones Are Not Enough: Analogues, Knowledge, and Interpretive Strategies in Zooarchaeology. *Journal of Anthropological Archaeology*, *10*(3), 215–254.

Gifford-Gonzalez, D. (2018a). A Perspective on Zooarchaeology. In D. Gifford-Gonzalez (Ed.), *An Introduction to Zooarchaeology* (pp. 51–70). Springer International Publishing. https://doi.org/10.1007/978-3-319-65682-3_3

Gifford-Gonzalez, D. (2018b). Avian Carnivore, Ungulate, and Effects on Bone. In D. Gifford-Gonzalez (Ed.), *An Introduction to Zooarchaeology* (pp. 255–280). Springer International Publishing. https://doi.org/10.1007/978-3-319-65682-3_13

Gifford-Gonzalez, D. (2018c). Human, Animal, Geological Causes of Bone Breakage. In D. Gifford-Gonzalez (Ed.), *An Introduction to Zooarchaeology* (pp. 203–224). Springer International Publishing. https://doi.org/10.1007/978-3-319-65682-3_11

Gifford-Gonzalez, D. (2018d). Skeletal Disarticulation, Dispersal, Dismemberment, Selective Transport. In D. Gifford-Gonzalez (Ed.), *An Introduction to Zooarchaeology* (pp. 413–434). Springer International Publishing. https://doi.org/10.1007/978-3-319-65682-3_19

Goldberg, P., Aldeias, V., Dibble, H., McPherron, S., Sandgathe, D., & Turq, A. (2017). Testing the Roc de Marsal Neandertal "Burial" with Geoarchaeology. *Archaeological and Anthropological Sciences*, *9*(6), 1005–1015. https://doi.org/10.1007/s12520-013-0163-2

Goldberg, P., & Bar-Yosef, O. (2002). Site formation processes in Kebara and Hayonim caves and their significance in Levantine prehistoric caves. In *Neandertals and modern humans in Western Asia* (pp. 107–125). Springer.

Goldberg, P., & Bar-Yosef, O. (2019). Chapter 25—Cave dwellers in Southwest Asia. In W. B. White, D. C. Culver, & T. Pipan (Eds.), *Encyclopedia of Caves (Third Edition)* (pp. 218–222). Academic Press. https://doi.org/10.1016/B978-0-12-814124-3.00024-8

Goldberg, P., McPherron, S. J. P., Dibble, H. L., & Sandgathe, D. M. (2018). Stratigraphy, Deposits, and Site Formation. In H. L. Dibble, S. J. P. McPherron, P. Goldberg, & D. M. Sandgathe (Eds.), *The Middle Paleolithic Site of Pech de l'Azé IV* (pp. 21–74). Springer International Publishing. https://doi.org/10.1007/978-3-319-57524-7_2

Goldberg, P., Weiner, S., Bar-Yosef, O., Xu, Q., & Liu, J. (2001). Site formation processes at Zhoukoudian, China. *Journal of Human Evolution*, *41*(5), 483–530.

Gorjanović-Kramberger, D. (1906). *Der diluviale Mensch von Krapina in Kroatien*. C. W. Kreidel.

Griggo, C., Ingrid, G., ARGANT, A., Argant, J., Christian, D., Eva, F., Hobléa, F., Lebreton, L., & Philippe, M. (2019). *Tempiette Cave (entremont-Le-Vieux, Savoie, France): Paleoecology, Seasonality and Taphonomy of an Ibex and Chamois Trap-Cave. Xxxixe*

Rencontre Internationale D'archéologie Et D'histoire D'antibes, Juan-Les Pins, 16 Au 18 Octobre 2018. Ed. Apdca, Sophia Antipolis: 43-59.

Grupe, G., & Harbeck, M. (2014). Taphonomic and Diagenetic Processes. *Handbook of Paleoanthropology*, *2*, 417–440.

Harp, E. L., Dart, R. L., & Reichenbach, P. (2011). Rock Fall Simulation at Timpanogos Cave National Monument, American Fork Canyon, Utah, Usa. *Landslides*, *8*(3), 373–379. https://doi.org/10.1007/s10346-010-0251-7

Haynes, G. (1983). Frequencies of Spiral and Green-Bone Fractures on Ungulate Limb Bones in Modern Surface Assemblages. *American Antiquity*, *48*(1), 102–114. https://doi.org/10.2307/279822

Haynes, G. (2015). *Bone Breakage and Other Disturbances at the Inglewood Mammoth Site*.

Henry-Gambier, D., Nespoulet, R., & Chiotti, L. (2013). An Early Gravettian cultural attribution for the human fossils from the Cro-Magnon rock shelter (Les Eyzies-de-Tayac, Dordogne). *PALEO. Revue d'archéologie Préhistorique*, *24*, 121–138.

Herries, A. I. R., Pickering, R., Adams, J. W., Curnoe, D., Warr, G., Latham, A. G., & Shaw, J. (2013). A Multi-Disciplinary Perspective on the Age of Australopithecus in Southern Africa. In K. E. Reed, J. G. Fleagle, & R. E. Leakey (Eds.), *The Paleobiology of Australopithecus* (pp. 21–40). Springer Netherlands. https://doi.org/10.1007/978-94-007-5919-0_3

Hershkovitz, I., Weber, G. W., Quam, R., Duval, M., Grün, R., Kinsley, L., Ayalon, A., Bar-Matthews, M., Valladas, H., & Mercier, N. (2018). The earliest modern humans outside Africa. *Science*, *359*(6374), 456–459.

Hill, M. G. (2003). *Dictionary of Geology & Mineralogy*. McGraw-Hill Education. https://books.google.com/books?id=ydJ8QgAACAAJ

Hutton, J. (1788). Theory of the Earth; or an Investigation of the Laws observable in the Composition, Dissolution, and Restoration of Land upon the Globe. *Transactions of the Royal Society of Edinburgh*, *1*(2), 209–304. Cambridge Core. https://doi.org/10.1017/S0080456800029227

Jacobs, Z., Duller, G. A., Wintle, A. G., & Henshilwood, C. S. (2006). Extending the chronology of deposits at Blombos Cave, South Africa, back to 140 ka using optical dating of single and multiple grains of quartz. *Journal of Human Evolution*, *51*(3), 255–273.

Johnson, E. (1985). Current Developments in Bone Technology. In *Advances in archaeological method and theory* (pp. 157–235). Elsevier.

Karavanić, I., & Smith, F. H. (1998). The Middle/Upper Paleolithic interface and the relationship of Neanderthals and early modern humans in the Hrvatsko Zagorje, Croatia. *Journal of Human Evolution*, *34*(3), 223–248. https://doi.org/10.1006/jhev.1997.0192

Karavanić, I., Vukosavljević, N., Janković, I., Ahern, J., & Smith, F. (2017). Paleolithic hominins and settlement in Croatia from MIS 6 to MIS 3: Research history and current interpretations. *Quaternary International*. https://doi.org/10.1016/j.quaint.2017.09.034

Karr, L. P., & Outram, A. K. (2012a). Actualistic Research into Dynamic Impact and Its Implications for Understanding Differential Bone Fragmentation and Survivorship. *Journal of Archaeological Science*, *39*(11), 3443–3449.

Karr, L. P., & Outram, A. K. (2012b). Tracking Changes in Bone Fracture Morphology Over Time: Environment, Taphonomy, and the Archaeological Record. *Journal of Archaeological Science*, *39*(2), 555–559. https://doi.org/10.1016/j.jas.2011.10.016

Karr, L. P., & Outram, A. K. (2015). Bone Degradation and Environment: Understanding, Assessing and Conducting Archaeological Experiments Using Modern Animal Bones. *International Journal of Osteoarchaeology*, *25*(2), 201–212. https://doi.org/10.1002/oa.2275

Kehl, M., Burow, C., Hilgers, A., Navazo, M., Pastoors, A., Weniger, G.-C., Wood, R., & Pardo, J. F. J. (2013). Late Neanderthals at Jarama VI (central Iberia)? *Quaternary Research*, *80*(2), 218–234. https://doi.org/10.1016/j.yqres.2013.06.010

Koch, W. (1935). The Age Order of Epiphyseal Union in the Skeleton of the European Bison (Bos bonasus l.). *The Anatomical Record*, *61*(3), 371–376. https://doi.org/10.1002/ar.1090610313

Kokkov, K. (2019). Warrants, Middle-Range Theories, and Inferential Scaffolding in Archaeological Interpretation. *Perspectives on Science*, *27*(2), 171–186. https://doi.org/10.1162/posc_a_00304

Kos, A. M. (2003). Characterisation of Post-Depositional Taphonomic Processes in the Accumulation of Mammals in a Pitfall Cave Deposit from Southeastern Australia. *Journal of Archaeological Science*, *30*(6), 781–796. https://doi.org/10.1016/S0305-4403(02)00252-2

Kover, T. R. (2017). Of Killer Apes and Tender Carnivores: A Shepardian Critique of Burkert and Girard on Hunting and the Evolution of Religion. *Studies in Religion/Sciences Religieuses*, *46*(4), 536–567.

Kurtén, B. (1995). *The Cave Bear Story: Life and Death of a Vanished Animal*. Columbia University Press.

Lam, Y. M., Chen, X., Marean, C. W., & Frey, C. J. (1998). Bone Density and Long Bone Representation in Archaeological Faunas: Comparing Results from CT and Photon Densitometry. *Journal of Archaeological Science*, *25*(6), 559–570. https://doi.org/10.1006/jasc.1997.0256

Langdon, J. H. (2016). Case Study 8. Taming the Killer Ape: The Science of Taphonomy. In J. H. Langdon (Ed.), *The Science of Human Evolution: Getting it Right* (pp. 59–65). Springer International Publishing. https://doi.org/10.1007/978-3-319-41585-7_8

Li, F., Bae, C. J., Ramsey, C. B., Chen, F., & Gao, X. (2018). Re-dating Zhoukoudian Upper Cave, northern China and its regional significance. *Journal of Human Evolution*, *121*, 170–177. https://doi.org/10.1016/j.jhevol.2018.02.011

Lisiecki, L. E., & Raymo, M. E. (2005). A Pliocene-Pleistocene stack of 57 globally distributed benthic δ18O records. *Paleoceanography*, *20*(1). https://doi.org/10.1029/2004PA001071

Lyman, R. (1987). Zooarchaeology and Taphonomy: A General Consideration. *J Ethnobiol*, *7*.

Lyman, R. L. (1984). Broken Bones, Bone Expediency Tools, and Bone Pseudotools: Lessons from the Blast Zone Around Mount St. Helens, Washington. *American Antiquity*, *49*(2), 315–333. JSTOR. https://doi.org/10.2307/280021

Lyman, R. L. (1994). *Vertebrate Taphonomy*. Cambridge University Press. https://doi.org/10.1017/CBO9781139878302

Mangiafico, S. (2018). *Re: How to interpret Spearman Correlation when p value is not significant?* [Response]. ResearchGate. https://www.researchgate.net/post/How_to_interpret_Spearman_Correlation_when_p_value_is_not_significant

Mann, A., & Monge, J. (2006). A Neandertal Parietal Fragment from Krapina (croatia) with a Serious Cranial Trauma. *Periodicum Biologorum*, *108*, 495–502.

Marean, C. W., Abe, Y., Frey, C. J., & Randall, R. C. (2000). Zooarchaeological and Taphonomic Analysis of the Die Kelders Cave 1 Layers 10 and 11 Middle Stone Age Larger Mammal Fauna. *Journal of Human Evolution*, *38*(1), 197–233. https://doi.org/10.1006/jhev.1999.0356

Marean, C. W., & Kim, S. Y. (1998). Mousterian Large-Mammal Remains from Kobeh Cave Behavioral Implications for Neanderthals and Early Modern Humans. *Current Anthropology*, *39*(S1), S79–S114. https://doi.org/10.1086/204691

Marra, A., Villa, P., Beauval, C., Laura, B., & Goldberg, P. (2004). Same Predator, Variable Prey: Taphonomy of Two Upper Pleistocene Hyena Dens in Sicily and Sw France. *Revue de Paleobiologie*, *23*, 787–801.

Martin, L., & Gilbert, B. (1978). Excavations at Natural Trap Cave. *Transactions of the Nebraska Academy of Sciences and Affiliated Societies*. https://digitalcommons.unl.edu/tnas/336

Meagher, M. (1986). Bison bison. *Mammalian Species*, *266*, 1–8.

Mina, W.-E., Tsatskin, A., Weiner, S., Shahack-Gross, R., Yeshurun, R., & Zaidner, Y. (2010). A Window into Early Middle Paleolithic Human Occupational Layers: Misliya Cave, Mount Carmel, Israel. *PaleoAnthropology*, *2010*, 202−228. https://doi.org/10.4207/PA.2012.ART75

Morlan, R. E. (1994). Bison Bone Fragmentation and Survivorship: A Comparative Method. *Journal of Archaeological Science*, *21*(6), 797–807.

Myers, T. P., Voorhies, M. R., & Corner, R. G. (1980). Spiral Fractures and Bone Pseudotools at Paleontological Sites. *American Antiquity*, *45*(3), 483–490. https://doi.org/10.2307/279863

Nejman, L., Lisá, L., Doláková, N., Horáček, I., Bajer, A., Novák, J., Wright, D., Sullivan, M., Wood, R., Gargett, R. H., Pacher, M., Sázelová, S., Nývltová Fišáková, M., Rohovec, J., & Králík, M. (2018). Cave Deposits as a Sedimentary Trap for the Marine Isotope Stage 3 Environmental Record: The Case Study of Pod Hradem, Czech Republic. *Palaeogeography, Palaeoclimatology, Palaeoecology*, *497*, 201–217. https://doi.org/10.1016/j.palaeo.2018.02.020

Njau, J. K., & Blumenschine, R. J. (2006). A Diagnosis of Crocodile Feeding Traces on Larger Mammal Bone, with Fossil Examples from the Plio-Pleistocene Olduvai Basin, Tanzania. *Journal of Human Evolution*, *50*(2), 142–162. https://doi.org/10.1016/j.jhevol.2005.08.008

Norton, C. J., & Gao, X. (2008). Zhoukoudian Upper Cave Revisited. *Current Anthropology*, *49*(4), 732–745. https://doi.org/10.1086/588637

Oliver, J. S. (1989). Analogues and Site Context: Bone Damages from Shield Trap Cave (24cb91), Carbon County, Montana, Usa. *In Bone Modification , Ed. Robson Bonnichsen and Marcello H. Sorg*, *Center for the Study of the First Americans, Orono, Maine.*, 73–98.

Olsen, S. L., & Shipman, P. (1988). Surface Modification on Bone: Trampling Versus Butchery. *Journal of Archaeological Science*, *15*(5), 535–553. https://doi.org/10.1016/0305-4403(88)90081-7

Pacher, M., & Rabeder, G. (2016). The leopard (Panthera pardus), the rare hunter of the Alpine area during the Upper Pleistocene. *Cranium*, *33*(1), 42–50.

Pante, M. C., Muttart, M. V., Keevil, T. L., Blumenschine, R. J., Njau, J. K., & Merritt, S. R. (2017). A New High-Resolution 3-D Quantitative Method for Identifying Bone Surface Modifications with Implications for the Early Stone Age Archaeological Record. *Journal of Human Evolution*, *102*, 1–11. https://doi.org/10.1016/j.jhevol.2016.10.002

Pickering, T. R., & Egeland, C. P. (2006). Experimental Patterns of Hammerstone Percussion Damage on Bones: Implications for Inferences of Carcass Processing by Humans. *Journal of Archaeological Science*, *33*(4), 459–469.

Piperno, M., & Giacobini, G. (1990). A taphonomic study of the paleosurface of Guattari Cave (Monte Circeo, Latina, Italy). *Quaternaria Nova*, *1*, 143–161.

Pirson, S., Toussaint, M., Bonjean, D., & Di Modica, K. (2018). Spy and Scladina Caves: A Neandertal's Story. In A. Demoulin (Ed.), *Landscapes and Landforms of Belgium and Luxembourg* (pp. 357–383). Springer International Publishing. https://doi.org/10.1007/978-3-319-58239-9_21

Pomeroy, E., Bennett, P., Hunt, C. O., Reynolds, T., Farr, L., Frouin, M., Holman, J., Lane, R., French, C., & Barker, G. (2020). New Neanderthal Remains Associated with the 'Flower Burial' at Shanidar Cave. *Antiquity*, *94*(373), 11–26. https://doi.org/10.15184/aqy.2019.207

Reed, E. H. (2006). In Situ Taphonomic Investigation of Pleistocene Large Mammal Bone Deposits from The Ossuaries, Victoria Fossil Cave, Naracoorte, South Australia. *Helictite*, *39*, 5–15.

Reynolds, T., Farr, L., Hill, E., Hunt, C., Jones, S., Gratuze, B., Nymark, A., Abdulmutalb, D., & Barker, G. (2018). Shanidar Cave and the Baradostian, a Zagros Aurignacian industry. *L'Anthropologie*, *122*(5), 737–748. https://doi.org/10.1016/j.anthro.2018.10.007

Richter, D., Rink, W., Schwarcz, H., Julig, P., & Schroeder, H. (2001). The Middle to Upper Palaeolithic transition in the Levant and new thermoluminescence dates for a late Mousterian assemblage from Jerf al-Ajla Cave (Syria). *Paléorient*, 29–46.

Richter, J. (2006). Neanderthals in Their Landscape. In *Neanderthals in Europe* (Vol. 117, pp. 51–66).

Rink, W. J., Schwarcz, H., Lee, H., Rees-Jones, J., Rabinovich, R., & Hovers, E. (2001). Electron spin resonance (ESR) and thermal ionization mass spectrometric (TIMS) 230Th/234U dating of teeth in Middle Paleolithic layers at Amud Cave, Israel. *Geoarchaeology: An International Journal*, *16*(6), 701–717.

Sala, N., Pantoja-Pérez, A., Arsuaga, J. L., Pablos, A., & Martínez, I. (2016). The Sima De Los Huesos Crania: Analysis of the Cranial Breakage Patterns. *Journal of Archaeological Science*, *72*, 25–43. https://doi.org/10.1016/j.jas.2016.06.001

Shipman, P. (1981). Applications of Scanning Electron Microscopy to Taphonomic Problems. *Annals of the New York Academy of Sciences*, *376*(1), 357–385.

Solecki, R. S. (1957). Shanidar Cave. *Scientific American*, *197*(5), 58–65. JSTOR.

Stavrova, T., Borel, A., Daujeard, C., & Vettese, D. (2019). A Gis Based Approach to Long Bone Breakage Patterns Derived from Marrow Extraction. *PloS One*, *14*(5), e0216733.

Talamo, S., Aldeias, V., Goldberg, P., Chiotti, L., Dibble, H. L., Guérin, G., Hublin, J.-J., Madelaine, S., Maria, R., Sandgathe, D., Steele, T. E., Turq, A., & Mcpherron, S. J. P. (2020). The new 14C chronology for the Palaeolithic site of La Ferrassie, France: The

disappearance of Neanderthals and the arrival of Homo sapiens in France. *Journal of Quaternary Science*, *35*(7), 961–973. https://doi.org/10.1002/jqs.3236

Toussaint, M., & Pirson, S. (2006). Neandertal Studies in Belgium: 2000–2005. *Periodicum Biologorum*, *108*(3), 373–387.

Trinkaus, E. (1983). *The Shanidar Neandertals*. Academic Press. https://books.google.com/books?id=fi2AAAAAMAAJ

Trinkaus, E. (1985). Cannibalism and Burial at Krapina. *Journal of Human Evolution*, *14*(2), 203–216.

Trinkaus, E., & Biglari, F. (2006). Middle Paleolithic Human Remains from Bisitun Cave, Iran. *Paléorient*, *32*(2), 105–111. JSTOR.

Ullrich, H. (2005). Cannibalistic Rites Within Mortuary Practices from the Paleolithic to Middle Ages in Europe. *Anthropologie (1962-)*, *43*(2/3), 249–261. JSTOR.

Valensi, P., Crégut-Bonnoure, E., & Defleur, A. (2012). Archaeozoological data from the Mousterian level from Moula-Guercy (Ardèche, France) bearing cannibalised Neanderthal remains. *Quaternary International*, *252*, 48–55. https://doi.org/10.1016/j.quaint.2011.07.028

Vettese, D., Blasco, R., Cáceres, I., Gaudzinski-Windheuser, S., Moncel, M.-H., Hohenstein, U. T., & Daujeard, C. (2020). Towards an Understanding of Hominin Marrow Extraction Strategies: A Proposal for a Percussion Mark Terminology. *Archaeological and Anthropological Sciences*, *12*(2), 48. https://doi.org/10.1007/s12520-019-00972-8

Villa, P. (1992). Cannibalism in Prehistoric Europe. *Evolutionary Anthropology: Issues, News, and Reviews*, *1*(3), 93–104.

Villa, P., & Mahieu, E. (1991). Breakage Patterns of Human Long Bones. *Journal of Human Evolution*, *21*(1), 27–48. https://doi.org/10.1016/0047-2484(91)90034-S

White, T. D. (1992). *Prehistoric Cannibalism at Mancos 5MTUMR-2346*. Princeton University Press.

White, T. D., Toth, N., Chase, P. G., Clark, G. A., Conrad, N. J., Cook, J., d'Errico, F., Donahue, R. E., Gargett, R. H., Giacobini, G., Pike-Tay, A., & Turner, A. (1991). The Question of Ritual Cannibalism at Grotta Guattari [and Comments and Replies]. *Current Anthropology*, *32*(2), 118–138. https://doi.org/10.1086/203931

Wolpoff, M. H., Smith, F. H., Malez, M., Radovčić, J., & Rukavina, D. (1981). Upper pleistocene human remains from Vindija cave, Croatia, Yugoslavia. *American Journal of Physical Anthropology*, *54*(4), 499–545. https://doi.org/10.1002/ajpa.1330540407

Wunn, I. (2000). Beginning of Religion. *Numen*, *47*(4), 417–452. https://doi.org/10.1163/156852700511612

Wunn, I. (2001). Cave bear worship in the Palaeolithic. *Cadernos Do Laboratorio Xeolóxico de Laxe*, *26*, 457–463.